Opportunities for the bio-based production of Methyl Propionate via 2-Butanol

Pereira, Joana P.C.

DOI
10.4233/uuid:04fc99da-9e9e-4e31-bd02-4076786e0c16

Publication date
2018

Document Version
Final published version

Citation (APA)
Pereira, J. P. C. (2018). *Opportunities for the bio-based production of Methyl Propionate via 2-Butanol*. [Dissertation (TU Delft), Delft University of Technology]. https://doi.org/10.4233/uuid:04fc99da-9e9e-4e31-bd02-4076786e0c16

Opportunities for the bio-based production of Methyl Propionate via 2-Butanol

Dissertation

for the purpose of obtaining the degree of doctor
at Delft University of Technology
by the authority of the Rector Magnificus, prof.dr.ir. T.H.J.J. van der Hagen
chair of the Board of Doctorates
to be defended publicly on
Monday 29 October 2018 at 10:00 o'clock

by

Joana Patrícia CARVALHO PEREIRA

Master of Science in Environmental Engineering,
Universidade de Aveiro, Portugal
born in Aveiro, Portugal

This dissertation has been approved by the promotors.

Composition of the doctoral committee:

Rector Magnificus	Chairperson
Prof. dr. ir. L.A.M. van der Wielen	Delft University of Technology, promotor
Dr. ir. A.J.J. Straathof	Delft University of Technology, promotor
Independent members:	
Prof. dr. H.J. Noorman	Delft University of Technology
Prof. dr. P. Osseweijer	Delft University of Technology
Prof. dr. ir. C.A. Ramirez Ramirez	Delft University of Technology
Prof. dr. M.R.M.S. Aires Barros	Técnico de Lisboa, Portugal
Dr. A.M. Lopez Contreras	Wageningen University and Research

The research described in this thesis was performed at the Bioprocess Engineering Group, Department of Biotechnology, Faculty of Applied Sciences, Delft University of Technology, the Netherlands.

This project has been financially supported by the Netherlands Organization for Scientific Research (NWO), under the framework of Technology Area TA-Biomass.

Printed by: Ridderprint BV | www.ridderprint.nl

An electronic version of this dissertation is available at
http://repository.tudelft.nl/.

ISBN 978-94-6186-971-5

"Para ser grande, sê inteiro: nada
Teu exagera ou exclui.
Sê todo em cada coisa. Põe quanto és
No mínimo que fazes.
Assim em cada lago a lua toda
Brilha, porque alta vive."
"Odes de Ricardo Reis", Fernando Pessoa, 1933

“To be great, be whole; exclude
Nothing, exaggerate nothing that is you.
Be whole in everything. Put all you are
Into the smallest thing you do.
As in each lake the whole moon gleams
Because it stands tall.”
“Odes de Ricardo Reis”, Fernando Pessoa, 1933

Summary

(Poly)methyl methacrylate is a valuable thermoplastic with wide application in several fields. Currently, methyl methacrylate (MMA) can be produced from ethene via methyl propionate using the Alpha technology, a more environmentally friendly method than the typical acetone-cyanohydrin route. Nevertheless, the use of lignocellulosic materials as feedstock to produce bio-based MMA would potentiate the recycling of agricultural waste biomass, theoretically resulting in zero-carbon emissions, contrasting with the current use of petrochemical feedstocks. This would also mitigate the industrial impact on climate change.

In the present thesis, a bio-based approach for the production of methyl propionate, the precursor of MMA, has been proposed. The overall process involves a two-step biotransformation, starting with the anaerobic fermentation of lignocellulosic sugars into 2-butanol, pursuing a metabolic route via butanone (a.o.). 2-Butanol is further used as chemical precursor in a cascade enzymatic reaction, where methyl propionate and ethyl acetate are formed from the Baeyer-Villiger (BV) oxidation of butanone. The techno-economic feasibility of this bio-based approach has been assessed, and critical issues affecting the practicability of the proposed process have been identified at a very early stage of strain engineering and process design.

In **Chapter 2**, the inhibiting effect of some key lignocellulose-derived and fermentation products on three potential hosts for the bio-based production of methyl propionate, namely *Escherichia coli*, *Bacillus subtilis*, and *Saccharomyces cerevisiae*, has been assessed. The microbial growth in the presence of these products was characterized by means of a lag-time model, and the inhibitory thresholds were determined using product-inhibition models. It has been observed that all the hosts were completely inhibited by lignocellulose-derived products with concentrations as low as 2.0 g/L. From the fermentation products tested, methyl propionate had the most severe impact, resulting in complete growth inhibition of the strains when exposed to concentrations in the range of 13–23 g/L. The inhibiting effect of the intermediate 2-butanol was slightly milder, but resulted in full inhibition of all the strains when growing in the presence of concentrations in the range of 20–36 g/L.

To avoid microbial inhibition, these products must be kept below their inhibiting concentrations. However, the purification of such diluted product streams, for instance by conventional

distillation, becomes highly energy-consuming. Product recovery costs can be mitigated by means of *in-situ* product recovery (ISPR) techniques.

Taking advantage of the products' high relative volatilities, as compared with the other compounds in the fermentation broth, the technical feasibility of a two-stage separation process combining vacuum stripping and adsorption has been investigated in **Chapter 3**, primarily aiming at the selective recovery of 2-butanol produced by fermentation. Given the lack of an engineered strain able to produce 2-butanol, spiked model solutions and hydrolysates have been used. This study revealed that the relative volatility of 2-butanol was enhanced in the presence of hydrolysate compounds, anticipating high energy requirements for the efficient product recovery by condensation. As a result, the integration of vacuum stripping with adsorption can become advantageous. Among the adsorbents tested, silicalite materials revealed higher efficiency to selectively recover 2-butanol from the stripped vapor mixture, particularly at low alcohol partial pressures.

Based on these results, the conceptual design of the process for 2-butanol production by vacuum fermentation, integrated with product recovery, has been developed in **Chapter 4**. Engineering software Aspen Plus has been used for simulation purposes. Aiming at a fair comparison among different product recovery options, three downstream scenarios have been examined for product recovery: 1) multi-stage vapor recompression, 2) temperature swing adsorption (TSA), and 3) vapor absorption. The performance of these scenarios has been evaluated using a consistent framework, based on global energy requirements and capital expenditure. This study revealed that the use of integrated adsorption and absorption minimized the energy duty required for azeotrope purification. The highest fixed capital investment was observed for scenario 2, driven by the numerous adsorption units required for the TSA task. The energy requirements per kg of highly-pure 2-butanol (99 wt.%) were determined as 25.3 MJ/kg, 21.9 MJ/kg, and 17.6 MJ/kg considering scenarios 1), 2) and 3), respectively, which is within the ranges reported for its isomer, 1-butanol. However, the feedstock costs represented the most significant expenditure in all the scenarios. Overall, this study showed that a profitable process for 2-butanol production could be achieved, if efficient microbial strains were used in a suitably integrated configuration such as the ones suggested.

Finally, the prospects for the full-scale methyl propionate production integrated with product recovery by *in-situ* stripping, have been analyzed in **Chapter 5**. Recombinant *E. coli* cells harboring a fused enzyme have been used to perform the cascade reaction, where methyl propionate and ethyl acetate were obtained from 2-butanol via butanone oxidation. The

conversion was in line with a model comprising product formation and stripping kinetics. The maximum conversion rates were 1.14 g-butanone/(L h), 0.11 g-ethyl acetate/(L h), and 0.09 g-methyl propionate/(L h). The enzyme regioselectivity towards methyl propionate was 43% of total ester. Under these conditions, the estimated feedstock costs for the full-scale process were ca. 4-fold higher than the sales revenue. Considering an optimized strain, the operational costs translated into 1.16 €/kg_{ester}, which is beyond the current petrochemical price. As a result, full-scale ester production could only become competitive with petrochemical production if the BV oxidation was enhanced, and the costs of bio-based 2-butanol were minimized.

Pursuing a one-step biotransformation of lignocellulosic sugars into methyl propionate would avoid the need for the recovery of chemical precursors, and could enhance the maximum yield to 0.489 $g_{ester}/g_{glucose}$. Overall, as shown in **Chapter 6**, even though the novel pathway for bio-based methyl propionate has been implemented in *E. coli*, significant strain optimization is still required. The outcome of this thesis indicates that the ideal microorganism would: 1) ferment lignocellulosic sugars; 2) harbor oxygen-insensitive enzymes; 3) form one methyl propionate per glucose equivalent, effectively closing the redox balance and circumventing the formation of ethyl acetate; 4) require no additional cobalamin; and 5) depict sufficient stability for cell retention and recycling.

Samenvatting

(Poly) methylmethacrylaat is een waardevol thermoplast met brede toepassing op verschillende gebieden. Momenteel kan methylmethacrylaat (MMA) worden geproduceerd uit etheen via methylpropionaat met behulp van de Alpha-technologie, een milieuvriendelijker methode dan de typische aceton-cyaanhydrine route. Niettemin zou het gebruik van lignocellulosematerialen als grondstof voor de productie van biogebaseerd MMA de recycling van biomassa van landbouwafval versterken. Theoretisch voorkomt dit in koolstofemissies, in tegenstelling tot het huidige gebruik van petrochemische grondstoffen. Dit zou ook de industriële impact op de klimaatverandering verminderen.

In dit proefschrift wordt een biobased benadering voor de productie van methylpropionaat, de voorloper van MMAgepresenteerd. Het totale proces omvat een biotransformatie in twee stappen, te beginnen met de anaerobe fermentatie van lignocellulosesuikers naar 2-butanol, waarbij een metabole route wordt gevolgd via (onder andere) butanon. 2-Butanol wordt verder gebruikt als chemische precursor in een enzymatische cascade reactie, waarbij methylpropionaat en ethylacetaat worden gevormd uit de Baeyer-Villiger (BV) oxidatie van butanon. De techno-economische haalbaarheid van deze biobased benadering is beoordeeld. Kritieke problemen die van invloed zijn op de uitvoerbaarheid van het voorgestelde proces zijn in een zeer vroeg stadium van strain engineering en procesontwerp geïdentificeerd.

In **Hoofdstuk 2** is het inhiberende effect van enkele van de belangrijkste uit lignocellulose afkomstige en fermentatieproducten op drie potentiële gastheer stammen voor de biogebaseerde productie van methylpropionaat, namelijk *Escherichia coli*, *Bacillus subtilis* en *Saccharomyces cerevisiae*, beoordeeld. De microbiële groei in de aanwezigheid van deze producten werd gekenmerkt door een lag-time model en de drempelwaardes van inhiberende producten werden bepaald met behulp van inhibitiemodellen. Er is waargenomen dat alle gastheer stammen volledig werden geremd door van lignocellulose afgeleide producten met concentraties zo laag als 2.0 g/L. Van de geteste fermentatieproducten had methylpropionaat de meest ernstige impact, resulterend in volledige groei-inhibitie van de stammen bij blootstelling aan concentraties in het bereik van 13-23 g/L. Het inhiberende effect van het tussenproduct 2-butanol was enigszins milder, maar resulteerde in volledige remming van alle stammen bij groei in de aanwezigheid van concentraties tussen 20-36 g/L.

Om microbiële inhibitie te voorkomen, moeten de concentraties van deze producten onder hun drempelwaardes worden gehouden. De zuivering van dergelijke verdunde productstromen, bijvoorbeeld door conventionele destillatie leiden echter tot een hoge energie consumptie. De kosten voor te terugwinnign van de producten kunnen worden verminderd met in-situ-productterugwinning (ISPR).

In **Hoofdstuk 3** is de technische haalbaarheid van een tweetraps scheidingsproces dat vacuümstrippen en adsorptie combineert onderzocht door, voornamelijk gericht op het selectieve herstel van 2-butanol geproduceerd door fermentatie. Gezien het ontbreken van een gemanipuleerde stam die in staat is om 2-butanol te produceren, zijn verrijkte modeloplossingen en hydrolysaten gebruikt. Deze studie toonde aan dat de relatieve vluchtigheid van 2-butanol verhoogd was in de aanwezigheid van hydrolysaatverbindingen, wat leidt tot hoge energievereisten voor een efficiënte productterugwinning door condensatie. Hierdoor kan de integratie van vacuümstrippen met adsorptie voordelig worden. Van de geteste adsorbentia toonden silicalietmaterialen hogere efficiëntie om selectief 2-butanol uit het gestripte dampmengsel terug te winnen, in het bijzonder bij lage partiële drukken van alcohol.

Op basis van deze resultaten is het conceptuele ontwerp van het proces voor 2-butanolproductie door vacuümfermentatie, geïntegreerd met productterugwinning, ontwikkeld in **Hoofdstuk 4**. Aspen Plus software is gebruikt voor simulatie doeleinden. Met het oog op een eerlijke vergelijking tussen verschillende productterugwinningsopties, zijn drie downstreamscenario's onderzocht voor productterugwinning: 1) meerstaps-damprecompressie, 2) adsorptie met temperatuurschommelingen (TSA) en 3) dampabsorptie. De prestaties van deze scenario's zijn geëvalueerd met behulp van een consistent kader, gebaseerd op wereldwijde energiebehoeften en kapitaaluitgaven. Uit deze studie bleek dat het gebruik van geïntegreerde adsorptie en absorptie de energiebelasting minimaliseerde die nodig is voor azeotroopzuivering. De hoogste investering in vast kapitaal werd waargenomen voor scenario 2, veroorzaakt door de vele adsorptie-eenheden die nodig zijn voor de TSA-taak. De energievraag per kg zeer zuivere 2-butanol (99 wt.%) werd bepaald als 25.3 MJ/kg, 21.9 MJ/kg, en 17.6 MJ/kg rekening houdend met scenario's 1), 2) en 3), respectievelijk, die ligt binnen het bereik dat wordt gerapporteerd voor zijn isomeer, 1-butanol. De grondstofkosten vertegenwoordigden echter de meest significante uitgaven in alle scenario's. Over het algemeen liet deze studie zien dat een winstgevend proces voor de productie van 2-butanol kon worden bereikt als efficiënte microbiële stammen werden gebruikt in een geschikt geïntegreerde configuratie, zoals voorgesteld.

Ten slotte zijn de vooruitzichten voor de volledige methylpropionaatproductie, geïntegreerd met productterugwinning door in-situ stripping, geanalyseerd in **Hoofdstuk 5**. Recombinante *E. coli*-cellen die een gefuseerd enzym bevatten, zijn gebruikt om de cascade-reactie uit te voeren, waarbij methylpropionaat en ethylacetaat werden verkregen uit 2-butanol via butanonoxidatie. De conversie was in overeenstemming met een model dat kinetiek van productvorming en terugwinning omvat. De maximale omzettingssnelheden waren 1.14 g-butanon/(Lh), 0.11 g-ethylacetaat/(Lh) en 0.09 g-methylpropionaat/(Lh). De regioselectiviteit van het enzym ten opzichte van methylpropionaat was 43% van de totale ester. Onder deze omstandigheden waren de geschatte grondstofkosten voor het volledige proces ongeveer vier maal hoger dan de omzet. Wanner gebruik werd gemaakt van een geoptimailseerde stam, vertaalden de operationele kosten zich in 1.16 €/kg_{ester}, wat hoger is dan de huidige petrochemische prijs. Als gevolg hiervan kon de volledige esterproductie alleen concurrerend worden met de petrochemische productie als de BV-oxidatie werd verbeterd en de kosten van biobased 2-butanol tot een minimum werden beperkt.

Het ontwikkelen van een biotransformatie in één stap van lignocellulosesuikers in methylpropionaat zou de noodzaak voor de terugwinning van chemische precursoren voorkomen en zou de maximale opbrengst kunnen verhogen tot 0.489 $g_{ester}/g_{glucose}$. Over het algemeen is, ondanks het feit dat de nieuwe route voor biogebaseerd methylpropionaat in *E. coli* is geïmplementeerd, nog steeds een aanzienlijke stamoptimalisatie nodig. De uitkomst van dit proefschrift geeft aan dat het ideale micro-organisme: 1) lignocellulosesuikers vergist; 2) zuurstof-ongevoelige enzymen bevat; 3) één methylpropionaat per glucoserequivalent vormt, waarbij de redoxbalans effectief wordt gesloten en de vorming van ethylacetaat wordt omzeild; 4) geen extra cobalamine vereist; en 5) voldoende stabiliteit voor celretentie en recycling vertoont.

Table of Contents

Chapter 1: General introduction

Contents

1.1 Lignocellulosic feedstock for the production of commodity chemicals

The use of renewable resources for the production of biofuels and biocommodity chemicals can minimize the existing industrial dependence on petrochemical resources, promoting a net zero carbon footprint, and ultimately mitigating climate change. Among the diverse sources of renewable feedstocks, lignocellulosic biomass is the most abundant and promising alternative feedstock, mainly due to its worldwide availability, low carbon footprint, and low cost, usually in the range of 24–60 €/ton [1]. Since lignocellulosic feedstocks range from energy crops to agriculture and forestry residues, as well as organic industrial wastes, their large scale application avoids competition with land requirements related to food crop production. Currently, corn stover is the most abundant lignocellulosic feedstock in the USA, particularly in corn-producing regions such as Iowa or Illinois, with an estimated amount of 64 million dry tonnes of collectable corn stover per year [2].

Lignocellulosic feedstocks are mainly composed of cellulose, hemicellulose, and lignin. To provide the monosaccharides required for microbial conversion, the polysaccharides (i.e., cellulose and hemicellulose) are first degraded using chemical and enzymatic methods [3]. During the monomerization process, numerous lignocellulose degradation products are also generated, such as weak acids (acetic acid, formic acid, levulinic acid), phenolic compounds (vanillin, syringaldehyde, coniferyl aldehyde), and furans (furfural, 5-hydroxymethyl-2-furaldehyde) [4]. These products usually inhibit the growth and productivity of the microbial biocatalysts, and therefore represent a major challenge for the commercial application of bio-based processes [3].

The fermentative conversion of monosaccharides to commodity chemicals typically involves long enzymatic pathways, occurring within wild type or specifically engineered microbial hosts. Cell-free enzymatic pathways have also been developed [5], but the production of the enzymes requires a fermentative process, besides additional laborious and cost-intensive enzyme purification processes [6]. Therefore, significant research has been dedicated to metabolic engineering, focusing on the improvement of intracellular enzyme activity, microbial robustness, and co-consumption of multiple monosaccharides, i.e. pentose and hexose, often with successful outcome [7]. Currently, numerous chemicals are produced by fermentation on industrial scale. Well-known industrial fermentations include the production of alcohols (ethanol, 1-butanol, isobutanol, 1,3-propanediol, 1,4-butanediol), amino acids ($_{L}$-lysine, $_{L}$-glutamate), and carboxylic acids (itaconic, lactic, and succinic acids) [8].

1.2 Bio-based (poly)methyl methacrylate

(Poly)methyl methacrylate (PMMA) is a valuable thermoplastic known for its excellent performance characteristics [9], which promoted its vast application in several fields (Fig. 1).
According to the most recent market analysis, the supply of methyl methacrylate (MMA) faces a strong demand, which requires a quick and responsive market to fully satisfy the needs of Asia and Europe [10]. Due to this increasing demand, the market size of PMMA is expected to exceed 11 billion USD by 2022 [11].

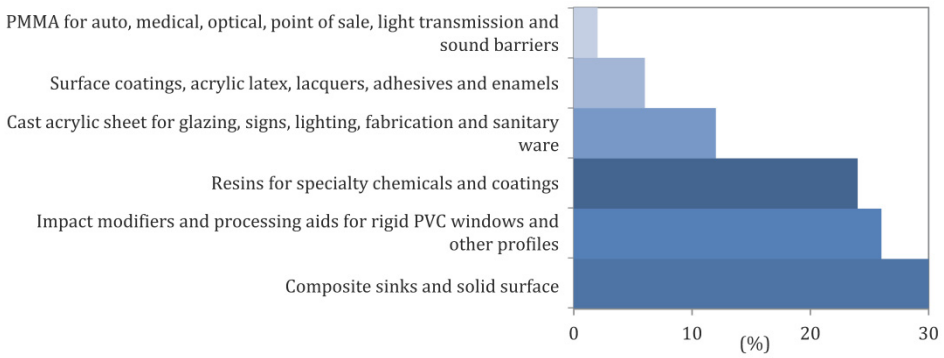

Figure 1. Downstream use of PMMA, as reported in October 2017 [10]

Several petrochemical and biomass-based routes have been proposed for the production of MMA, and an overview of these routes is provided in Fig. 2. Detailed information about the existing petrochemical routes can be found elsewhere [12]. Typically, MMA is produced via the acetone-cyanohydrin route, but the extreme toxicity and corrosivity of the reagents used in this method led to environmental pressure against their use [13]. In 2008, Lucite International has commissioned the first commercial MMA plant using the Alpha technology, a more environmentally friendly method to produce MMA from ethene via methyl propionate, in two reaction steps (see Fig. 2) [14,15]. The Alpha technology, which is also to be used in the world's largest MMA plant currently under commissioning, proved to be 30–40% cheaper to build and run than other conventional systems, producing virtually no waste [10].
However, given the petrochemical nature of the resources supporting the current industrial MMA production, great concern has emerged regarding the continued emission of greenhouse

gases (GHG), which increase the industrial GHG footprint and promote climate change. To mitigate their GHG footprint, as well as their dependence on petrochemical resources, the major opportunity for the producers lies towards the development of biomass-based approaches for MMA production.

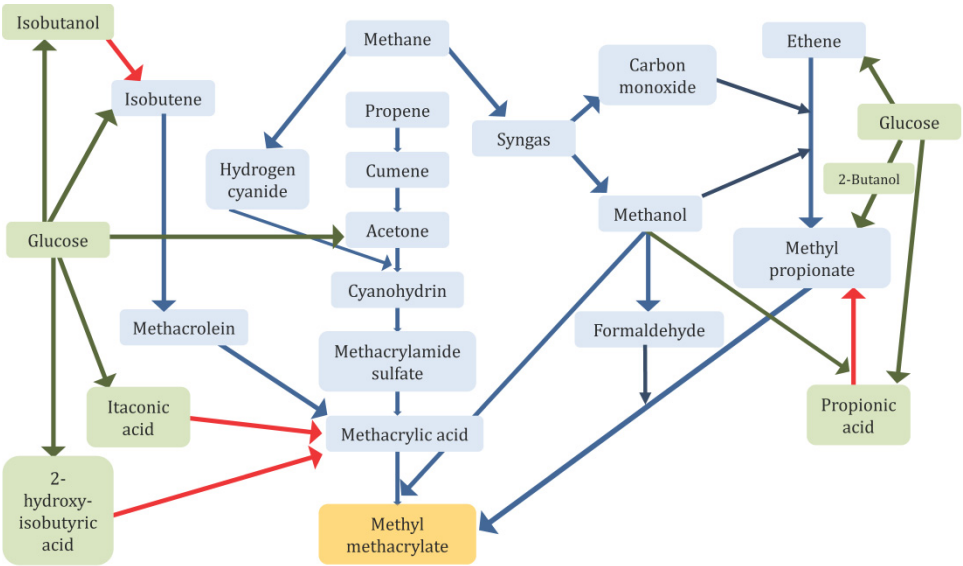

Figure 2. Routes to methyl methacrylate production from petrochemical resources (blue), and potential biomass-based routes starting from glucose (green), including some chemical conversions (red arrows)

Lucite International patented the application of unusual enzymes in a biotransformation to produce MMA, starting from lignocellulosic corn stover hydrolysate. The proposed pathway comprises a series of different enzymatic reactions, summarized in Fig. 3 [16].

The first step of the biotransformation yields butanone and 2-butanol from the anaerobic fermentation of sugars, via meso-2,3-butanediol. This pathway has been first explored by Speranza et al. [17] using *Lactobacillus brevis*, and later engineered for *Escherichia coli* [18], *Saccharomyces. cerevisiae* [19], and *Klebsiella pneumoniae* [20]. Despite the efforts to enhance the production of bio-based 2-butanol, the maximum titer achieved was 1.03 g/L, with a productivity of ca. 0.029 g/(L h) [20], which is still far from the required commercial targets.

The second step of the biotransformation is an enzymatic oxidation, accomplished by a newly developed fusion enzyme, combining an alcohol dehydrogenase and a Baeyer-Villiger monooxygenase (BVMO) [21]. 2-Butanol is first oxidized to butanone, which is further oxidized to

methyl propionate, in a true cascade reaction. The purified methyl propionate is finally condensed with formaldehyde to produce MMA, using the state-of-the-art downstream chemistry of Lucite's Alpha process [16].

The Baeyer-Villiger oxidation of butanone would normally produce ethyl acetate, but it has been observed that certain BVMOs, namely cyclohexanone monooxygenases (CHMOs), can also produce the abnormal product, methyl propionate [22]. Since the endogenous reaction yielding the normal product cannot be totally suppressed, ethyl acetate is an unavoidable side-product of the biotransformation [23]. Compared to other biomass-based approaches (recall Fig. 2), the proposed pathway is a short route, and presents a potentially high yield on glucose: the maximum achievable theoretical yield is 0.453 g-ester/g-glucose, similar to that observed for ethyl acetate produced from direct glucose conversion [24].

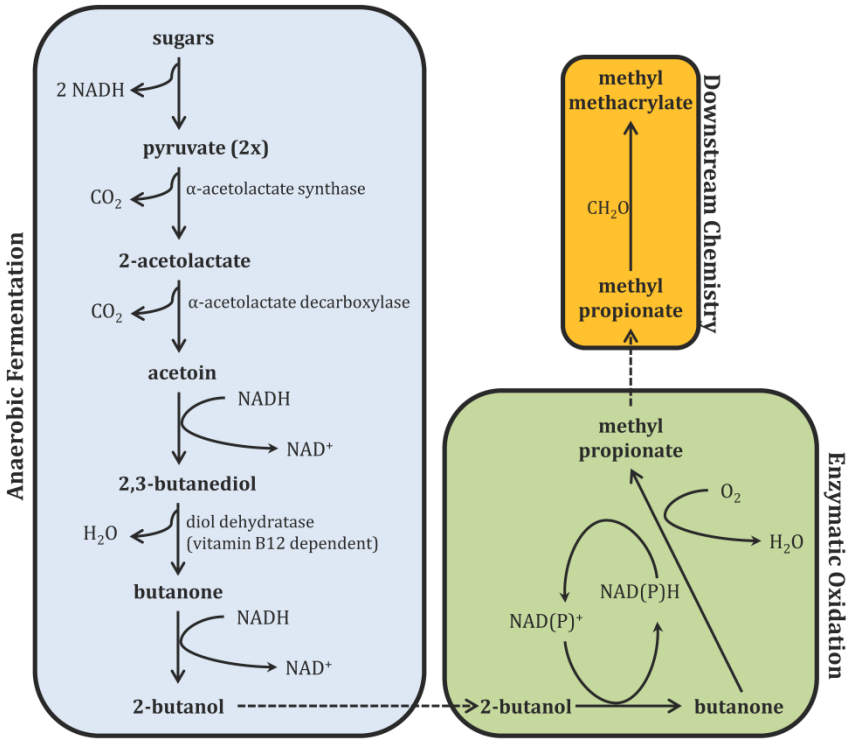

Figure 3. Metabolic pathway for the production of methyl methacrylate from sugars via 2-butanol

1.2.1 Rational approach for the production of bio-based methyl methacrylate

As shown in Fig. 3, the overall biotransformation presents distinct oxygen requirements in the different steps. In the first step, if aerobic conditions are used, the α-acetolactate synthase is rapidly and irreversibly inactivated, ceasing the formation of the intermediate meso-2,3-butanediol [25], and thus the production of the main intermediate 2-butanol. In the second step, however, 2-butanol is the chemical precursor in a cascade of oxidative enzymatic reactions, and side-reactions can only be prevented by effectively closing the redox balances. Therefore, it is crucial to ensure a continuous flux of oxygen and cofactor through the pathway.

Due to these constraints, controlling anaerobic and aerobic conditions within the same bioreactor, using a single engineered microorganism, appears to be a demanding and challenging task. As a result, the most rational approach for first-generation production of bio-based MMA considers a two-step process, where 2-butanol is first produced by anaerobic fermentative conversion of lignocellulosic sugars, and then transferred to an aerobic bioreactor, where the enzymatic cascade reaction yields methyl propionate. The state-of-the-art downstream chemistry step yielding MMA from methyl propionate is left outside the scope of this study.

1.2 Scope and thesis outline

The present research evaluates the feasibility of a two-step biotransformation for methyl propionate production, via 2-butanol, aiming to identify the major process bottlenecks at a very early stage of strain engineering and process design.

A typical drawback in bio-based processes is product toxicity. Besides the lignocellulosic degradation products, fermentation products such as 1-butanol, isobutanol, and ethyl acetate, are also known to be toxic to the fermenting microorganisms [26,27]. The toxicity of products such as 2-butanol and methyl propionate on microbial hosts is therefore anticipated, but has not yet been reported in the available literature.

To overcome product toxicity, several *in-situ* product removal (ISPR) techniques exist, and have often proven effective to circumvent product inhibition and reduce energy requirements for product recovery. Detailed reviews on these technologies and their efficiency for biobutanol removal and recovery can be found in the literature [28-30]. Given the novelty of the bio-based production of methyl propionate via 2-butanol, information regarding the effective recovery of these products from fermentation broth is lacking from the literature. As a result, the state-of-

the-art strategies in process engineering for biobutanol (1-butanol and isobutanol) and ethyl acetate recovery have been considered as a starting point for the studies herein developed. Moreover, given the lack of an engineered microbial host able to produce 2-butanol at the relevant rates for this process, the selective recovery of the alcohol was studied using spiked model solutions and hydrolysates.

The present thesis is structured as follows (Fig. 4):

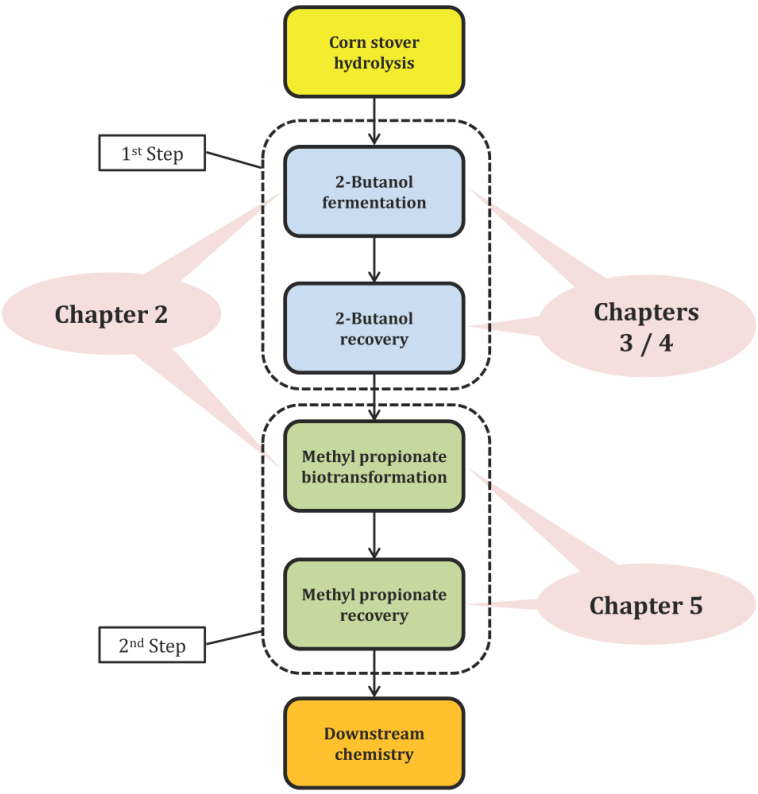

Figure 4. Schematic research framework and thesis outline

In **Chapter 2**, the effect of lignocellulosic and fermentation inhibitors on three potential hosts for the bio-based production of methyl propionate, namely *E. coli*, *S. cerevisiae*, and *Bacillus subtilis*, will be assessed. As a result of this study, the potential of each microbial host for recombinant solvent production will be disclosed. The product concentrations at which the microbial growth

is pointedly inhibited will be determined, and can therefore be used as reference for the maximum titers allowed to accumulate in the bioreactor.

In **Chapter 3**, the experimental feasibility of vacuum fermentation as ISPR technique for the selective removal of 2-butanol from fermentation broths will be assessed. Aiming at the selective recovery of 2-butanol from the fermentation vapor, four different types of adsorbents will be screened. This study will allow to troubleshoot the vacuum fermentation process, and its overall integration with product recovery by adsorption.

In **Chapter 4**, the conceptual design of the full-scale process considering 2-butanol production by vacuum fermentation, integrated with product recovery from the fermentation vapor, will be presented. Three downstream scenarios will be examined for product recovery: 1) multi-stage vapor recompression; 2) temperature swing adsorption; and 3) vapor absorption. This study will provide insights into the overall process economics, ultimately outlining the metabolic targets required for the bio-based production of 2-butanol to become profitable.

In **Chapter 5**, recombinant *E. coli* cells harboring a fused enzyme will be used to produce methyl propionate and ethyl acetate, starting from 2-butanol. The conceptual design of the full-scale ester production process, integrated with conventional product recovery by distillation, will be presented. This study will give a new insight into the feasibility of the proposed two-step process for methyl propionate production via 2-butanol, also reflecting the overall metabolic targets that must be aimed at for the process to become feasible.

Finally, **Chapter 6** will provide an overview on the prospects for the integrated biotransformation and recovery of methyl propionate at large-scale, based on the findings provided by the overall research.

1.3 References

(1) de Jong, W.; van Ommen, J. R. *Biomass as a Sustainable Energy Source for the Future: Fundamentals of Conversion Processes*, Wiley, New Jersey, 2014.

(2) Graham, R. L.; Nelson, R.; Sheehan, J.; Perlack, R. D.; Wright, L. L. Current and Potential U.S. Corn Stover Supplies. *Agronomy Journal* **2007**, *99*, 1-11.

(3) van der Pol, E.; Bakker, R.; Baets, P.; Eggink, G. By-Products Resulting from Lignocellulose Pretreatment and Their Inhibitory Effect on Fermentations for (Bio)Chemicals and Fuels. *Appl. Microbiol. Biotechnol.* **2014**, *98*, 9579-9593.

(4) Jönsson, L. J.; Alriksson, B.; Nilvebrant, N.-O. Bioconversion of Lignocellulose: Inhibitors and Detoxification. *Biotechnol. Biofuels* **2013**, *6*, 16-16.

(5) Guterl, J. K.; Garbe, D.; Carsten, J.; Steffler, F.; Sommer, B.; Reisse, S.; Philipp, A.; Haack, M.; Ruhmann, B. et al. Cell-Free Metabolic Engineering: Production of Chemicals by Minimized Reaction Cascades. *ChemSusChem* **2012**, *5*, 2165-72.

(6) Shuler, M. L.; Kargi, F.; DeLisa, M. *Bioprocess Engineering: Basic Concepts*, Prentice Hall, Upper Saddle River, NJ, 2017.

(7) Yao, R.; Shimizu, K. Recent Progress in Metabolic Engineering for the Production of Biofuels and Biochemicals from Renewable Sources with Particular Emphasis on Catabolite Regulation and Its Modulation. *Process Biochem.* **2013**, *48*, 1409-1417.

(8) Straathof, A. J. J. Transformation of Biomass into Commodity Chemicals Using Enzymes or Cells. *Chem. Rev.* **2014**, *114*, 1871–1908.

(9) Ali, U.; Karim, K. J. B. A.; Buang, N. A. A Review of the Properties and Applications of Poly (Methyl Methacrylate) (Pmma). *Polym. Rev.* **2015**, *55*, 678–705.

(10) Taking a Closer Look at the Methacrylates Markets. http://www.luciteinternational.com accessed 18 Dec 2017.

(11) Global Market Insights, I., *Synthetic and Bio-Based Pmma (Polymethyl Methacrylate) Market Size by Product (Extruded Sheets, Pellets, Beads, Cell Cast Sheet & Blocks), by Application (Automotive, Electronics, Construction, Signs & Display), Industry Analysis Report, Regional Outlook, Downstream Application Development Potential, Price Trend, Competitive Market Share & Forecast, 2012-2022*. 2016. p. 190.

(12) Ullmann, F.; Gerhartz, W.; Yamamoto, Y. S.; Campbell, F. T.; Pfefferkorn, R.; Rounsaville, J. F. *Ullmann's Encyclopedia of Industrial Chemistry*, VCH, 1991.

(13) Li, B.; Yan, R.; Wang, L.; Diao, Y.; Li, Z.; Zhang, S. Synthesis of Methyl Methacrylate by Aldol Condensation of Methyl Propionate with Formaldehyde over Acid–Base Bifunctional Catalysts. *Catal. Lett.* **2013**, *143*, 829-838.

(14) Clegg, W.; R. J. Elsegood, M.; R. Eastham, G.; P. Tooze, R.; Lan Wang, X.; Whiston, K. Highly Active and Selective Catalysts for the Production of Methyl Propanoate Via the Methoxycarbonylation of Ethene. *Chem. Commun.* **1999**, 1877–1878.

(15) Lorusso, P.; Coetzee, J.; Eastham, G. R.; Cole-Hamilton, D. J. A-Methylenation of Methyl Propanoate by the Catalytic Dehydrogenation of Methanol. *ChemCatChem* **2016**, *8*, 222–227.

(16) Eastham, G. R.; Johnson, D. W.; Straathof, A. J. J.; Fraaije, M. W.; Winter, R. T. Process for the Production of Methyl Methacrylate. EP2855689 A1, 2015.

(17) Speranza, G.; Corti, S.; Fontana, G.; Manitto, P.; Galli, A.; Scarpellini, M.; Chialva, F. Conversion of Meso-2,3-Butanediol into 2-Butanol by Lactobacilli. Stereochemical and Enzymatic Aspects. *J. Agric. Food. Chem.* **1997**, *45*, 3476–3480.

(18) Yoneda, H.; Tantillo, D. J.; Atsumi, S. Biological Production of 2-Butanone in *Escherichia Coli*. *ChemSusChem* **2014**, *7*, 92–95.

(19) Ghiaci, P.; Norbeck, J.; Larsson, C. 2-Butanol and Butanone Production in *Saccharomyces Cerevisiae* through Combination of a B12 Dependent Dehydratase and a Secondary Alcohol Dehydrogenase Using a Tev-Based Expression System. *PLoS One* **2014**, *9*, e102774.

(20) Chen, Z.; Wu, Y.; Huang, J.; Liu, D. Metabolic Engineering of Klebsiella Pneumoniae for the De

Novo Production of 2-Butanol as a Potential Biofuel. *Bioresour. Technol.* **2015**, *197*, 260–265.

(21) Aalbers, F. S.; Fraaije, M. W. Coupled Reactions by Coupled Enzymes: Alcohol to Lactone Cascade with Alcohol Dehydrogenase-Cyclohexanone Monooxygenase Fusions. *Appl. Microbiol. Biotechnol.* **2017**, *101*, 7557–7565.

(22) van Beek, H. L.; Winter, R. T.; Eastham, G. R.; Fraaije, M. W. Synthesis of Methyl Propanoate by Baeyer-Villiger Monooxygenases. *Chem. Commun.* **2014**, *50*, 13034–13036.

(23) van Beek, H. L.; Romero, E.; Fraaije, M. W. Engineering Cyclohexanone Monooxygenase for the Production of Methyl Propanoate. *ACS Chem. Biol.* **2017**, *12*, 291–299.

(24) Löser, C.; Urit, T.; Bley, T. Perspectives for the Biotechnological Production of Ethyl Acetate by Yeasts. *Appl. Microbiol. Biotechnol.* **2014**, *98*, 5397–5415.

(25) Ji, X. J.; Huang, H.; Ouyang, P. K. Microbial 2,3-Butanediol Production: A State-of-the-Art Review. *Biotechnol. Adv.* **2011**, *29*, 351-64.

(26) Aiba, S.; Shoda, M.; Nagatani, M. Kinetics of Product Inhibition in Alcohol Fermentation. *Biotechnol. Bioeng.* **1968**, *10*, 845-64.

(27) Urit, T.; Manthey, R.; Bley, T.; Löser, C. Formation of Ethyl Acetate by *Kluyveromyces Marxianus* on Whey: Influence of Aeration and Inhibition of Yeast Growth by Ethyl Acetate. *Eng. Life Sci.* **2013**, *13*, 247-260.

(28) Ezeji, T. C.; Qureshi, N.; Blaschek, H. P. Bioproduction of Butanol from Biomass: From Genes to Bioreactors. *Curr. Opin. Biotechnol.* **2007**, *18*, 220-227.

(29) Groot, W. J.; van der Lans, R. G. J. M.; Luyben, K. C. A. M. Technologies for Butanol Recovery Integrated with Fermentations. *Process Biochem.* **1992**, *27*, 61–75.

(30) Oudshoorn, A.; van der Wielen, L. A. M.; Straathof, A. J. J. Assessment of Options for Selective 1-Butanol Recovery from Aqueous Solution. *Ind. Eng. Chem. Res.* **2009**, *48*, 7325–7336.

Chapter 2: Growth inhibition of *S. cerevisiae*, *B. subtilis*, and *E. coli* by lignocellulosic and fermentation products

Abstract This paper describes the effect of several inhibiting components on three potential hosts for the bio-based production of methyl propionate, namely wild type *Escherichia coli* and *Bacillus subtilis*, and evolved *Saccharomyces cerevisiae* IMS0351. The inhibition by the lignocellulose-derived products 5-hydroxymethyl-2-furaldehyde, vanillin and syringaldehyde, and the fermentation products 2-butanol, 2-butanone, methyl propionate and ethyl acetate, has been assessed for these strains in defined medium and microaerobic conditions. Multiple screenings were performed using small scale cultures in both shake flasks and microtiter plates. Technical drawbacks revealed the limited applicability of the latter in this study. The microbial growth was characterized by means of a lag-time model, and the inhibitory thresholds were determined using product-inhibition models. The lignocellulose-derived products were found to be highly inhibitory, and none of the strains could grow in the presence of 2.0 g L^{-1} of product. From the fermentation products tested, methyl propionate had the most severe impact resulting in complete inhibition of all the strains when exposed to concentrations in the range of 13–23 g L^{-1}. In general, *S. cerevisiae* and *B. subtilis* were comparatively more tolerant than *E. coli* to all the fermentation products, despite *E. coli*'s lower sensitivity towards vanillin. The results suggest that, overall, the strains investigated have good potential to be engineered and further established as hosts for the bio-based production of methyl esters.

Keywords: Bio based products · Growth inhibition · Lag time model · Product inhibition models

---

Published as: Pereira, J.P.C., Verheijen, P.J.T., and Straathof, A.J.J., Growth inhibition of *S. cerevisiae*, *B. subtilis*, and *E. coli* by lignocellulosic and fermentation products. *Appl. Microbiol. Biotechnol*. 2016, *100*, 9069–9080.

Contents

2.1 Introduction

Methyl methacrylate is a valuable building block for acrylic paints and organic glass [1]. The global demand for methyl methacrylate has grown annually, and it is expected to increase at an average rate of 4.0% up to 2016 [2]. Currently, methyl methacrylate is produced from fossil feedstocks, such as methyl propionate [3,4]. Therefore, its market growth is vulnerable to rising and volatile fossil feedstock prices. The development of a bio-based production process would mitigate these effects and exploit the potential of these methyl esters. Recent findings show that methyl propionate can be formed by enzymatic oxidation of 2-butanone [5]. The fermentative production of 2-butanone has also been proposed, both in *E. coli* [6] and *S. cerevisiae* [7]. Despite the low conversion efficiencies reached so far, the coupling of these processes would enable the use of renewable feedstocks such as lignocellulose, instead of fossil feedstocks, for the long-term production of methyl methacrylate. However, in addition to demanding pathway engineering, product toxicity is a major drawback in the microbial production of commodity chemicals.

Lignocellulose is the most abundant biomass on earth, and it is the substrate of choice to produce bulk products by fermentation [8,9]. Given its complex structure consisting of cellulose, hemicellulose and lignin, lignocellulose requires pretreatment to facilitate depolymerization to simple sugars. Several pretreatment methods have been inspected comprising both chemical and enzymatic hydrolysis, but the unavoidable release of inhibitory degradation products is often emphasized and strongly correlated to the type of feedstock and pretreatment used [10-12]. Typical potential inhibitors include weak acids, phenolic compounds like vanillin and syringaldehyde, and furanic compounds such as 2-furaldehyde (furfural) and 5-hydroxymethyl-2-furaldehyde (HMF) [12-14]. The effect of these compounds on the growth and productivity of different microorganisms has been reviewed by many authors, but the levels of inhibition reported vary strikingly with inhibitor concentrations and microbial strain [12,15-17].

Besides lignocellulosic degradation products, fermentation products are also toxic to the fermenting microorganisms [18-20]. In addition to methyl propionate, intermediates such as 2-butanone, 2-butanol and ethyl acetate are also expected to be produced. 2-Butanone has been reported to decrease the cell density of *E. coli* and *S. cerevisiae* strains by 85% and 53%, respectively, for concentrations around 2.5% (v/v) [21]. The inhibiting effect of different butanol isomers on the growth of *S. cerevisiae* has also been investigated [22,23], and the studies report that the growth rate of *S. cerevisiae* is barely affected when growing in 2-butanol concentrations

up to 1.2% (v/v) [22]. Other inhibition studies have shown that the microbial growth of *K. marxianus* and *H. anomala* is totally inhibited by nearly 2.0% (v/v) ethyl acetate [20,24]. Surprisingly, the effect of methyl propionate on fermenting microorganisms has not yet been described.

The inhibition of microbial hosts by both lignocellulosic and fermentation products often leads to low yields and productivity, increasing product recovery and energy costs significantly [25]. As a result, the bio-based production cannot compete economically with the chemical synthesis. Therefore, finding a user-friendly tolerant host will enhance the productivity and promote the bio-based methyl ester production.

While *E. coli* has been widely used as platform microorganism for metabolic engineering regarding 2-butanone and butanol production [6,19,26-28], *S. cerevisiae* IMS0351 has already been identified as highly tolerant to alcohols [23], and *B. subtilis* has been recognized as a potential platform for biocommodity production from non-food biomass [29-31]. In this paper, the inhibition of these three potential hosts by lignocellulose degradation products, namely HMF, vanillin and syringaldehyde, and fermentation products, namely 2-butanol, 2-butanone, methyl propionate and ethyl acetate, has been assessed. Multiple inhibition assays were conducted on small scale cultures, using both shake flasks (SFs) and microtiter plates (MTPs). The maximum growth rates at high dilution and microbial lag-times were determined for each assay using the lag-time model proposed by Baranyi and Roberts [32]. The inhibitory thresholds were further assessed using known product-inhibition models [18,33,34]. Based on the results, this study ultimately evaluates the potential of each microbial host for recombinant solvent production, which can enable the bio-based production of methyl propionate.

2.2 Materials and Methods

2.2.1 Microbial strains and culture media

The laboratory strains *E. coli* K12 DH5α, *B. subtilis* NCCB 70064 and *S. cerevisiae* IMS0351 [23] were kindly provided by the Industrial Microbiology group, Delft University of Technology. Stock cultures were stored at -80°C in a mixture containing fermentation media and 20% glycerol.

The strains were grown in appropriate chemically-defined mineral media: *E. coli* and *B. subtilis* were grown in medium as in Cuellar *et al*. [35], and *S. cerevisiae* was grown in medium as in Verduyn *et al*. [36]. Fresh solutions were prepared aseptically immediately before each experiment, using 15 g L^{-1} glucose as carbon source. All the reagents used were analytical grade.

Prior to each inhibition assay, 100 mL fermentation medium was directly inoculated with cells taken from the frozen stocks, and incubated aerobically overnight at 200 rpm and appropriate temperature (37°C for *E. coli* and *B. subtilis*; 30°C for *S. cerevisiae*). Solutions of inhibiting agents i were prepared according to the concentrations C_i (g L^{-1}) depicted in the Results section. The reference stands for fresh fermentation medium without any inhibitor. The initial pH of each solution was adjusted using KOH (4 mol L^{-1}) and H_2SO_4 (2 mol L^{-1}), aiming at a pH 6.5 for *E. coli* and *B. subtilis*, and pH 4.5 for *S. cerevisiae*. The pH was not controlled during the experiments.

2.2.2 Inhibition assays in shake flasks

For manual growth measurements, 80 mL glass flasks were aseptically filled with 19 mL fresh fermentation medium containing inhibitor concentrations in the defined ranges. Each flask was inoculated with 1 mL aliquots from the overnight grown cultures to an initial OD_{600} of approximately 0.15. After inoculation, the flasks were sealed with pierceable rubber stoppers to prevent evaporation during sampling, and incubated at 150 rpm in an orbital shaker with 5 cm shaking diameter and suitable temperature (37°C±1°C for *E. coli* and *B. subtilis*; 30°C±1°C for *S. cerevisiae*). The mixing performance and oxygen transfer rate (OTR) were assessed using the correlations proposed by Maier and Büchs [37] and Klockner and Büchs [38], and a value of 7 mmol O_2 L^{-1} h^{-1} was found for the OTR under these conditions. The growth curves were determined by measuring the OD_{600} of each flask every 2 h during 14 h in a Biochrom Libra S11 Visible Spectrophotometer, and a final measurement was performed after 24 h. All the measurements were performed within the linear OD range of the instrument, using fresh fermentation medium for sample dilution when required. To determine whether evaporation or microbial consumption occurred throughout the experiments, the initial and final concentrations of the volatile inhibitors were determined via GC (Focus GC, InterScience, Thermo Electron), using an aqueous solution of 325 mg L^{-1} 1-pentanol as internal standard. Two independent experiments were run in duplicate.

2.2.3 Inhibition assays in microtiter plates

For growth measurements in microtiter plates, 392 µL Greiner 96 well MTPs with flat bottom and low evaporation lid were used. The wells were aseptically filled with 190 µL fresh fermentation medium containing inhibitor concentrations in the defined ranges. Each well was inoculated with 10 µL from the cultures grown overnight to an initial OD_{600} of approximately

0.15, and at least 16 replicates were used per condition. Given the large amount of conditions to be tested, three similar microplate readers were used: TECAN GENIos Pro, TECAN M200 Infinite Pro, and BioTek Synergy™ 2. The MTPs were incubated with orbital intermediate shaking at suitable temperature (37°C±1°C for *E. coli* and *B. subtilis*; 30°C±1°C for *S. cerevisiae*). The mixing performance and oxygen transfer rate were evaluated using the correlations suggested by Hermann *et al.* [39], and an OTR of 7 mmol O_2 L^{-1} h^{-1} was estimated for these operational conditions. The growth curves were determined by measuring the OD_{600} of each well every 15 min, during 24 h. All the measurements were performed within the linear OD range of the instrument. The data were exported from the microplate reader in ASCII format and further processed in Excel (Microsoft Office 2010).

2.2.4 Modeling the microbial growth rates and lag-times

The maximum growth rate μ_{max} (h^{-1}) and lag-time λ (h) are parameters typically used to characterize the kinetics of microbial growth. To assess these parameters, the lag-time model proposed by Baranyi and Roberts [32] has been used:

$$\frac{dx}{xdt} = \mu_{max}\, \alpha(t) f(x), \text{ with } x(t=0) = x_0 \quad (1)$$

In this model, x_0 (g L^{-1}) and x (g L^{-1}) are the initial and actual cell densities respectively, t (h) is the time, $\alpha(t)$ is the adjustment function delaying the transition from the lag-time to the exponential phase, and $f(x)$ is the inhibition function defining the transition of the curve to the stationary phase. As only data from the lag-phase and exponential growth phase have been considered in the present work, the inhibition function, where oxygen limitation plays a fundamental role, can be omitted. The adjustment function has been defined according to the literature [32,40]:

$$\alpha(t) = \frac{q_0}{q_0 + \exp(-\mu_{max} t)} \quad (2)$$

where q_0 quantifies the physiological viability of the inoculum for each specific environment. Baranyi and Roberts [32] linked this parameter to μ_{max} and λ according to:

$$q_0 = [\exp(\mu_{max}\lambda) - 1]^{-1} \quad (3)$$

As a result, the solution for equation 1 is:

$$x(t) = x_0 \left[1 + \exp\big(\mu_{max}(t-\lambda)\big) - \exp(-\mu_{max}\lambda)\right] \quad (4)$$

Parameter estimation in equation 4 was performed by iterative nonlinear regression using Matlab 2013b (Mathworks). The parameter dependency and sensitivity of Matlab's *lsqnonlin* function were inspected and minimized. The initial values for the parameters were chosen based on the experimental observations, and the measurement error in the initial cell density was tackled by estimating x_0 along with μ_{max} and λ. The upper bound for the regression, i.e. the transition of the growth curves to the stationary phase, was chosen based on visual inspection accounting for all the curves belonging to each strain–C_i dataset. As a result, data points beyond the linear part of the logarithmic growth curves were excluded from the fit. Simultaneous optimization was performed for each curve by minimizing the sum of squared residuals. The parameter q_0 was ultimately determined from μ_{max} and λ using equation 3. The average values of μ_{max}, λ, and $q_0$were determined for each dataset, and finally compared using Welch's unequal variance t-test, with a significance level of 5 % [41].

2.2.5 Modeling the microbial tolerance to product inhibition

Several mathematical models have been proposed to quantify product inhibition kinetics, focusing mainly on the inhibiting effect of alcohols [18,33], weak acids [34] and ethyl esters [20] on different microorganisms. These models have been extensively reviewed elsewhere [20,42,43]. In the present work three product-inhibition models (Table 1) were inspected, mainly for their simplicity and applicability regarding similar strains and inhibitors to those used herein.

Table 1 Product-inhibition models used to fit the experimental data

Type	Authors	Equation	#Eq.
linear	Dagley and Hinshelwood [33]	$\mu_{max} = \mu_{max,0}\left(1 - \frac{C_i}{C_{max,i}}\right)$	(5)
exponential	Aiba et al. [18]	$\mu_{max} = \mu_{max,0}\left[\exp\left(-\frac{C_i}{K_{exp,i}}\right)\right]$	(6)
hyperbolic	Quintas et al. [34]	$\mu_{max} = \mu_{max,0}\left(1 + \frac{C_i}{K_{hyp,i}}\right)^{-1}$	(7)

C_i (g L^{-1}) is the concentration of inhibiting agent in the fermentation medium, μ_{max} (h^{-1}) is the maximum growth rate observed in the presence of each C_i, $\mu_{max,0}$ (h^{-1}) is the maximum growth

rate in the absence of inhibitor, and $C_{max,i}$, $K_{exp,i}$ and $K_{hyp,i}$ are indicators of microbial tolerance, for which higher values denote a higher tolerance to the inhibitors. In the linear approach, $C_{max,i}$ (g L^{-1}) stands for the inhibitory threshold at which the microbial growth is completely inhibited, considering that $0 \leq C_i \leq C_{max,i}$ [33]. On the other hand, $K_{exp,i}$ (g L^{-1}) represents the inhibitory threshold in the exponential relation between the growth rate and the product concentration [18], and $K_{hyp,i}$ (g L^{-1}) represents the inhibitor concentration at which half of the rate of substrate consumption is used for cell maintenance rather than growth, as described by Quintas *et al.* [34] on the basis of cell energy requirements. Parameter estimation in equations 5 – 7 was performed by iterative nonlinear regression using the generalized reduced gradient (GRG) algorithm in Excel add-in Solver (Microsoft Office 2010). The initial values for the parameters were chosen based on the experimental observations, and the error in $\mu_{max,0}$ was tackled by estimating this parameter along with $C_{max,i}$, $K_{exp,i}$ or $K_{hyp,i}$. Simultaneous optimization was performed by minimizing the sum of weighted squared residuals (relative weighting), imposing the same $\mu_{max,0}$ for the whole set of inhibitors regarding each strain. The goodness of the fit was assessed based on the standard error of the estimate for each case, σ_i (%), and the microbial tolerance to the inhibitors was ultimately compared using the indicators provided by the model with the lowest overall weighted standard error of the estimate, σ_{est} (%).

2.3 Results

2.3.1 Inhibition assays in shake flasks

Although shake flasks are widely used as less expensive bioreactors for multiple tasks, manual flask sampling has been proved to disturb cell growth [44]. The sampling procedure was therefore limited to a sample every 2 h, allowing to gather sufficient data points to characterize the microbial growth. The concentration of volatile compounds in solution was consistent throughout the experiments, showing that no evaporation or microbial consumption occurred. Extreme cases were observed where none of the replicates grew at higher inhibitor concentrations, exhibiting extended lag-times ($\lambda > 24$ h), and unquantifiable growth rates. This precluded parameter regression using equation 4, and further calculation of q_0 in these cases. Apart from these occurrences, good fits were observed for the growth curves using the lag-time model. To facilitate the comprehension of the results, the maximum growth rates obtained for each strain–C_i dataset are presented as the ratio of μ_{max} to $\mu_{max,0}$. This is shown in Fig. 1a. The regressed lag-times λ for each case are shown in Fig. 1b. The standard errors determined from

two independent experiments are comparatively low, suggesting a good reproducibility (Fig. 1). For all the cases investigated, the microbial growth displayed a slowing trend with increasing inhibitor concentrations. The majority of the cases displayed a virtually linear relation between μ_{max} and the inhibitor concentration, with the striking exception of *B. subtilis*, for which this is only observed when growing in medium containing methyl propionate. The statistical analysis showed that all the strains were significantly affected by the inhibitors at their lowest concentrations, with the exception of *S. cerevisiae*, that was not significantly affected by ethyl acetate at 4.5 g L^{-1}, nor by 2-butanone or 2-butanol up to 8 g L^{-1}.

In these cases, a progressive inhibition of growth is suggested to occur with higher inhibitor concentrations. Strikingly, *S. cerevisiae* tolerated up to 18.1 g L^{-1} ethyl acetate, and grew in the presence of 16 g L^{-1} 2-butanol with a relative growth rate of 50%. In fact, this strain proved to have a higher tolerance for 2-butanol, methyl propionate and ethyl acetate when compared to the other strains, as its growth rates were affected to a lesser extent by higher inhibitor concentrations. Although *B. subtilis* could also tolerate up to 16 g L^{-1} 2-butanol, the growth rate was only about 20% of that without any inhibitor. Both *S. cerevisiae* and *B. subtilis* exhibited similar tolerance to 2-butanone up to 16 g L^{-1}.

Among the fermentation products, methyl propionate had the most severe impact, resulting in complete inhibition of all the strains when exposed to 18.1 g L^{-1}. Regarding the lignocellulose-derived products, these revealed a high inhibitory activity, as none of the strains grew in product concentrations of 2.0 g L^{-1}. *S. cerevisiae* and *E. coli* showed comparable tolerance regarding HMF and syringaldehyde, growing in concentrations up to 1.5 g L^{-1}. On the other hand, *B. subtilis* could not grow in syringaldehyde concentrations higher than 0.5 g L^{-1}. Vanillin was the most inhibiting for the yeast, reducing its growth rate by 95% at 1.5 g L^{-1}.

Regarding the lag-times (Fig. 1b), although these were expected to increase with inhibiting concentrations, we failed to find a clear trend in the behavior of the strains. Longer λ (h) were indeed observed for all the strains when growing in the presence of increased concentrations of 2-butanone, methyl propionate, vanillin and syringaldehyde. However, *B. subtilis* and *E. coli* were clearly more affected than yeast by 2-butanol, ethyl acetate, and HMF at high concentrations. Strikingly, *E. coli* presented $\lambda > 24$ h for the highest concentrations of all the inhibitors tested, suggesting its higher sensitivity when compared to the other microbial hosts. Recalling equation 3, the parameters μ_{max}, λ and q_0 are intertwined, and thus the physiological viability of a culture growing in a specific test condition depends on the growth rate and lag-time

observed in that condition only. As a result, no direct relation was found between the inhibitor concentration and the values of q_0 (data not shown).

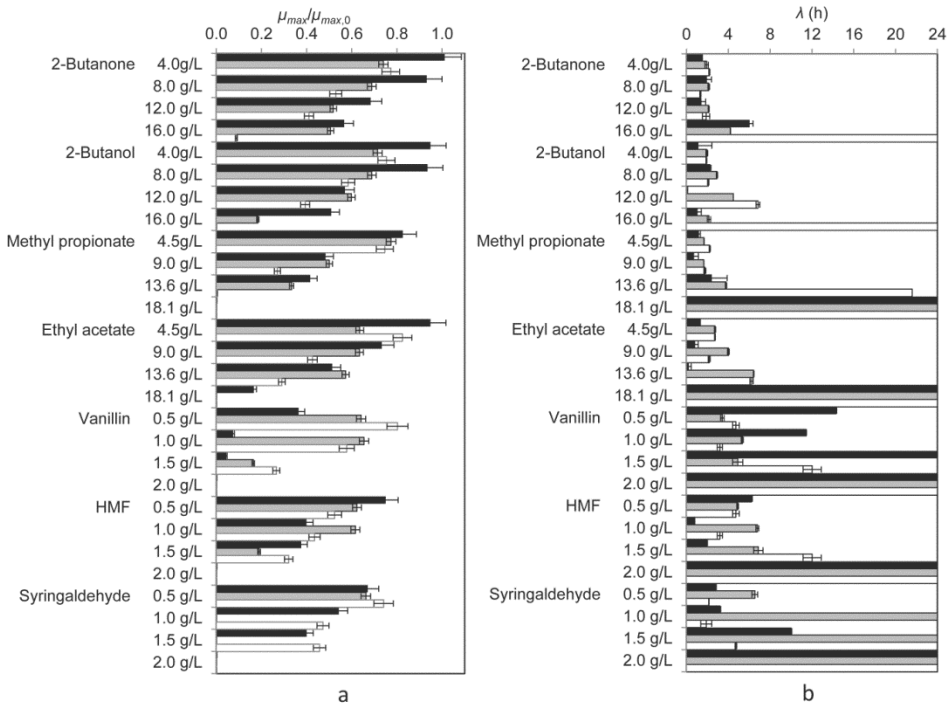

Fig. 1 Kinetic parameters of microbial growth determined from inhibition assays in shake flasks with *S. cerevisiae* (■), *B. subtilis* (□), and *E. coli* (▨) growing in defined mineral media containing different concentrations of inhibitors: (a) Ratios of the maximum growth rates observed in the presence of inhibitors (μ_{max}) to those observed in the absence of inhibitor ($\mu_{max,0}$) and (b) lag-times (λ); error bars represent standard errors

2.3.2 Inhibition assays in microtiter plates

Fig. 2 shows some examples of worst-case model fittings for the growth of *B. subtilis* in different concentrations of 2-butanol, both in MTPs and shake flasks. It is clear from Fig. 2a that the cells experienced oxygen limitation in the MTPs, as the slopes of the curves declined slightly before the stationary phase was reached. This was not observed in the growth curves in shake flasks (Fig. 2b). The upper bounds chosen for the regression analysis of MTP data accounted for this observation, as shown by the dotted line representing the upper bound for the reference fermentation, and the dashed line for the other conditions, in Fig. 2a.

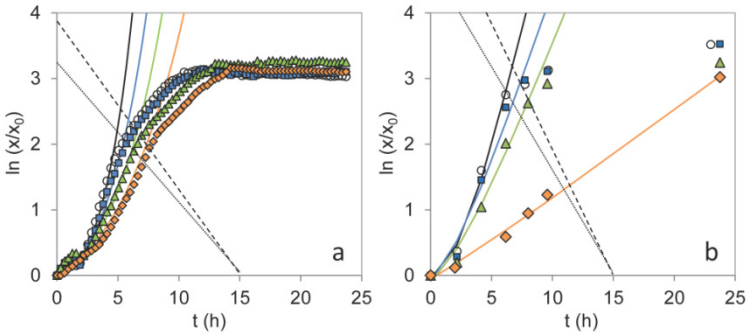

Fig. 2 Comparative example of upper bounds in model fitting: logarithmic growth curves of *B. subtilis* measured in (a) MTPs and (b) shake flasks, in the absence (circles) and in the presence of 4 g L^{-1} (squares), 8 g L^{-1} (triangles) and 16 g L^{-1} (diamonds) 2-butanol; markers represent experimental data, full lines represent model predictions, dotted line represents upper bound chosen in the absence of 2-butanol, dashed line represents upper bound chosen for the remaining conditions

The same upper bound was used for different conditions in this particular case. In general, the experimental growth curves were well fitted by the simplified lag-time model, based on the average fitting deviation of 7.4%. Nevertheless, great well-to-well disparity was observed for replicates within the same datasets, not only in the presence, but also in the absence of inhibitors. The average variation found for μ_{max} was 13.7% with a general increasing trend for increasing C_i, much higher than that observed amid the replicates of shake flasks (5.4%). As an attempt to verify the similarity between the assays, the average $\mu_{max,0}$ values estimated for each strain were compared using Welch's t-test, and the outcome is presented in Table 2.

Table 2 Maximum growth rates of *S. cerevisiae*, *B. subtilis*, and *E. coli* in defined mineral media without inhibitor ($\mu_{max,0}$), determined from experimental shake flask and MTP data

	$\mu_{max,0}$ (h^{-1})	
	SF	MTP
S. cerevisiae	0.34±0.01	0.35±0.06
B. subtilis	0.76±0.02	0.8±0.2
E. coli	0.7±0.1	0.6±0.1

The $\mu_{max,0}$ values observed for *S. cerevisiae* and *B. subtilis* were identical in both assays at a significance level of 5%, while the $\mu_{max,0}$ values of *E. coli* were identical at a significance level of 10%. This suggests that the cultivation conditions were fairly identical in both assays. However, when comparing the estimated μ_{max}, considerable discrepancies were found, and the validation of the automated growth assay failed for the present case, as no correlation was found for any

of the strains investigated. To address this matter, we investigated potential causes for well-to-well variability in the MTPs.

In this work, the shaking mode was normalized for all the strains based on the calculated OTR, and identical growth rates were obtained for a minimum of 16 replicates growing in reference medium (Fig. 3), indicating the low impact of the shaking mode on the growth reproducibility. Noticeably, a significant variability was observed for *B. subtilis* and *E. coli* at higher cell densities (Fig. 3b and 3c, respectively), which was not observed in *S. cerevisiae*. Overall, *S. cerevisiae* had the lowest well-to-well variation, 9.5%, while *B. subtilis* and *E. coli* had average variations of 15.3% and 15.9%, respectively. This suggests that the operational temperature also plays a role in the reproducibility of the results in MTPs. In fact, the microtiter wells were clearly affected by evaporation and cell sedimentation, especially at 37°C. As an attempt to determine the influence of evaporation on the optical density measurements, the optical density of water at 999 nm (OD_{999}) was monitored at 37°C during 24 h. The rates of evaporation were observed to vary strikingly depending on the well position, as the values of OD_{999} on the outer rows of the MTP decreased within a range of 15 – 100%. Additionally, the evaporation of 2-butanol and methyl propionate, two volatile compounds with distinct boiling points of 100°C and 80°C respectively, was examined at 30°C and 37°C. The evaporation rate of these compounds, γ_i (g $L^{-1}h^{-1}$), was modelled according to $\gamma_i = k_s a \cdot C_i$ [45], where $k_s a$ (h^{-1}) is the evaporation rate constant. At 30°C, the evaporation rate of 2-butanol was nearly unquantifiable after 24 hours, while the $k_s a$ value of methyl propionate was 0.0433±0.0005 h^{-1}. At 37°C, the $k_s a$ values increased significantly to 0.00638±0.00002 h^{-1} for 2-butanol, and 0.073±0.003 h^{-1} for methyl propionate. It is clear that the evaporation rate not only depends on temperature, but also on the volatile concentration and thus on the evaporation rate of water, varying with the well position in the MTP. Aware of these occurrences, attempts were made to prevent evaporation by filling the outer positions of the MTPs with distilled water, and using special covers for 96 MTPs (Enzyscreen low-evaporation sandwich covers). Unfortunately, the results obtained at such conditions were analogous to the previous experiments. Another curious observation was the enhanced turbidity in wells containing higher concentrations of 2-butanone, methyl propionate and ethyl acetate, which significantly increased the OD_{600} values in these cases. This was also observed in control wells without cells, indicating some sort of reactivity. Although these products have been reported as good solvents for polystyrene [46,47], swelling and dissolution of the polymer is a slow process that has only been observed in the presence of pure compounds, and thus it was not expected to happen in these dilute aqueous solutions.

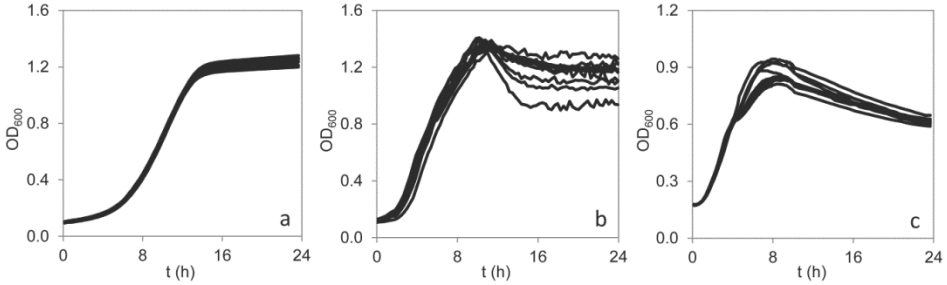

Fig. 3 Experimental growth curves of (a) *S. cerevisiae*, (b) *B. subtilis*, and (c) *E. coli* in defined mineral media without inhibitor, measured in MTP with orbital intermediate shaking at suitable temperature (37°C±1°C for *E. coli* and *B. subtilis*; 30°C±1°C for *S. cerevisiae*)

2.3.3 Microbial tolerance to product inhibition

Due to the perceived uncertainty in the MTP assay, the tolerance of each strain to the inhibitors was assessed using the shake flask data exclusively. The correlation between the experimental data and the predicted values of μ_{max} using the product-inhibition models described in equations 5 – 7 is shown in Fig. 4, accounting for all the strains and inhibitors investigated. A good correlation was found between the observed microbial growth rates of the strains and those estimated using the linear model (Fig. 4a). Comparatively, and although the majority of the observations lies within a ±20% deviation, the exponential and the hyperbolic models (Fig. 4b and Fig. 4c, respectively) under-predicted the microbial growth for a considerable number of cases.

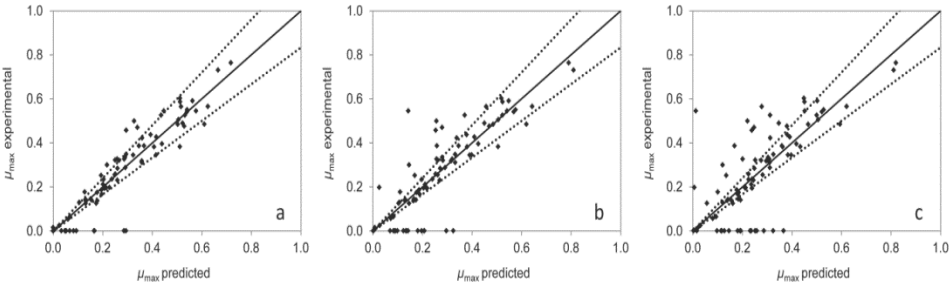

Fig. 4 Parity plot showing the maximum growth rates (μ_{max}) determined from experimental shake flask data, against those predicted by the (a) linear model, (b) exponential model and (c) hyperbolic model; full line $x = y$ added as reference; dotted lines represent a standard error of ± 20%

The predictability of the models for each inhibitor was inspected by looking at the overall standard errors of the estimates, σ_{est} (%), accounting for the individual fits obtained for each strain. The results are presented in Table 3, and also depict what is shown in Fig. 4: the model proposed by Dagley and Hinshelwood [33] exhibited the lowest standard errors, and allowed

better predictions for the effect of all the inhibitors on the strains. Two-parameter models have been reported to outperform the simple one-parameter models tested herein, when describing the growth inhibition of *K. marxianus* by ethyl acetate [20]. These models account for an additional regression parameter n, whose magnitude determines whether the inhibition trend is linear (n = 1), progressive (n > 1) or declining (n < 1). For the sake of comparison, the experimental shake flask data were fitted using the progressive model proposed by Luong [48]. The parameter estimation and goodness of fit were assessed using the same approach as previously described. The standard errors of the estimates found when fitting the data with the progressive model were slightly lower, but analogous to those determined for the simpler linear model. The fit of both models was thus compared by means of a model reduction test (F test), where the improvement of adding the extra parameter in the progressive model was quantified as the difference in the resulting sum-of-squares.

Table 3 Overall standard error of the estimates σ_{est} (%) for the predictions by each product-inhibition model; the lowest σ_{est} (%) indicate the best fits to shake flask experimental data

	σ_{est} (%)		
Model	Linear	Exponential	Hyperbolic
#Eq.	(5)	(6)	(7)
2-Butanone	11.8	20.0	29.0
2-Butanol	13.9	17.9	22.7
Methyl propionate	10.8	34.4	41.2
Ethyl acetate	16.2	20.5	27.0
Vanillin	17.8	19.9	31.2
HMF	18.0	19.2	20.0
Syringaldehyde	10.4	12.1	10.5

The p-values calculated using this approach were much higher than the traditional value of 0.05 (0.8, 0.6 and 0.5 for the fittings of *B. subtilis*, *E. coli* and *S. cerevisiae*, respectively), showing that it is not statistically significant to add a parameter, and thus complexity, to the product-inhibition model used. Based on these observations, the indicators of microbial tolerance $C_{max,i}$ estimated using the linear model were chosen for further comparison amongst the strains. The results are depicted in Table 4, where the individual standard errors of the estimates σ_i (%) are also presented. All the estimates show standard errors lower than 20%, with rare exceptions: the effect of vanillin on the growth of *S. cerevisiae* and the effect of HMF on the growth of *E. coli*, which were better described by the exponential model ($\sigma_i = 15.4\%$) and hyperbolic model

($\sigma_i = 10.9\%$), respectively. Based on the Welch's test results, *S. cerevisiae* and *B. subtilis* are significantly more tolerant than *E. coli* to 2-butanone, methyl propionate and ethyl acetate.

In fact, the thresholds predicted for *S. cerevisiae* are higher than those of *B. subtilis* for all the fermentation products, with the exception of ethyl acetate. On the other hand, the threshold concentrations found for the lignocellulose-derived products are comparable regarding all the strains, although *E. coli* is slightly more tolerant to vanillin.

Table 4 Inhibitor concentrations at which the microbial growth is completely inhibited ($C_{max,i}$, g L^{-1}), estimated from experimental data (shake flasks) using the linear product-inhibition model; σ_i (%) are the standard errors of the estimates

	S. cerevisiae	σ_i (%)	*B. subtilis*	σ_i (%)	*E. coli*	σ_i (%)
2-Butanone	45 ± 17	11.4	31 ± 6	9.1	17.8 ± 0.4	14.4
2-Butanol	36 ± 9	12.6	20 ± 1	18.7	21 ± 3	6.5
M. propionate	23 ± 5	11.6	21 ± 2	6.0	13.68 ± 0.02	13.4
E. acetate	22 ± 1	19.6	30 ± 8	14.6	19 ± 2	12.6
Vanillin	1.08 ± 0.02	22.9	1.84 ± 0.08	18.3	2.2 ± 0.2	12.0
HMF	2.2 ± 0.3	18.0	1.9 ± 0.1	15.7	2.2 ± 0.2	20.1
Syringaldehyde	2.5 ± 0.5	8.2	2 ± 1	6.0	2.7 ± 0.4	13.7

Interestingly, when comparing the data in Table 4 with the observations presented in Fig. 1, the thresholds predicted for *B. subtilis* regarding ethyl acetate appear to be overestimated, as this strain was unable to grow in 18 g L^{-1} ethyl acetate. This might be justified by an apparent lag of inhibition at low ester concentrations, which has also been observed for *K. marxianus* [20]. Overall, the results in Table 4 are in agreement with previous studies reporting that inhibition thresholds strongly depend on the microbial strain and inhibitor tested [12].

2.4 Discussion

2.4.1 The limited applicability of microtiter plates in the present study

In a growth tolerance assay, the inhibitors in the fermentation medium impose a continuous stress on the cells. Under these circumstances, the cells are expected to adapt while growing, which leads to a differential expression of the genes required for growth, and thus great variation is expected in latency times and maximum growth rates [23,49]. However, in the present work we noticed that the variance found in the MTP assay, not observed in the shake flasks, was mostly related to technical issues instead of intraspecies variability. Many advances have been

reported concerning MTP bioreactors for rapid and reliable bioprocess development [38,44,50,51]. However, as cells grow under suboptimal conditions, such as inhibiting environments, they might experience apoptosis resulting in cell adhesion and aggregates, ultimately disturbing the cell density measurements [52]. To reduce cell sedimentation and enhance growth reproducibility, the shaking mode of MTP readers has been optimized by some researchers [51,53]. The optimal shaking mode varied depending on the strain [53], and good reproducibility has only been achieved when intermittent shaking modes were used [51,53]. This leads to different operational conditions for each strain, which becomes unfeasible when several strains are to be compared under the same circumstances. The evaporation observed in this work also promoted a trendless well-to-well variability. Gonzalez-Ramos *et al*. [23] reported 50% 1-butanol evaporation in unsealed MTPs, and reduced this to 10% by sealing the plates with a gas-impermeable film that also prevented aeration. In this case, a micro-aerobic instead of a fully anaerobic environment was desired, which led us to avoid this approach. Despite the efforts to correct the optical density based on water evaporation, great discrepancy was still observed. The vapor pressures of aqueous mixtures of 2-butanone, 2-butanol, methyl propionate and ethyl acetate are higher than those of the pure compounds, depending on the temperature and mixture concentration at ambient pressure. Thus, the evaporation rates of water and inhibitors varied with the concentrations investigated and working temperatures in the MTPs. While the volatile products would easily evaporate along with water resulting in unknown medium concentrations, the lignocellulose-derived inhibitors would become more concentrated as water evaporated, leading to their sedimentation along with the dead cells. None of these issues was observed in the shake flasks, since these could be properly sealed without compromising micro-aeration. Given all these reasons, and opposed to what has been achieved by other researchers [34,54,55], the observations made in shake flask tests could not be fairly validated in MTPs. The datasets provided by the MTPs facilitated the model fitting and parameter estimation with small residuals and errors; however, the technical issues encountered could have led to severe misinterpretation of the collected data.

2.4.2 Quantification of inhibition on microbial growth rates

The simplified lag-time model proved to be a useful and reliable tool to describe the experimental growth curves of the strains in the presence of all the inhibitors investigated. Similarly to what has been previously reported in microbial growth studies [49], no linear

correlation was found between μ_{max} and λ for any of the strains (R^2 = 0.66 for *S. cerevisiae*, R^2 = 0.76 for *E. coli*, and R^2 = 0.72 for *B. subtilis*). As a result, no correlation was found between the parameters and the physiological viability of the inoculum. It is known that the lag-phase estimation is greatly influenced by the technique used to monitor bacterial growth [40]. In the present case, the observed lag-phase duration results not only from the adaptation of the microbial hosts to the adverse environment, but also from the death of a fraction of cells that could not survive the inhibition, followed by growth of the enduring cells. The OD growth measurements accounted for both living and dead cells, which can mask the lag-phase duration. This fact is supported by Swinnen *et al*. [49], who reported that the actual lag of enduring cells is significantly shorter than that detected by OD measurements.

The linear product-inhibition model was an important tool to predict critical concentrations of inhibitors, allowing a fair comparison of inhibitory thresholds amid the strains investigated. The exponential and hyperbolic models, on the other hand, tended to predict a declining inhibition with increasing inhibitor concentrations. In the present work, this trend has been mostly observed for *S. cerevisiae* and *E. coli* growing in medium containing vanillin and HMF, respectively. A progressive model could have also been used to predict the effect of the inhibitors on the strains, but we proved that the results were not significantly improved by this approach. Overall, the results showed that *S. cerevisiae* and *B. subtilis* are comparatively more tolerant than *E. coli* to the fermentation products tested, namely 2-butanone, methyl propionate, and ethyl acetate. *S. cerevisiae* revealed the highest critical concentration for 2-butanol, which might be explained by the fact that this strain is a spontaneous mutant resulting from an evolved population growing under increased 1-butanol concentrations, which could also grow in approximately 3% (v/v) 2-butanol [23]. The threshold estimated for 2-butanol in the present study, 36 ± 9 g L^{-1}; is in agreement with this observation. Methyl propionate had a severe impact on the strains, resulting in complete inhibition of all the strains when exposed to the highest concentration tested. This is clear from Table 4, where the critical concentration values have been estimated as 23 ± 5 g L^{-1}, 21 ± 2 g L^{-1} and 13.68 ± 0.02 g L^{-1} for *S. cerevisiae*, *B. subtilis* and *E. coli* respectively. Strikingly, the thresholds determined for ethyl acetate were higher than that previously reported for *K. marxianus* (17 g L^{-1}) [20]. Despite the fact that ethyl acetate is an isomer of methyl propionate, the strains were slightly more tolerant to this ester, which is also demonstrated by the values in Table 4. This might be related to the different hydrophobicity of the isomers, since it has been suggested that more hydrophobic compounds would be expected to easily permeate microbial membranes, exhibiting an increased toxicity [56].

In fact, methyl propionate exhibits a more hydrophobic behavior, since its $log\ P_{oct/water}$ is higher than that of ethyl acetate (0.82 versus 0.73, respectively) [57,58]. The fact that certain organisms are able to metabolize ethyl acetate, namely *H. anomala* [24] might also enhance the microbial tolerance to this inhibitor. Nevertheless, our observations are insufficient to explain this behavior herein.

Among the lignocellulosic degradation products tested, vanillin had the most severe effect on yeast, which could barely tolerate 1.5 g L^{-1} of inhibitor. Although this observation is in agreement with what has been previously reported by Delgenes *et al*. [59], the yeast tolerance observed for syringaldehyde in the present study is remarkably higher than that reported by the same author: 40% of the reference growth rate against 19% for a concentration of 1.5 g L^{-1}. All the strains depicted analogous values for the threshold concentrations regarding HMF and syringaldehyde. However, and opposed to what has been reported [12], none of the strains investigated in this work showed significant growth in medium containing lignocellulosic product concentrations of 2.0 g L^{-1}.

Overall, based on the observed growth rates and lag-times, *S. cerevisiae* was slightly more tolerant than the other strains to the majority of the inhibitors, having great potential to be engineered and further established as host for the bio-based production of methyl esters. Even though *B. subtilis* showed similar tolerance to some of the inhibitors investigated, namely 2-butanone, methyl propionate, ethyl acetate, HMF and syringaldehyde, the lag-times observed were recurrently higher than those of *S. cerevisiae*. Additionally, it must be recalled that this strain is not as robust in microaerobic environments [60]. The *S. cerevisiae* IMS0351 used in the present study proves that evolutionary methods, such as natural selection and evolutionary dynamics, are highly valuable to improve inhibitor tolerance [23]. Repetitive growth under increasing inhibitor concentrations might be a promising and effective technique to further enhance inhibitor tolerance in *S. cerevisiae* IMS0351, and accelerate the methyl propionate bio-based production.

2.5 Acknowledgments

The authors would like to acknowledge Max Zomerdijk, Stef van Hateren, Rosario Medici, Linda Otten, Luuk van der Wielen, Ton van Maris and Walter van Gulik for their advice and analytical support.

2.6 References

(1) Kent, J. A. *Handbook of Industrial Chemistry and Biotechnology: Volume 1 and 2*, Springer, New York, 2013.

(2) Ceh: Methyl Methacrylate. chemical.ihs.com/CEH/Public/Reports/674.4500/.

(3) Li, B.; Yan, R.; Wang, L.; Diao, Y.; Li, Z.; Zhang, S. Synthesis of Methyl Methacrylate by Aldol Condensation of Methyl Propionate with Formaldehyde over Acid–Base Bifunctional Catalysts. *Catal. Lett.* **2013**, *143*, 829-838.

(4) Shreiber, E. H.; Mullen, J. R.; Gogate, M. R.; Spivey, J. J.; Roberts, G. W. Thermodynamics of Methacrylate Synthesis from Methanol and a Propionate. *Ind. Eng. Chem. Res.* **1996**, *35*, 2444-2452.

(5) van Beek, H. L.; Winter, R. T.; Eastham, G. R.; Fraaije, M. W. Synthesis of Methyl Propanoate by Baeyer-Villiger Monooxygenases. *Chem. Commun.* **2014**, *50*, 13034–13036.

(6) Yoneda, H.; Tantillo, D. J.; Atsumi, S. Biological Production of 2-Butanone in *Escherichia Coli. ChemSusChem* **2014**, *7*, 92–95.

(7) Ghiaci, P.; Norbeck, J.; Larsson, C. 2-Butanol and Butanone Production in *Saccharomyces Cerevisiae* through Combination of a B12 Dependent Dehydratase and a Secondary Alcohol Dehydrogenase Using a Tev-Based Expression System. *PLoS One* **2014**, *9*, e102774.

(8) Straathof, A. J. J. Transformation of Biomass into Commodity Chemicals Using Enzymes or Cells. *Chem. Rev.* **2014**, *114*, 1871–1908.

(9) Eriksson, K. E. L.; Bermek, H. Lignin, Lignocellulose, Ligninase, in: *Encyclopedia of Microbiology;* Schaechter, M., (Eds.); Oxford, 2009, pp 373-384.

(10) Du, B.; Sharma, L. N.; Becker, C.; Chen, S. F.; Mowery, R. A.; van Walsum, G. P.; Chambliss, C. K. Effect of Varying Feedstock-Pretreatment Chemistry Combinations on the Formation and Accumulation of Potentially Inhibitory Degradation Products in Biomass Hydrolysates. *Biotechnol. Bioeng.* **2010**, *107*, 430-40.

(11) Ibraheem, O.; Ndimba, B. K. Molecular Adaptation Mechanisms Employed by Ethanologenic Bacteria in Response to Lignocellulose-Derived Inhibitory Compounds. *Int J Biol Sci* **2013**, *9*, 598-612.

(12) van der Pol, E.; Bakker, R.; Baets, P.; Eggink, G. By-Products Resulting from Lignocellulose Pretreatment and Their Inhibitory Effect on Fermentations for (Bio)Chemicals and Fuels. *Appl. Microbiol. Biotechnol.* **2014**, *98*, 9579-9593.

(13) Jönsson, L. J.; Alriksson, B.; Nilvebrant, N.-O. Bioconversion of Lignocellulose: Inhibitors and Detoxification. *Biotechnol. Biofuels* **2013**, *6*, 16-16.

(14) Luo, C.; Brink, D. L.; Blanch, H. W. Identification of Potential Fermentation Inhibitors in Conversion of Hybrid Poplar Hydrolyzate to Ethanol. *Biomass Bioenergy* **2002**, *22*, 125-138.

(15) Larsson, S.; Quintana-Sainz, A.; Reimann, A.; Nilvebrant, N. O.; Jonsson, L. J. Influence of Lignocellulose-Derived Aromatic Compounds on Oxygen-Limited Growth and Ethanolic Fermentation by *Saccharomyces Cerevisiae. Appl. Biochem. Biotechnol.* **2000**, *84-86*, 617-32.

(16) Pienkos, P.; Zhang, M. Role of Pretreatment and Conditioning Processes on Toxicity of Lignocellulosic Biomass Hydrolysates. *Cellulose* **2009**, *16*, 743-762.

(17) Wierckx, N.; Koopman, F.; Ruijssenaars, H. J.; de Winde, J. H. Microbial Degradation of Furanic Compounds: Biochemistry, Genetics, and Impact. *Appl. Microbiol. Biotechnol.* **2011**, *92*, 1095-105.

(18) Aiba, S.; Shoda, M.; Nagatani, M. Kinetics of Product Inhibition in Alcohol Fermentation. *Biotechnol. Bioeng.* **1968**, *10*, 845-64.

(19) Kanno, M.; Katayama, T.; Tamaki, H.; Mitani, Y.; Meng, X.-Y.; Hori, T.; Narihiro, T.; Morita, N.; Hoshino, T. et al. Isolation of Butanol- and Isobutanol-Tolerant Bacteria and Physiological Characterization of Their Butanol Tolerance. *Appl. Environ. Microbiol.* **2013**, *79*, 6998-7005.

(20) Urit, T.; Manthey, R.; Bley, T.; Löser, C. Formation of Ethyl Acetate by *Kluyveromyces Marxianus* on Whey: Influence of Aeration and Inhibition of Yeast Growth by Ethyl Acetate. *Eng. Life Sci.* **2013**, *13*, 247-260.

(21) Burk, M. J.; Pharkya, P.; Burgard, A. P. Microorganisms for the Production of Methyl Ethyl Ketone and 2-Butanol. U.S. Patent 20100184173, 2010.

(22) Ghiaci, P.; Norbeck, J.; Larsson, C. Physiological Adaptations of *Saccharomyces Cerevisiae* Evolved for Improved Butanol Tolerance. *Biotechnol. Biofuels* **2013**, *6*, 101.

(23) Gonzalez-Ramos, D.; van den Broek, M.; van Maris, A. J.; Pronk, J. T.; Daran, J. M. Genome-Scale Analyses of Butanol Tolerance in *Saccharomyces Cerevisiae* Reveal an Essential Role of Protein Degradation. *Biotechnol. Biofuels* **2013**, *6*, 48.

(24) Tabachnick, J.; Joslyn, M. A. Formation of Esters by Yeast. Ii. Investigations with Cellular Suspensions of *Hansenula Anomala. Plant Physiol* **1953**, *28*, 681-692.

(25) Oudshoorn, A.; van den Berg, C.; Roelands, C. P. M.; Straathof, A. J. J.; van der Wielen, L. A. M. Short-Cut Calculations for Integrated Product Recovery Options in Fermentative Production of Bio-Bulk Chemicals. *Process Biochem.* **2010**, *45*, 1605-1615.

(26) Reyes, L. H.; Almario, M. P.; Winkler, J.; Orozco, M. M.; Kao, K. C. Visualizing Evolution in Real Time to Determine the Molecular Mechanisms of N-Butanol Tolerance in *Escherichia Coli. Metab. Eng.* **2012**, *14*, 579-90.

(27) Atsumi, S.; Cann, A. F.; Connor, M. R.; Shen, C. R.; Smith, K. M.; Brynildsen, M. P.; Chou, K. J.; Hanai, T.; Liao, J. C. Metabolic Engineering of *Escherichia Coli* for 1-Butanol Production. *Metab. Eng.* **2008**, *10*, 305-311.

(28) Atsumi, S.; Liao, J. C. Metabolic Engineering for Advanced Biofuels Production from *Escherichia Coli. Curr. Opin. Biotechnol.* **2008**, *19*, 414-9.

(29) Anderson, T. D.; Miller, J. I.; Fierobe, H. P.; Clubb, R. T. Recombinant *Bacillus Subtilis* That Grows on Untreated Plant Biomass. *Appl. Environ. Microbiol.* **2013**, *79*, 867-76.

(30) Kataoka, N.; Tajima, T.; Kato, J.; Rachadech, W.; Vangnai, A. Development of Butanol-Tolerant *Bacillus Subtilis* Strain Grsw2-B1 as a Potential Bioproduction Host. *AMB Express* **2011**, *1*, 10-10.

(31) Zhang, X.-Z.; Zhang, Y.-H. P. One-Step Production of Biocommodities from Lignocellulosic Biomass by Recombinant Cellulolytic *Bacillus Subtilis*: Opportunities and Challenges. *Eng Life Sci* **2010**, *10*, 398-406.

(32) Baranyi, J.; Roberts, T. A. A Dynamic Approach to Predicting Bacterial Growth in Food. *Int J Food Microbiol* **1994**, *23*, 277-94.

(33) Dagley, S.; Hinshelwood, C. N. Physicochemical Aspects of Bacterial Growth. Part Iii. Influence of Alcohols on the Growth of *Bact. Lactis Aerogenes. J. Chem. Soc.* **1938**, 1942-1948.

(34) Quintas, C.; Leyva, J. S.; Sotoca, R.; Loureiro-Dias, M. C.; Peinado, J. M. A Model of the Specific Growth Rate Inhibition by Weak Acids in Yeasts Based on Energy Requirements. *Int J Food Microbiol* **2005**, *100*, 125-130.

(35) Cuellar, M. C.; Zijlmans, T. W.; Straathof, A. J. J.; Heijnen, J. J.; van der Wielen, L. A. M. Model-Based Evaluation of Cell Retention by Crossflow Ultrafiltration During Fed-Batch Fermentations with *Escherichia Coli. Biochem. Eng. J.* **2009**, *44*, 280-288.

(36) Verduyn, C.; Postma, E.; Scheffers, W. A.; Van Dijken, J. P. Effect of Benzoic Acid on Metabolic Fluxes in Yeasts: A Continuous-Culture Study on the Regulation of Respiration and Alcoholic Fermentation. *Yeast* **1992**, *8*, 501-17.

(37) Maier, U.; Büchs, J. Characterisation of the Gas–Liquid Mass Transfer in Shaking Bioreactors. *Biochem. Eng. J.* **2001**, *7*, 99-106.

(38) Klockner, W.; Buchs, J. Advances in Shaking Technologies. *Trends Biotechnol* **2012**, *30*, 307-14.

(39) Hermann, R.; Lehmann, M.; Büchs, J. Characterization of Gas–Liquid Mass Transfer Phenomena in Microtiter Plates. *Biotechnol. Bioeng.* **2003**, *81*, 178-186.

(40) Baty, F.; Delignette-Muller, M. L. Estimating the Bacterial Lag Time: Which Model, Which Precision? *Int J Food Microbiol* **2004**, *91*, 261-77.

(41) Welch, B. L. The Significance of the Difference between Two Means When the Population Variances Are Unequal. *Biometrika* **1938**, *29*, 350-362.

(42) Han, K.; Levenspiel, O. Extended Monod Kinetics for Substrate, Product, and Cell Inhibition. *Biotechnol. Bioeng.* **1988**, *32*, 430-47.

(43) Mulchandani, A.; Luong, J. H. T. Microbial Inhibition Kinetics Revisited. *Enzyme Microb. Technol.* **1989**, *11*, 66-73.

(44) Büchs, J. Introduction to Advantages and Problems of Shaken Cultures. *Biochem. Eng. J.* **2001**, *7*, 91-98.

(45) Truong, K. N.; Blackburn, J. W. The Stripping of Organic Chemicals in Biological Treatment Processes. *Environ. Prog.* **1984**, *3*, 143–152.

(46) Brown, W.; Fundin, J. Dynamical Behavior of High Molecular Weight Polystyrene in the Marginal Solvent 2-Butanone. *Macromolecules* **1991**, *24*, 5171-5178.

(47) Imre, A.; Van Hook, W. A. Liquid–Liquid Demixing from Solutions of Polystyrene. 1. A Review. 2. Improved Correlation with Solvent Properties. *J Phys Chem Ref Data* **1996**, *25*, 637-661.

(48) Luong, J. H. T. Kinetics of Ethanol Inhibition in Alcohol Fermentation. *Biotech. Bioeng.* **1985**, *27*, 280-285.

(49) Swinnen, S.; Fernandez-Nino, M.; Gonzalez-Ramos, D.; van Maris, A. J.; Nevoigt, E. The Fraction of Cells That Resume Growth after Acetic Acid Addition Is a Strain-Dependent Parameter of Acetic Acid Tolerance in *Saccharomyces Cerevisiae. FEMS Yeast Res.* **2014**, *14*, 642-53.

(50) Funke, M.; Buchenauer, A.; Mokwa, W.; Kluge, S.; Hein, L.; Muller, C.; Kensy, F.; Buchs, J. Bioprocess Control in Microscale: Scalable Fermentations in Disposable and User-Friendly Microfluidic Systems. *Microb. Cell Fact.* **2010**, *9*, 86.

(51) Jung, P. P.; Christian, N.; Kay, D. P.; Skupin, A.; Linster, C. L. Protocols and Programs for High-Throughput Growth and Aging Phenotyping in Yeast. *PLoS ONE* **2015**, *10*, e0119807.

(52) Reinhart, D.; Damjanovic, L.; Kaisermayer, C.; Kunert, R. Benchmarking of Commercially Available Cho Cell Culture Media for Antibody Production. *Appl Microbiol Biotechnol* **2015**, *99*, 4645-57.

(53) Warringer, J.; Blomberg, A. Automated Screening in Environmental Arrays Allows Analysis of Quantitative Phenotypic Profiles in *Saccharomyces Cerevisiae. Yeast* **2003**, *20*, 53-67.

(54) Chaturvedi, K.; Sun, S. Y.; O'Brien, T.; Liu, Y. J.; Brooks, J. W. Comparison of the Behavior of Cho Cells During Cultivation in 24-Square Deep Well Microplates and Conventional Shake Flask Systems. *Biotechnol. Rep.* **2014**, *1–2*, 22-26.

(55) Huber, R.; Scheidle, M.; Dittrich, B.; Klee, D.; Buchs, J. Equalizing Growth in High-Throughput Small Scale Cultivations Via Precultures Operated in Fed-Batch Mode. *Biotechnol. Bioeng.* **2009**, *103*, 1095-102.

(56) Zaldivar, J.; Ingram, L. O. Effect of Organic Acids on the Growth and Fermentation of Ethanologenic *Escherichia Coli* Ly01. *Biotechnol. Bioeng.* **1999**, *66*, 203-10.

(57) Lide, D. R. *Crc Handbook of Chemistry and Physics, 85th Edition*, Taylor & Francis, Boca Raton, 2004.

(58) Smallwood, I. M. *Handbook of Organic Solvent Properties*, Wiley, London, 1996.

(59) Delgenes, J. P.; Moletta, R.; Navarro, J. M. Effects of Lignocellulose Degradation Products on Ethanol Fermentations of Glucose and Xylose by *Saccharomyces Cerevisiae, Zymomonas Mobilis, Pichia Stipitis*, and *Candida Shehatae. Enzyme Microb. Technol.* **1996**, *19*, 220-225.

(60) Cruz Ramos, H.; Hoffmann, T.; Marino, M.; Nedjari, H.; Presecan-Siedel, E.; Dreesen, O.; Glaser, P.; Jahn, D. Fermentative Metabolism of *Bacillus Subtilis*: Physiology and Regulation of Gene Expression. *J. Bacteriol.* **2000**, *182*, 3072-80.

Chapter 3: Integrated vacuum stripping and adsorption for the efficient recovery of (bio-based) 2-butanol

Abstract Bio-based 2-butanol offers high potential as biofuel, but its toxicity toward the microbial hosts calls for efficient techniques to alleviate product inhibition in fermentation processes. Aiming at the selective recovery of 2-butanol, the feasibility of a process combining in-situ vacuum stripping, followed by vapor adsorption, has been assessed using mimicked fermentation media.

The experimental vacuum stripping of model solutions and corn stover hydrolysate closely aligned with mass transfer model predictions. However, the presence of lignocellulosic impurities affected 2-butanol recovery yields resulting from vapor condensation, which decreased from 96 wt.% in model solutions, to 40 wt.% using hydrolysate. For the selective recovery of 2-butanol from a vapor mixture enriched in water and carbon dioxide, silicalite materials were the most efficient, particularly at low alcohol partial pressures. Integrating in-situ vacuum stripping with vapor adsorption using HiSiv3000 proved useful to effectively concentrate 2-butanol above its azeotropic composition (>68 wt.%), facilitating further product purification.

Keywords: Biomaterials · integrated product recovery · vacuum stripping · adsorption· ·

This chapter has been submitted for publication in *Industrial & Engineering Chemistry Research* as: Pereira, J.P.C., Overbeek, W., Gudiño-Reyes, N., Andrés-García, E., Kapteijn, F., van der Wielen, L.A.M., and Straathof, A.J.J., Integrated vacuum stripping and adsorption for the efficient recovery of (bio-based) 2-butanol.

Contents

3.1 Introduction

The use of renewable feedstocks for the production of biofuels and commodity chemicals enables carbon recycling, as opposed to the use of petrochemical feedstocks, therefore reducing the carbon footprint in the industrial sector. When competitively produced, bio-based products can effectively reach the markets, similarly to what happened with bioethanol and biobutanol[1], promoting a sustainable bioeconomy.

Among the butanol isomers that can be produced from biomass, 2-butanol appears as a promising biofuel, mainly due to its higher octane and motor numbers, and lower boiling temperature. 2-Butanol is also a crucial intermediate in bio-based production of methyl methacrylate, as recently suggested[2]. Therefore, it has attracted the attention of several researchers in the last decade[3-7]. Bio-based 2-butanol is known to be naturally produced by *Lactobacillus* strains in the wine-making industry, as a result of the dehydration of 2,3-butanediol into butanone, and its following reduction into 2-butanol[8]. Aiming at competitive production, Ghiaci[5] attempted to produce 2-butanol using engineered *Saccharomyces cerevisiae* strains, but due to the low activity of the adenosylcobalamin-dependent diol dehydratase, only 4 mg/L were achieved. Using a different approach, Chen[6] extended the natural meso-2,3-butanediol pathway in *Klebsiella pneumoniae*, and achieved 1.03 g/L 2-butanol from glucose, with a productivity of ca. 0.03 g/(L h). While this volumetric productivity is still far from industrial targets, previously estimated as 2 g/(L h)[9], the studies show that the enzyme constructs are functional, and competitive strains for industrial applications might be engineered within few years, as happened with other fermentation products[10]. However, 2-butanol severely inhibits microbial growth when product concentrations reach 10 g/L[11]. Metabolic engineering can be used to enhance the microbial tolerance to bio-based chemicals, but it is still challenging to increase tolerance levels up to economically feasible product titers[12]. Therefore, *in-situ* product recovery (ISPR) techniques are widely used to alleviate product inhibition, enhance volumetric productivities, and overcome the downstream processing costs resulting from low product titers in fermentation[13].

Among the different ISPR options, reviewed elsewhere[13-15], vacuum fermentation is a promising vapor-based technology that exploits the relative volatility of the fermentation products, facilitating their separation from the cells and non-volatile lignocellulosic impurities. This technology is particularly efficient in ethanol fermentation given its low boiling point[16], but its technical feasibility has also been demonstrated for 1-butanol in acetone-butanol-ethanol (ABE)

fermentation[17], depicting higher selectivity, and faster removal rates, than gas stripping. The recovery of 1-butanol from the stripped vapor is typically performed by condensation, and the heterogeneous azeotropic mixture formed in 1-butanol/water systems facilitates further product purification by means of conventional decantation and distillation[18-20]. The relative volatility of 2-butanol at infinite dilution, however, is 2.2-fold lower than that of 1-butanol, and 1.7-fold lower than that of isobutanol, which might hinder the selective recovery of this alcohol. Additionally, 2-butanol/water systems form a homogeneous azeotrope, which cannot be separated using conventional distillation methods[7]. Although 2-butanol can be concentrated up to ca. 62 wt.% by phase separation in a decanter, this composition is still below the azeotrope (ca. 68 wt.% 2-butanol). As a result, further product purification by distillation is impracticable. Therefore, a technically feasible alternative is required to recover 2-butanol from the stripped vapor, and further concentrate the alcohol above its azeotropic composition.

Adsorption-based technologies have often proved to be advantageous over other recovery technologies regarding energy requirements[15,18]. Combined with vacuum stripping, adsorption from fermentation vapor would avoid typical liquid-phase adsorption bottlenecks such as nutrient/substrate removal and adsorbent fouling[21,22]. To selectively remove alcohols from dilute aqueous solutions, adsorbents with higher affinity towards non-polar compounds are preferred[23]. For instance, aluminum-free silicalite and zeolites with high silica-aluminum (SiO_2/Al_2O_3) ratio exhibited high alcohol selectivity and adsorption capacities, and proved to be robust when handling regenerative temperature swing cycles[24-26]. Also, activated carbons were effective for the selective adsorption of alcohols from model solutions[27,28]; and polymeric resins such as Sepabeads 207®, based on a poly(styrenedivinylbenzene) matrix that enhances hydrophobicity, proved to be an effective option for ethanol recovery[29,30], yet significantly more expensive than zeolite, silicalite, or activated carbon materials.

The adsorptive behavior of water and 1-butanol onto materials such as silicalite[31], zeolites[32,33], and activated carbons[23,34], has been reported in the literature, as well as the adsorptive behavior of CO_2 onto zeolites and activated carbons[35]. However, studies focusing on the selective alcohol adsorption from stripped fermentation vapor, enriched in water and CO_2, are scarce[28,31].

In the present work, we investigate the feasibility of *in-situ* vacuum stripping for the selective removal of 2-butanol, from model solutions and corn stover hydrolysate. Aiming at product concentrations above the azeotropic composition of 2-butanol/water systems, four commercially available adsorbents, namely a zeolite, a silicalite, an activated carbon, and a polymeric resin, will be screened for the selective recovery of the alcohol from stripped vapor,

enriched in water and carbon dioxide. A mathematical model, initially developed by Löser[36], will be adapted to describe the vacuum stripping process. The efficiency of product recovery by condensation, as well as the achievable 2-butanol concentration in the condensate, will also be assessed. Pure component isotherm data will be used to model the multicomponent adsorption in a fixed bed column, and identify the most promising adsorbent for this process. To the best of the authors' knowledge, the technical feasibility of vacuum stripping using lignocellulosic hydrolysates has not yet been assessed. Additionally, this is the first study on the experimental feasibility of *in-situ* 2-butanol recovery, using vacuum stripping and adsorption technologies, and the data provided can be used for the conceptual design of a large-scale integrated process.

3.2 Materials and Methods

3.2.1 Materials

Analytical grade 2-butanol (99.5 wt.%) was supplied by Sigma-Aldrich. Glucose (99.9 wt%) was obtained from J.T Baker. The gaseous CO2 (>99.99 wt%) was supplied by Air Liquide. Deionized water was used to prepare the model solutions.

Corn stover hydrolysate, containing ca. 20.5 wt.% solids, 10.5 wt.% sugars, 0.5 wt.% acetic acid, 0.07 wt.% formic acid, 0.04 wt.% 5-hydroxymethylfurfural, and 0.01 wt.% furfural, was kindly provided by DSM (Delft, the Netherlands).

Table 1. Properties of the selected adsorbents according to the manufacturers; q_{max} according to the references ($T^{25,27,37,38}$ = 25°C; $T^{29,31}$ = 35°C)

Adsorbents	Surface area (m^2/g)	Pore volume (cm^3/g)	$q_{max,ROH}$ (g/g)	q_{max,H_2O} (g/g)
Zeolite powder	400	0.19	0.133[31]	0.061[25]
Silicalite pellets	282	0.15	0.100[27]	0.051[37]
Activated carbon	1090	0.43	0.206[27]	0.396[38]
Resin	600	1.10	1.250[29]	0.920[29]

Four commercial adsorbents were tested for selective product recovery: powdered ZSM-5 zeolite CBV28014 (SiO_2/Al_2O_3=280, Zeolyst International, USA), pelletized silicalite HiSiv3000 (SiO_2/Al_2O_3=218, UOP Products, Belgium), activated carbon F-400 (Chemviron Carbon, Belgium), and resin Sepabeads SP207® (Resindion S.R.L., Italy). These adsorbents have been selected

based on reported adsorption capacities for alcohols (1-butanol and ethanol) and water[23,25,27,29-31,37]. These values are depicted in Table 1, along with some physical properties of the adsorbents.

3.2.2 Vacuum stripping studies

Vacuum-stripping experiments under anaerobic conditions were performed at 30.0±0.5°C in a 20 L stainless steel reactor (Applikon BIO BENCH 20, the Netherlands), fitted with typical sensors for pH, temperature, and pressure (Fig. 1). The working volume was 10 L. To mimic microbial production, CO2 was sparged at a rate of ca. 0.054 mol/(L h). This rate was calculated stoichiometrically, assuming a hypothetical 2-butanol volumetric productivity of 0.027 mol/(L h)7. This rate translated into a CO2 gas flow of ca. 13±3 L/h, which was measured using a mass flow controller. The off-gas port of the reactor was attached to the condensation system, which comprised a series of two Liebig-type condensers (40 cm), coupled to Erlenmeyer flasks (250 mL) submerged at -7°C in the cryostat (ECO RE 620, Lauda). A vacuum pump (KNF Neuberger, SC920), positioned downstream of the condensation system, controlled the overall pressure at 5.5±0.5 kPa. The pump was equipped with two additional condensers, PC1 and PC2, both at room temperature, but different pressures: PC1 was at 5.5±0.5 kPa, while PC2 was at room pressure (vapor compression ratio ca. 18).

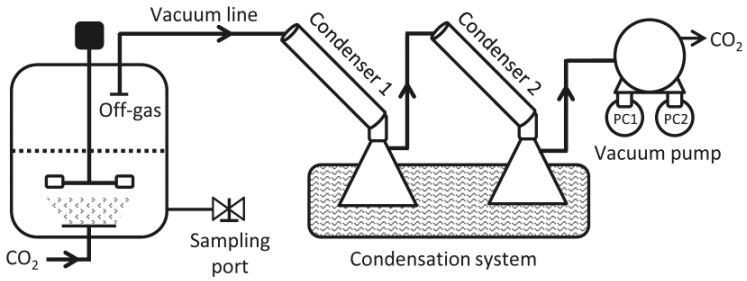

Figure 1. Experimental set-up for in-situ 2-butanol recovery by vacuum stripping

Two series of experiments were performed, viz. vacuum stripping of model solutions containing 2-butanol and glucose (ca. 45 g/L), and vacuum stripping of 2-butanol-containing corn stover hydrolysate. The vacuum pressure, along with the gaseous CO_2 flow, provided sufficient turbulence in the model solutions containing 2-butanol, and stirring was not applied. The corn

stover hydrolysate, however, was significantly denser than the model solutions, and stirring (150 RPM) was applied to facilitate mass transfer and prevent solid sedimentation.

The system was monitored using the MFCS/win 3.0 software (Sartorius), and aqueous samples (0.5 mL) were collected hourly, using an external sampling loop, which allowed sample collection without hampering the vacuum pressure. The samples of hydrolysate were first centrifuged at 13000 g for 1 min, after which the supernatant was collected. Upon termination of the experiments, the volume and mass of the condensates, as well as the remaining solution in the reactor, were determined. All the samples were stored at -20.0°C until 2-butanol quantification.

A mathematical model, describing the vacuum stripping of 2-butanol, has been adapted from the batch-process model proposed by Urit[39]. i stands for the specific components 2-butanol, water, and CO_2. The initial concentrations of i in the liquid and vapor phases, $C_{i,L}$ and $C_{i,G}$ respectively, have been used as model input parameters, and further translated into the respective molar fractions x_i and y_i (for more information, see Nomenclature section):

$$C_{i,L} = \frac{n_{i,L}}{V_L} \quad (1)$$

$$C_{i,G} = \frac{n_{i,G}}{V_{reactor} - V_L} \quad (2)$$

$$x_i = \frac{n_{i,L}}{\sum n_{i,L}} \quad (3)$$

$$y_i = \frac{n_{i,G}}{\sum n_{i,G}} \quad (4)$$

The concentration of CO_2 in the liquid has been determined as total soluble inorganic carbon, $C_{C_{tot},L}$, and subsequently translated into each species of the carbonate buffer system, i.e. dissolved CO_2, carbonic acid, bicarbonate, and carbonate, using the mathematical model proposed by Contreras[40]. The dissolved CO_2 is determined according to:

$$C_{C,L} = \frac{C_{C_{tot,L}} \times {C_{H^+,L}}^2}{{C_{H^+,L}}^2 + K_1 C_{H^+,L} + K_1 K_2} \quad (5)$$

K_1 and K_2 are the known dissociation constants of carbonic acid [41], and $C_{H^+,L}$ stands for the free proton concentration in solution.

The liquid volume, V_L, is a time-dependent variable determined according to:

$$V_L = \frac{\sum(n_{i,L} \times M_{wi})}{\rho_{mix}} \quad (6)$$

The density of aqueous 2-butanol, ρ_{mix}, was determined from its molar composition according to Senanayake et al. [42]. The experimental density of the corn stover hydrolysate was determined to be 1.08 kg/L, and its viscosity was estimated to be 0.09 Pa s, according to Hou et al. [43].

The material balances for 2-butanol, water, and CO_2 in the liquid phase consider their transfer from the liquid to the vapor phase, θ_i:

$$\frac{\mathrm{d}n_{i,L}}{\mathrm{d}t} = -\theta_i \quad (7)$$

In the vapor phase, the material balances consider the molar inflow of CO_2 ($F_{CO_2,in}$), and outflow (F_{out}) of each component i:

$$\frac{\mathrm{d}n_{i,G}}{\mathrm{d}t} = F_{CO_2,in} + \theta_i - F_{out} \times y_{i,out} \quad (8)$$

The overall pressure in the reactor is determined according to the ideal gas law:

$$P = \frac{\sum n_{i,G} \times R \times T}{(V_{reactor} - V_L)} \quad (9)$$

Ideally, to uphold a constant pressure in the reactor, the total amount of moles per volume of vapor phase ($\sum n_{i,G} / (V_{reactor} - V_L)$) should be constant, and therefore $F_{out} = F_{CO_2,in} + \sum \theta_i$. In the present case, the vacuum pump was affected by a pumping delay that caused up to 10% pressure buildup. This constrained the value of F_{out}. As an attempt to mimic this effect, F_{out} was calibrated as a function of the pressure in the reactor. Considering a constant vapor phase volume in the reactor ($V_{reactor} = 20$ L; $V_L = 0$ L), P was decreased over measured time steps, starting from room pressure down to 5.5 kPa. Using eq. (9), the number of moles stripped per time unit (F_{out}) was determined. The experimental values of F_{out} were then plotted as a

function of P, and the best fit to this series ($F_{out} = -8 \times 10^{-6}P^3 + 1.4 \times 10^{-3}P^2 + 0.2P - 0.8$; $R^2 = 0.99$) was used to estimate F_{out} in the simulation.

The transfer rate of compounds via the liquid/vapor interface, θ_i, is dependent on the mass transfer coefficient, $k_{L,i}a$, and the amount of moles of i at the liquid interface, $n^*_{i,L}$:

$$\theta_i = k_{L,i}a \times (n_{i,L} - n^*_{i,L}) \quad (10)$$

The mass transfer coefficient, $k_{L,i}a$, was determined for each component by using the experimental $k_{L,O_2}a$ value, and the relationship proposed by Truong and Blackburn[44]. At the liquid interface, $n^*_{i,L}$ is related to the partition coefficient, K_i:

$$n^*_{i,L} = K_i \times y_i \times \sum n_{i,L} \quad (11)$$

$$K_i = \frac{x_i}{y_i} = \frac{P}{\gamma_i P_i^{Sat}} \quad (12)$$

The modified-UNIFAC model[45] was used to compute the values of activity coefficients, γ_i, and the temperature-dependent P_i^{sat} value was determined using Antoine's equation[46]. CO_2 transfer via the interface, which depends on its aqueous saturation concentration, was predicted using the Henry coefficient:

$$n^*_{C,L} = y_i \times V_L \times \frac{P}{H_i} \quad (13)$$

H_i was determined for the operational temperature according to the parameters provided by Green and Perry [47].

The system of equations described was iteratively solved using Matlab ODE15s, Matlab R2014b (Mathworks), with t as the independent variable. The average relative error, δ, has been used to evaluate the fitting accuracy of the model to the experimental data:

$$\delta = \frac{100}{\mathrm{n}} \sum \left| \frac{C_{i,exp} - C_{i,mod}}{C_{i,exp}} \right| \quad (14)$$

3.2.3 Adsorption studies

ZSM-5 and HiSiv3000 were calcined for 8 h at 600°C. F-400 and the SP207 were dried overnight at 200°C and 70°C, respectively. The adsorbents were stored in an oven at 70°C until further use. Immediately before the experiments, the adsorbents were accurately weighed, and outgassed overnight at 1 kPa.

The single-component isotherms were determined at 30°C. Gas adsorption was performed by volumetric method, using a high-pressure gas adsorption system BELSORP-HP (BEL Japan, INC). with equilibration time of 0.33 h for each measurement. Vapor adsorption was performed using an Autosorb-1-C volumetric adsorption analyzer (Quantachrome GmbH & Co. KG, Germany). Equilibrium was assumed if the pressure variation in 0.17 h was < 0.01 %. Saturated vapor equilibrium experiments were performed in triplicate under controlled temperature, using sealed, depressurized desiccators, in which a weighed amount of adsorbent was placed in a plate above a flask containing liquid adsorbate. The mass variation of the adsorbent after 168 h was used to estimate the maximum vapor uptake.

Several equilibrium isotherm models exist, and reviews regarding their application and consistency can be found elsewhere[48]. In the present work, the Langmuir isotherm[49], the Sips isotherm[50], and the Brunauer-Emmett-Teller (BET) isotherm[51] were selected to correlate the single-component adsorption data. The well-known Freundlich isotherm model[52] depicted significantly higher relative errors for the majority of the cases (data not shown), and was therefore excluded from this study. The Sips isotherm model, shown in eq. 15, combines both Langmuir and Freundlich relations to predict heterogeneous adsorption systems via the index of heterogeneity, a. At high adsorbate concentration, $a = 1$, and a typical Langmuir isotherm is predicted. The BET isotherm (eq. 16) is used to describe finite multilayer adsorption systems: first, the parameters b_i and $q_{max,i}$ were determined from the slope and intercept of the line resulting from the linearization of eq. 17, using the low-pressure region of the experimental data ($P_i \leq 0.35$). These parameters were then used in eq. 16, and the average number of adsorption layers α was estimated by curve fitting[51]. The adsorption parameters in equations 15 and 16 were estimated by iterative nonlinear minimization of the sum of squared residuals, using Matlab R2014b (Mathworks). The average relative error δ and the coefficient of determination R^2 were used to measure the fitting accuracy of the models[48]. To predict competitive adsorption, the multicomponent Sips isotherm, shown in equation 18, was used[53]. For the cases in which Langmuir depicted better fits, Langmuir's parameters were used with $a = 1$. Regarding

the cases better described by the BET isotherm, multicomponent adsorption was predicted using the second best fit isotherm model (either Langmuir or Sips).

$$q_{eq,i} = \frac{q_{max,i}(b_i P_i)^{1/a}}{1+(b_i P_i)^{1/a}} \quad (15)$$

$$q_{eq,i} = \frac{q_{max,i}\, b_i(P_i/P_i^{Sat})}{1-(P_i/P_i^{Sat})}\left\{\frac{1-(\alpha+1)(P_i/P_i^{Sat})^{\alpha}+\alpha(P_i/P_i^{Sat})^{\alpha+1}}{1+(b_i-1)(P_i/P_i^{Sat})-b_i(P_i/P_i^{Sat})^{\alpha+1}}\right\} \quad (16)$$

$$q_{eq,i} = \frac{q_{max,i}\, b_i P_i}{(P_i^{Sat}-P_i)\left[1+(b_i-1)(P_i/P_i^{Sat})\right]} \quad (17)$$

$$q_{eq,i} = \frac{q_{max,i}\, b_i P_i(\sum b_j P_j)^{1/a-1}}{1+(\sum b_j P_j)^{1/a}} \quad (18)$$

3.2.4 Integrated vacuum stripping and adsorption

The integration of vacuum stripping and adsorption was evaluated by means of mathematical simulation, using Adsim®. The mathematical model previously developed in section 2.2 was used to predict the composition of the vapor stripped from a continuous fermentation at pseudo-steady-state, in which 2-butanol was produced at a rate of 2 g/(L h). A fixed bed column with plug flow was considered for vapor adsorption, assuming isothermal conditions and neglecting radial gradients. The pressure drop in the column was estimated using Ergun's equation[54]. The mass and heat transfer coefficients were derived from well-known correlations, suggested in the literature[55,56]. The mass transfer resistances were determined via the lumped linear driving force approximation[57], and the ideal gas theory was used to describe the thermodynamic process. The adsorbent requirements were estimated by means of mass balance, assuming fixed bed saturation, considering a production capacity of 101 kton-2-butanol/a. The breakthrough curves were evaluated for different vapor flow velocities, allowing for the loss of 1 wt.% 2-butanol. Therefore, at least 99 wt.% of the stripped 2-butanol was recovered by adsorption in the column.

3.2.5 Analytical methods

Aqueous concentrations of 2-butanol were determined via GC (InterScience, the Netherlands), using a Zebron™ ZB-WAX-PLUS column (30 m x 0.32 mm x 0.50 µm). 1-Pentanol (320 mg/L) was

used as internal standard. The temperature was 30°C for 5 min, followed by a gradient of 20°C/min for 5 min. The temperatures of the injector and FI detector were 200°C and 250°C, respectively.

3.3 Results and Discussion

3.3.1 Selective recovery of 2-butanol via *in-situ* vacuum stripping and vapor condensation

The efficiency of *in-situ* vacuum stripping was analyzed by targeting the selective removal of 2-butanol from model solutions. The effect of other fermentation compounds was evaluated using corn stover hydrolysate. The concentration profiles of 2-butanol in the reactor, resulting from the vacuum stripping of model solutions and hydrolysate, are shown in Fig. 2. The initial concentration of 2-butanol in the mixtures was within the range expected in fermentations, tolerating a 50% reduction in the maximum microbial growth rate due to toxicity[11]. Fig. 2 shows that the vacuum stripping process is in agreement with the model predictions for model solutions and hydrolysate, with low average relative errors of 1.6±0.1 % and 2.8±0.2 %, respectively. Thus, the model can accurately predict 2-butanol concentration profiles and condensate compositions for a wide range of operational conditions and mixtures. Overall, the stripping rate and the favorable 2-butanol removal over other compounds, namely water, were found to increase with the product concentration in the aqueous mixture, as observed in other studies[58,59].

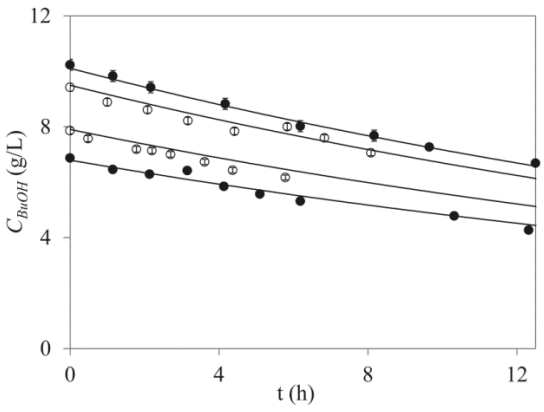

Figure 2. Comparison between experimental (markers) and predicted (lines) concentrations of 2-butanol in the aqueous phase, during the vacuum stripping of model solutions (full symbols), and hydrolysate (open symbols); T= 30ºC; P= 5.5 kPa.

The measured mass of 2-butanol stripped from model solutions and hydrolysate, as well as its mole fraction, concentration in the recovered condensates, and stripping selectivity, $S_{BuOH} = \left[\left(x_{BuOH,cond}/x_{wat,cond}\right)/\left(x_{BuOH,broth}/x_{wat,broth}\right)\right]$, are given in Table 2. These values were obtained after termination of the experiments. Water was stripped at a constant rate of 1.42±0.06 g/(L h), and 96.6±0.1 wt.% of the stripped water was collected in Condenser 1 (recall Fig.1). Conversely, the higher activity coefficient of 2-butanol (γ_{BuOH} ≈18.7) enhanced θ_{BuOH}, promoting its evaporation along the condensation system. In the pump condenser PC2, the high compression ratio caused 2-butanol to condense at 20 °C. This condenser contained the highest product mass fraction (61 wt.%), and ca. 19 wt.% of the total 2-butanol stripped from the model solutions.

Table 2. Masses, mole fractions, concentrations, and selectivities measured after vacuum stripping of model solutions; T= 30ºC; P= 5.5 kPa.

	Model solution	Hydrolysate
t_{exp} (h)	12	8
$C_{BuOH,t=0}$ (g/L)	10.2±0.2	9.4±0.2
$m_{BuOH,strip}$ (g)	34 ± 1	25 ± 3
$m_{BuOH,cond}$ (g)	32 ± 1	10.0 ± 0.2
recovery (%)	96 ± 3	40 ± 5
$m_{wat,cond}$ (g)	178.3 ± 0.8	111.5 ± 0.2
$x_{BuOH,cond}$ (mol/mol)	(421 ± 11)×10^{-4}	(214 ± 4)×10^{-4}
$C_{BuOH,cond}$ (g/L)	147 ± 4	81 ± 2
$S_{BuOH,cond}$ (–)	17.5 ± 0.5	9.3 ± 0.2
$S_{BuOH,cond}$* (–)	18.4 ± 0.6	22.9 ± 2.8

The extent of 2-butanol recovery by condensation decreased drastically to 40±5 % using hydrolysate mixtures, as opposed to model solutions. As a result, the stripping selectivity was roughly twice as low. Residual amounts of typical hydrolysate compounds, namely furfural, acetic and formic acids, among other unidentified compounds, were found in the condensate. The chemical composition of a mixture is known to influence vapor-liquid equilibria, and the addition of ternary species is widely used to facilitate the selective removal of alcohols, by promoting their relative volatility[60,61]. This effect was minimized in the reactor, due to the dilute

concentrations of product and hydrolysate compounds, but their comparatively higher molar fraction in the condensate enhanced γ_{BuOH} and, therefore, 2-butanol evaporation. The composition of the hydrolysate also caused technical issues not observed with model solutions, namely the obstruction of the sampling device, which led to shorter experimental runs (ca. 5–8 h, as opposed to ca. 12 h using model solutions).

The predictive model was used to analyze the effect of increasing the driving force for evaporation (F_{out}) on 2-butanol concentrations and condensate compositions, by increasing the CO_2 flow rate ($F_{CO_2,in}$) in the simulations accordingly. A continuous reactor at pseudo-steady state was considered, in which 2-butanol was produced at a rate of 2 g/(L h). $F_{CO_2,in}$ =0.54 mol/h represents the base-case, in which the stoichiometric microbial CO_2 production was considered. The results are shown in Fig. 3.

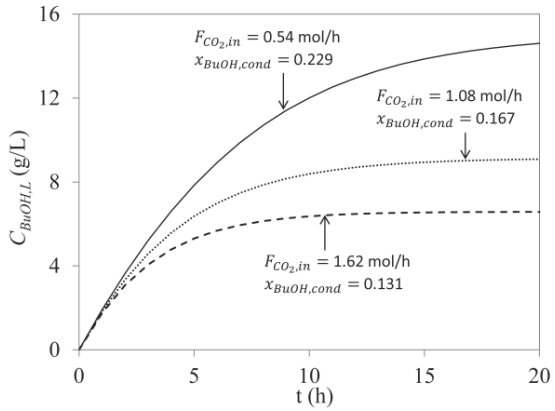

Figure 3. Predicted 2-butanol concentration profiles in the reactor during vacuum stripping at various values of $F_{CO_2,in}$; $x_{BuOH,cond}$ values assume full recovery from the vapor; T= 30ºC; P= 5.5 kPa.

The stripping rate of 2-butanol increased with the magnitude of F_{out}, and the concentration of 2-butanol in the reactor was kept below inhibiting levels without the requirement of additional stripping gas. However, decreasing $C_{BuOH,L}$ led to subsequent lower values of y_{BuOH}. Since $C_{wat,L}$ was comparatively unaffected, the stripping selectivity for 2-butanol declined, i.e., increasing F_{out} decreased $x_{BuOH,cond}$. Considering the base-case, the composition of the stripped vapor would contain roughly $y_{BuOH} = 0.077$, $y_{wat} = 0.769$, and $y_{CO_2} = 0.154$. The resulting condensate, containing nearly 23 wt.% 2-butanol, is 23-fold more concentrated than the hydrolysate, and would facilitate phase separation by decantation. However, this

composition is still below the azeotropic composition (ca. 68 wt.%), anticipating high costs for product purification by distillation.

3.3.2 Selective recovery of 2-butanol by adsorption

As discussed in the previous section, the stripped fermentation vapor is expected to comprise mostly water, 2-butanol, and CO_2. Therefore, it is convenient to find an adsorbent that can selectively separate the alcohol from the vapor, such that the resulting adsorbate contains 2-butanol beyond its azeotropic composition. The isotherms obtained for the adsorption of 2-butanol, water and CO_2 onto four potential adsorbents are depicted in Fig. 4 A), B) and C), respectively. For 2-butanol and water, the equilibrium capacity is presented up to the saturated vapor pressure at 30ºC, using the values determined under solvent vapor-saturated atmosphere. The lines represent the predictions by the isotherm model depicting the lowest δ for each case study, and the fitted parameters are presented in Table 3.

The resin revealed the highest adsorption capacity for 2-butanol in vapor-saturated atmosphere (723±5 mg/g) and, given its hydrophobicity, the lowest adsorption capacity for water. The latter cannot hold direct comparison with that reported by Delgado[29] (Table 1), since these authors did not make a distinction between the liquid phase filling the voids, and the adsorbed phase, in their study. Despite these results, Fig.4 A shows that the resin has the lowest affinity for the alcohol at low partial pressures. This suggests that large amounts of adsorbent are required for 2-butanol recovery from dilute vapor, leading to costly product recovery by adsorption. The clear multilayered adsorption behavior at high partial pressures suggests that capillary condensation might occur, promoting Van der Waals interactions between the vapor molecules inside the pores of the resin. Therefore, the BET model provided a good fit for the resulting S-shaped isotherm. The adsorption of 2-butanol onto the other materials was accurately described by Langmuir-type isotherms. The maximum loadings observed for 2-butanol adsorption onto zeolite powder (153 mg/g) and silicalite pellets (109 mg/g) are comparable to those reported for 1-butanol adsorption onto high Si/Al ratio materials[25,31,62] (recall Table 1). The $q_{max,BuOH}$ value achieved in zeolite, 40% higher than that of silicalite, is probably due to its larger pore volume[25]. The values of b_{BuOH} observed in the present work are much lower than those reported by Farzaneh[31] for the adsorption of 1-butanol onto silicalite-1 at 35°C. This shows that the adsorbent affinity for 1-butanol is higher than for the less organophilic 2-butanol. Activated carbon depicted a slightly higher $q_{max,BuOH}$ value than that observed by Abdehagh[27] regarding

1-butanol. This is probably due to the fact that the authors tested dilute aqueous solutions, in which the alcohol loading is strongly affected by the competitive adsorption of water. The high $q_{max,wat}$ value observed for the activated carbon, similar to what is reported in the literature[38], also suggests the low selectivity of this material.

Typical S-shaped isotherms were observed for the adsorption of water vapor onto the adsorbents (Fig.4 B): the low-pressure region of the isotherm revealed a low affinity for water, but at higher partial pressures water adsorption was enhanced, due to the formation of hydrogen bonds and water clusters[32]. While severe competitive adsorption is anticipated when using the activated carbon or the resin, this effect is mitigated regarding the zeolite and the silicalite, since the affinity for 2-butanol at lower pressures is comparatively high. The high value of δ observed for water adsorption onto resin relates to the small sample size, while for activated carbon it relates to the fitting errors in the low-pressure region.

The measured isotherms for CO_2 (Fig.4 C) were successfully fitted using Sips isotherm, suggesting heterogeneous adsorption onto the materials tested. Although the $q_{max,C}$ value for zeolite powder is within the range reported in the literature[35,63] (124–198 mg/g), it is significantly higher than that reported for activated carbon[37], possibly due to the different materials and operational conditions used. The equilibrium capacities observed for CO_2 at low partial pressures are almost negligible, particularly for the resin and the silicalite. Overall, less than 8 mg-CO_2/g were adsorbed onto the materials at 5.5 kPa. Although at room pressure CO_2 adsorption becomes more significant, the affinities for the gas are much lower than those observed for 2-butanol or water. This indicates that competitive adsorption of CO_2 does not play an important role when predicting multicomponent adsorption at the considered vacuum pressures.

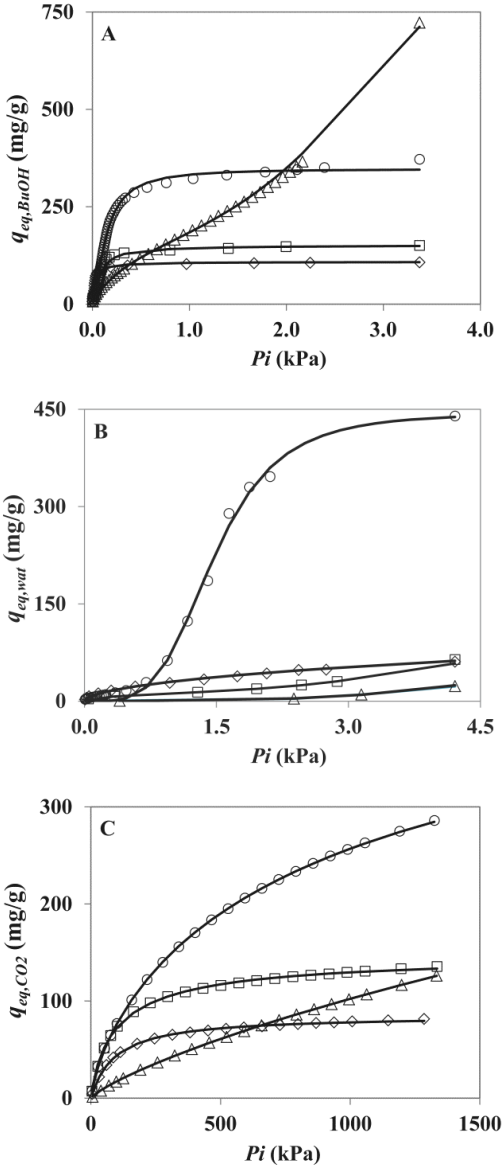

Figure 4. Adsorption isotherms of (A) 2-butanol; (B) water; and (C) CO_2 onto different adsorbents; markers represent the experimental data, and lines represent the isotherm model predictions (best fit); T= 30ºC; □ – Zeolite powder; ◇ – Silicalite pellets; ○ – Activated carbon; △ – Resin.

Table 4. Fitted parameters for the adsorption of 2-butanol, water, and CO_2 onto different adsorbents; T = 30ºC.

	Zeolite powder	Silicalite pellets	Activated carbon	Resin
2-Butanol				
Best fit model	Langmuir	Langmuir	Sips	BET
$q_{max,i}$ (mg/g)	153 ± 6	109 ± 3	350 ± 3	160 ± 5
b_i (1/kPa)	11 ± 1	41 ± 4	6.9 ± 0.1	10.1 ± 0.2
a / α (–)	n.a.	n.a.	0.64 ± 0.02	8.0 ± 0.7
δ (%)	14.7	9.8	8.9	8.4
R^2 (–)	0.965	0.973	0.994	0.997
Water				
Best fit model	BET	Sips	Sips	Langmuir
$q_{max,i}$ (mg/g)	11 ± 2	651 ± 98	445 ± 11	3432 ± 3350
b_i (1/kPa)	19 ± 2	$(3 \pm 1)\times10^{-3}$	0.68 ± 0.01	$(1 \pm 1)\times10^{-3}$
a / α (–)	10.0 ± 0.7	1.9 ± 0.2	0.25 ± 0.02	n.a.
δ (%)	7.3	5.5	64	98
R^2 (–)	0.999	0.998	0.996	0.793
CO_2				
Best fit model	Sips	Langmuir	Sips	Sips
$q_{max,i}$ (mg/g)	149 ± 2	85.3 ± 0.5	531 ± 4	1154 ± 157
b_i (1/kPa)	$(93 \pm 3)\times10^{-4}$	$(107 \pm 3)\times10^{-4}$	$(9.1 \pm 0.2)\times10^{-4}$	$(5.5 \pm 1.2)\times10^{-5}$
a / α (–)	1.18 ± 0.03	n.a.	1.3 ± 0.3	1.25 ± 0.01
δ (%)	1.7	1.3	0.6	2.3
R^2 (–)	0.999	0.998	1.000	1.000

n.a. – not applicable

Given the diverse adsorption profiles obtained, choosing an adsorbent for the selective recovery of 2-butanol from the fermentation vapor is not straightforward: it is clear that the affinity for 2-butanol at lower partial pressures is of major importance. As an attempt to better understand competitive adsorption, the multicomponent Sips isotherm has been used, considering the vapor composition of the base-case study, depicted in Fig. 3. Regarding the adsorption of 2-butanol onto the resin and the adsorption of water onto the zeolite, better described by the BET

isotherm, the estimated values for the Langmuir model parameters have been used ($q_{max,BuOH}$ =110.6 g/g, b_{BuOH} =1.6×10^{-3} (1/kPa), δ =29% and q_{max,H_2O} =1534.8 g/g, b_{H_2O} =7.8×10^{-6} (1/kPa), δ =31%, respectively). Based on estimated values of $q_{eq,i}$ (mg/g), the adsorbent selectivity for 2-butanol has been determined as $\varepsilon_{BuOH} = q_{eq,BuOH}/\sum q_{eq,i}$. The results are depicted in Table 5.

Table 5. Estimated equilibrium adsorption of 2-butanol, water, and CO_2 from stripped fermentation vapor onto different adsorbents; T= 30ºC; P= 5.5 kPa.

	$q_{eq,i}$ (mg/g)			
	Zeolite powder	Silicalite pellets	Activated carbon	Resin
2-Butanol	126 ± 12	103 ± 10	166 ± 6	76 ± 31
Water	9 ±4	0.4 ± 0.2	220 ± 19	14 ± 20
CO_2	0.20 ± 0.01	0.042 ± 0.001	0.06 ± 0.01	0.15 ± 0.04
ε_{BuOH} (–)	0.9 ± 0.4	1.0 ± 0.4	0.4 ± 0.1	0.8 ± 1.2

Although adsorbents such as activated carbon are often pointed out as the most promising option for the selective recovery of bio-butanol[27,64,65], the present study suggests that silicalite materials, particularly HiSiv3000, offer higher selectivity over water at lower alcohol partial pressures. However, the adsorbent selectivity for 2-butanol is affected by great errors, mostly due to the impracticability of describing the adsorption behavior using a single model. It is important to note that the prediction of multicomponent adsorption is challenging using simple adsorption models for hydrogen bonding systems[66]. Therefore, it is strongly recommended that the multicomponent equilibrium data presented in this work are further validated using actual stripped fermentation vapor. Silicalite materials are known to be more selective for 1-butanol when compared to other solvents such as ethanol or acetone, since more organophilic components are adsorbed preferentially[62,67]. Bearing in mind the log *P* values of the hydrolysate compounds that might be vacuum stripped, considerably lower than that of 2-butanol, the alcohol is expected to be adsorbed favorably.

3.3.3 Prospects for the vacuum stripping of fermentation broth integrated with adsorption

The feasibility of integrated vacuum stripping and adsorption of 2-butanol using silicalite HiSiv3000 was further investigated using Adsim®. The column feed matched the base-case off-gas composition (recall Fig. 3), as described in section 3.1.

Although the first option was to use the vapor stream directly from the bioreactor (T =33°C, P =5.5 kPa), it became clear that the maximum attainable vapor velocity (0.05 m/s) was limited by the pressure drop in the column. This affected significantly the bed volume (1067 m^3) and cross sectional area (ca. 4500 m^2), compromising the equipment sizing. By compressing the vapor feed to 10.0 kPa, the vapor velocity increased to 0.10 m/s. As a result, the required mass of adsorbent decreased by 2.4-fold, and the adsorption productivity increased from 0.011 $kg_{BuOH}/(kg_{ads}$ h) to 0.024 $kg_{BuOH}/(kg_{ads}$ h). Further vapor compression to 20.0 kPa reduced the 2-butanol fraction in the vapor by 44%, anticipating significant costs due to product recovery from the resulting dilute condensate. Therefore, a preliminary vapor compression step, up to 10.0 kPa, has been considered. The effect of the feed pressure on 2-butanol breakthrough curve is depicted in Fig. 5, along with the 2-butanol content (wt.%) in the resulting adsorbate. Taking into account the recovery target of 99 wt.% of the stripped 2-butanol, the adsorption step must be stopped when this specification is reached, i.e., around 4.5 h considering the adsorption pressure of 10.0 kPa. At this point, the adsorbate within the column contained roughly 93 wt.% 2-butanol, which is substantially higher than the azeotrope composition.

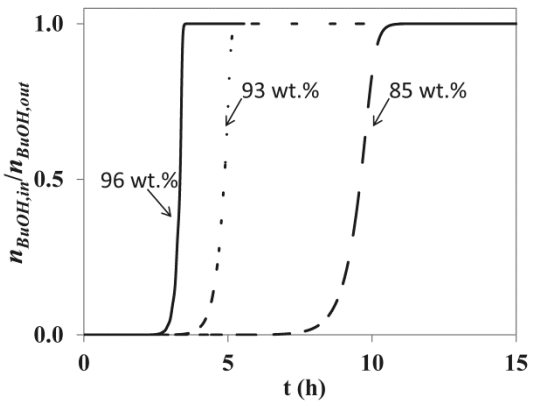

Figure 5. Breakthrough curves of 2-butanol using different feed pressures: P= 5.5 kPa (dashed line), P= 10.0 kPa (dotted line), and P= 20.0 kPa (full line)

The prospects for the adsorption-based recovery of 2-butanol produced by vacuum fermentation have been discussed in Pereira[7], on basis of preliminary data. The overall energy duty was estimated to be 21.9 MJ/kg with highly pure 2-butanol (99wt.%) as the final product. Although the overall energy duty of the integrated configuration is expected to be high using the current adsorption data, a convenient stream of 2-butanol beyond azeotropic composition can be obtained.

3.4 Conclusions

Aiming at the selective recovery of bio-based 2-butanol, the feasibility of an integrated process combining *in-situ* vacuum stripping and adsorption has been assessed. As a result of vacuum stripping, the concentration of 2-butanol in the bioreactor was kept below inhibiting levels without the requirement of additional stripping gas. However, the presence of hydrolysate impurities hindered the efficiency of 2-butanol recovery by condensation, which decreased from 96 wt.% in model solutions, to 40 wt.% using hydrolysate. While the content of 2-butanol in the condensate was ca. 23-fold higher than in the bioreactor, this was still below the azeotropic composition of 2-butanol/water systems.

Integrating vacuum stripping with vapor adsorption using silicalite HiSiv3000 proved advantageous to achieve 2-butanol contents beyond the azeotropic composition. Based on the results provided by the mathematical simulation, adsorbates containing up to 93 wt.% 2-butanol can be obtained after desorption. However, it is strongly recommended that the data presented in this work are further validated using actual fermentation broth, and the resulting stripped fermentation vapor.

3.5 Acknowledgments

We would like to acknowledge Willy Rook, Yi Song, Max Zomerdijk, Dirk Geerts, and Stef van Hateren for their analytical support. We would also like to thank Chris Jugters (UOP Products, Belgium BVBA) for providing the HiSiv 3000, Chemviron Carbon (Belgium) for providing the activated carbon F-400, Resindion S.R.L. (Italy) for providing the Sepabeads SP207®, and DSM (Delft, the Netherlands) for providing the corn stover hydrolysate.

3.6 Nomenclature

a	–	Index of heterogeneity in Sips equation
A	m^2	Solid interface area
b	1/bar	Affinity constant for adsorption
C	mol/L	Concentration
C^*	mol/L	Concentration at the liquid interface
F	mol/h	Mole flow rate
H	L bar/mol	Henry's coefficient
$k_L a$	1/h	Volume-specific mass transfer coefficient
K_i	bar/bar	Distribution coefficient
M_w	g/mol	Molecular mass
n	–	Number of observations
n	mol	Number of moles
n^*	mol	Number of moles at the liquid interface
P	bar	Pressure
P^{Sat}	bar	Saturation pressure
r	mol/(L h)	Rate of formation
R	L bar/(K mol)	Ideal gas constant
S	–	Selectivity
q	mg/g	Adsorption capacity
t	h	Time
T	K	Temperature
V	L	Volume
x	–	Mole fraction in the liquid phase
y	–	Mole fraction in the vapor phase
Greek Symbols		
α	–	Average number of adsorption layers in BET isotherm
δ	%	Average relative error
γ	–	Activity coefficient
ε	–	Adsorbent selectivity
θ	mol/h	Transfer rate from liquid to gas phase
ρ	g/L	Density

Subscripts

$broth$	Fermentation broth
$BuOH$	2-Butanol
C	Carbon dioxide
$cond$	Condensate
eq	Equilibrium
exp	Experimental
G	Vapor phase
i	Component i
in	In
j	Component j
L	Liquid phase
max	Maximum
mix	Mixture
mod	Predicted by model
out	Out
$strip$	Stripped
tot	Total
wat	Water

3.7 References

(1) Straathof, A. J. J. Transformation of Biomass into Commodity Chemicals Using Enzymes or Cells. *Chem. Rev.* **2014**, *114*, 1871–1908.

(2) Pereira, J. P. C.; van der Wielen, L. A. M.; Straathof, A. J. J. Perspectives for the Microbial Production of Methyl Propionate Integrated with Product Recovery. *Bioresour. Technol.* **2018**, *256*, 187-194.

(3) Bramucci, M. G.; Flint, D.; Miller, E. S.; Nagarajan, V.; Sedkova, N.; Singh, M.; Van Dyk, T. K. Method for the Production of 2-Butanol. U.S. Patent 8426174, 2013.

(4) Burk, M. J.; Pharkya, P.; Burgard, A. P. Microorganisms for the Production of Methyl Ethyl Ketone and 2-Butanol. U.S. Patent 20100184173, 2010.

(5) Ghiaci, P.; Norbeck, J.; Larsson, C. 2-Butanol and Butanone Production in *Saccharomyces Cerevisiae* through Combination of a B12 Dependent Dehydratase and a Secondary Alcohol Dehydrogenase Using a Tev-Based Expression System. *PLoS One* **2014**, *9*, e102774.

(6) Chen, Z.; Wu, Y.; Huang, J.; Liu, D. Metabolic Engineering of Klebsiella Pneumoniae for the De Novo Production of 2-Butanol as a Potential Biofuel. *Bioresour. Technol.* **2015**, *197*, 260–265.

(7) Pereira, J. P. C.; Lopez-Gomez, G.; Reyes, N. G.; van der Wielen, L. A. M.; Straathof, A. J. J. Prospects and Challenges for the Recovery of 2-Butanol Produced by Vacuum Fermentation - a Techno-Economic Analysis. *Biotechnol. J.* **2017**, *12*, 1600657.

(8) Speranza, G.; Corti, S.; Fontana, G.; Manitto, P.; Galli, A.; Scarpellini, M.; Chialva, F. Conversion of Meso-2,3-Butanediol into 2-Butanol by Lactobacilli. Stereochemical and Enzymatic Aspects. *J. Agric. Food. Chem.* **1997**, *45*, 3476–3480.

(9) Van Dien, S. From the First Drop to the First Truckload: Commercialization of Microbial Processes for Renewable Chemicals. *Curr. Opin. Biotechnol.* **2013**, *24*, 1061–1068.

(10) Park, S. J.; Lee, S. H.; Lee, S. Y.; Lee, E. J. Mutants Having Capability to Produce 1,4-Butanediol and Method for Preparing 1,4-Butanediol. U.S. Patent 9096860, 2009.

(11) Pereira, J. P. C.; Verheijen, P. J. T.; Straathof, A. J. J. Growth Inhibition of S. Cerevisiae, B. Subtilis, and E. Coli by Lignocellulosic and Fermentation Products. *Appl. Microbiol. Biotechnol.* **2016**, *100*, 9069–9080.

(12) Mukhopadhyay, A. Tolerance Engineering in Bacteria for the Production of Advanced Biofuels and Chemicals. *Trends Microbiol.* **2015**, *23*, 498-508.

(13) Van Hecke, W.; Kaur, G.; De Wever, H. Advances in in-Situ Product Recovery (Ispr) in Whole Cell Biotechnology During the Last Decade. *Biotechnol. Adv.* **2014**, *32*, 1245–1255.

(14) Xue, C.; Zhao, J.-B.; Chen, L.-J.; Bai, F.-W.; Yang, S.-T.; Sun, J.-X. Integrated Butanol Recovery for an Advanced Biofuel: Current State and Prospects. *Appl. Microbiol. Biotechnol.* **2014**, 3463–3474.

(15) Outram, V.; Lalander, C.-A.; Lee, J. G. M.; Davis, E. T.; Harvey, A. P. A Comparison of the Energy Use of in Situ Product Recovery Techniques for the Acetone Butanol Ethanol Fermentation. *Bioresour. Technol.* **2016**, *220*, 590–600.

(16) Nguyen, V. D.; Auresenia, J.; Kosuge, H.; Tan, R. R.; Brondial, Y. Vacuum Fermentation Integrated with Separation Process for Ethanol Production. *Biochem. Eng. J.* **2011**, *55*, 208–214.

(17) Mariano, A. P.; Qureshi, N.; Filho, R. M.; Ezeji, T. C. Assessment of in Situ Butanol Recovery by Vacuum During Acetone Butanol Ethanol (Abe) Fermentation. *J. Chem. Technol. Biotechnol.* **2012**, *87*, 334–340.

(18) Vane, L. M. Separation Technologies for the Recovery and Dehydration of Alcohols from Fermentation Broths. *Biofuels, Bioprod. Biorefin.* **2008**, *2*, 553–588.

(19) Díaz, V. H. G.; Tost, G. O. Butanol Production from Lignocellulose by Simultaneous Fermentation, Saccharification, and Pervaporation or Vacuum Evaporation. *Bioresour. Technol.* **2016**, *218*, 174–182.

(20) Patraşcu, I.; Bîldea, C. S.; Kiss, A. A. Eco-Efficient Butanol Separation in the Abe Fermentation Process. *Sep. Purif. Technol.* **2017**, *177*, 49-61.

(21) Qureshi, N.; Hughes, S.; Maddox, I. S.; Cotta, M. A. Energy-Efficient Recovery of Butanol from Model Solutions and Fermentation Broth by Adsorption. *Bioprocess Biosyst. Eng.* **2005**, *27*, 215–222.

(22) Xue, C.; Liu, F.; Xu, M.; Tang, I. C.; Zhao, J.; Bai, F.; Yang, S.-T. Butanol Production in Acetone-Butanol-Ethanol Fermentation with in Situ Product Recovery by Adsorption. *Bioresour. Technol.* **2016**, *219*, 158-168.

(23) Taqvi, S. M.; Appel, W. S.; LeVan, M. D. Coadsorption of Organic Compounds and Water Vapor on Bpl Activated Carbon. 4. Methanol, Ethanol, Propanol, Butanol, and Modeling. *Ind. Eng. Chem. Res.* **1998**, *38*, 240–250.

(24) Águeda, V. I.; Delgado, J. A.; Uguina, M. A.; Sotelo, J. L.; García, Á. Column Dynamics of an Adsorption–Drying–Desorption Process for Butanol Recovery from Aqueous Solutions with Silicalite Pellets. *Sep. Purif. Technol.* **2013**, *104*, 307–321.

(25) Oudshoorn, A.; van der Wielen, L. A. M.; Straathof, A. J. J. Adsorption Equilibria of Bio-Based Butanol Solutions Using Zeolite. *Biochem. Eng. J.* **2009**, *48*, 99–103.

(26) Oudshoorn, A.; van der Wielen, L. A. M.; Straathof, A. J. J. Desorption of Butanol from Zeolite Material. *Biochem. Eng. J.* **2012**, *67*, 167–172.

(27) Abdehagh, N.; Tezel, F. H.; Thibault, J. Adsorbent Screening for Biobutanol Separation by Adsorption: Kinetics, Isotherms and Competitive Effect of Other Compounds. *Adsorption* **2013**, *19*, 1263–1272.

(28) Pyrgakis, K. A.; de Vrije, T.; Budde, M. A. W.; Kyriakou, K.; López-Contreras, A. M.; Kokossis, A. C. A Process Integration Approach for the Production of Biological Iso-Propanol, Butanol

and Ethanol Using Gas Stripping and Adsorption as Recovery Methods. *Biochem. Eng. J.* **2016**, *116*, 176–194.

(29) Delgado, J. A.; Águeda, V. I.; Uguina, M. A.; Sotelo, J. L.; García, A.; Brea, P.; García-Sanz, A. Separation of Ethanol–Water Liquid Mixtures by Adsorption on a Polymeric Resin Sepabeads 207®. *Chem. Eng. J.* **2013**, *220*, 89–97.

(30) Delgado, J. A.; Uguina, M. A.; Sotelo, J. L.; Águeda, V. I.; Gómez, P.; Hernández, V. Modeling the Regeneration of a Polymeric Resin Column Saturated with Ethanol by Air Purge and External Heating. *Separ. Sci. Technol.* **2011**, *46*, 1740–1749.

(31) Farzaneh, A.; Zhou, M.; Potapova, E.; Bacsik, Z.; Ohlin, L.; Holmgren, A.; Hedlund, J.; Grahn, M. Adsorption of Water and Butanol in Silicalite-1 Film Studied with in Situ Attenuated Total Reflectance–Fourier Transform Infrared Spectroscopy. *Langmuir* **2015**, *31*, 4887–4894.

(32) Jentys, A.; Warecka, G.; Derewinski, M.; Lercher, J. A. Adsorption of Water on Zsm 5 Zeolites. *J. Phys. Chem. A* **1989**, *93*, 4837–4843.

(33) Gorbach, A.; Stegmaier, M.; Eigenberger, G. Measurement and Modeling of Water Vapor Adsorption on Zeolite 4a—Equilibria and Kinetics. *Adsorption* **2004**, *10*, 29–46.

(34) Nastaj, J.; Chybowska, M. Adsorption Equilibria of Butan-1-Ol, Toluene and Water Vapour onto Sorbonorit 4 Activated Carbon and the Co-Adsorption of Organic Compounds and Water Vapour onto Skt Activated Carbon. *Adsorpt. Sci. Technol.* **2006**, *24*, 283–300.

(35) Lopes, F. V. S.; Grande, C. A.; Ribeiro, A. M.; Loureiro, J. M.; Evaggelos, O.; Nikolakis, V.; Rodrigues, A. E. Adsorption of H2, Co2, Ch4, Co, N2 and H2o in Activated Carbon and Zeolite for Hydrogen Production. *Separ. Sci. Technol.* **2009**, *44*, 1045-1073.

(36) Löser, C.; Schröder, A.; Deponte, S.; Bley, T. Balancing the Ethanol Formation in Continuous Bioreactors with Ethanol Stripping. *Eng. Life Sci.* **2005**, *5*, 325–332.

(37) Nastaj, J.; Aleksandrzak, T. Adsorption Isotherms of Water, Propan-2-Ol, and Methylbenzene Vapors on Grade 03 Silica Gel, Sorbonorit 4 Activated Carbon, and Hisiv 3000 Zeolite. *J. Chem. Eng. Data* **2013**, *58*, 2629–2641.

(38) Rudisill, E. N.; Hacskaylo, J. J.; LeVan, M. D. Coadsorption of Hydrocarbons and Water on Bpl Activated Carbon. *Ind. Eng. Chem. Res.* **1992**, *31*, 1122–1130.

(39) Urit, T.; Löser, C.; Wunderlich, M.; Bley, T. Formation of Ethyl Acetate by *Kluyveromyces Marxianus* on Whey: Studies of the Ester Stripping. *Bioprocess Biosyst. Eng.* **2011**, *34*, 547–559.

(40) Contreras, E. M. Carbon Dioxide Stripping in Bubbled Columns. *Ind. Eng. Chem. Res.* **2007**, *46*, 6332–6337.

(41) Millero, F. J.; Pierrot, D.; Lee, K.; Wanninkhof, R.; Feely, R.; Sabine, C. L.; Key, R. M.; Takahashi, T. Dissociation Constants for Carbonic Acid Determined from Field Measurements. *Deep Sea Res. Part 1 Oceanogr. Res. Pap.* **2002**, *49*, 1705–1723.

(42) Senanayake, P. C.; Gee, N.; Freeman, G. R. Viscosity and Density of Isomeric Butanol/Water Mixtures as Functions of Composition and Temperature. *Can. J. Chem.* **1987**, *65*, 2441–2446.

(43) Hou, W.; Li, L.; Bao, J. Oxygen Transfer in High Solids Loading and Highly Viscous Lignocellulose Hydrolysates. *ACS Sustain. Chem. Eng.* **2017**, 11395–11402.

(44) Truong, K. N.; Blackburn, J. W. The Stripping of Organic Chemicals in Biological Treatment Processes. *Environ. Prog.* **1984**, *3*, 143–152.

(45) Gmehling, J.; Wittig, R.; Lohmann, J.; Joh, R. A Modified Unifac (Dortmund) Model. 4. Revision and Extension. *Ind. Eng. Chem. Res.* **2002**, *41*, 1678-1688.

(46) Poling, B.; Prausnitz, J.; Connell, J. O. *The Properties of Gases and Liquids*, McGraw-Hill Education, 2000.

(47) Green, D.; Perry, R. *Perry's Chemical Engineers' Handbook, Eighth Edition*, McGraw-Hill Education, 2007.

(48) Foo, K. Y.; Hameed, B. H. Insights into the Modeling of Adsorption Isotherm Systems. *Chem. Eng. J.* **2010**, *156*, 2–10.

(49) Langmuir, I. The Constitution and Fundamental Properties of Solids and Liquids. Part 1. Solids. *J. Am. Chem. Soc.* **1916**, *38*, 2221–2295.

(50) Sips, R. Combined Form of Langmuir and Freundlich Equations. *J. Chem. Phys.* **1948**, *16*, 490–495.

(51) Brunauer, S.; Emmett, P. H.; Teller, E. Adsorption of Gases in Multimolecular Layers. *J. Am. Chem. Soc.* **1938**, *60*, 309–319.

(52) Freundlich, H. M. F. Over the Adsorption in Solution. *J. Phys. Chem. A* **1906**, *57*, 385–471.

(53) Do, D. D. *Adsorption Analysis: Equilibria and Kinetics*, Imperial College Press, London, U.K., 1998.

(54) Ergun, S.; Orning, A. A. Fluid Flow through Randomly Packed Columns and Fluidized Beds. *Ind. Eng. Chem.* **1949**, *41*, 1179–1184.

(55) Bonjour, J.; Chalfen, J.-B.; Meunier, F. Temperature Swing Adsorption Process with Indirect Cooling and Heating. *Ind. Eng. Chem. Res.* **2002**, *41*, 5802–5811.

(56) Joss, L.; Gazzani, M.; Hefti, M.; Marx, D.; Mazzotti, M. Temperature Swing Adsorption for the Recovery of the Heavy Component: An Equilibrium-Based Shortcut Model. *Ind. Eng. Chem. Res.* **2015**, *54*, 3027–3038.

(57) Sircar, S.; Hufton, J. R. Why Does the Linear Driving Force Model for Adsorption Kinetics Work? *Adsorption* **2000**, *6*, 137–147.

(58) de Vrije, T.; Budde, M.; van der Wal, H.; Claassen, P. A. M.; López-Contreras, A. M. "*In Situ*" Removal of Isopropanol, Butanol and Ethanol from Fermentation Broth by Gas Stripping. *Bioresour. Technol.* **2013**, *137*, 153–159.

(59) Chen, Y.; Ren, H.; Liu, D.; Zhao, T.; Shi, X.; Cheng, H.; Zhao, N.; Li, Z.; Li, B. et al. Enhancement of *N*-Butanol Production by in Situ Butanol Removal Using Permeating–Heating–Gas Stripping in Acetone–Butanol–Ethanol Fermentation. *Bioresour. Technol.* **2014**, *164*, 276–284.

(60) Tan, T. C.; Gan, S. H. Vapour–Liquid Equilibrium of Water/Ethanol/1-Butanol/Salt: Prediction and Experimental Verification. *Chem. Eng. Res. Des.* **2005**, *83*, 1361–1371.

(61) Oudshoorn, A.; Peters, M. C. F. M.; van der Wielen, L. A. M.; Straathof, A. J. J. Exploring the Potential of Recovering 1-Butanol from Aqueous Solutions by Liquid Demixing Upon Addition of Carbohydrates or Salts. *J. Chem. Technol. Biotechnol.* **2011**, *86*, 714–718.

(62) Saravanan, V.; Waijers, D. A.; Ziari, M.; Noordermeer, M. A. Recovery of 1-Butanol from Aqueous Solutions Using Zeolite Zsm-5 with a High Si/Al Ratio; Suitability of a Column Process for Industrial Applications. *Biochem. Eng. J.* **2010**, *49*, 33–39.

(63) Ohlin, L.; Bazin, P.; Thibault-Starzyk, F.; Hedlund, J.; Grahn, M. Adsorption of Co2, Ch4, and H2o in Zeolite Zsm-5 Studied Using in Situ Atr-Ftir Spectroscopy. *J. Phys. Chem. C* **2013**, *117*, 16972-16982.

(64) Cao, Y.; Wang, K.; Wang, X.; Gu, Z.; Gibbons, W.; Vu, H. Butanol Vapor Adsorption Behavior on Active Carbons and Zeolite Crystal. *Appl. Surf. Sci.* **2015**, *349*, 1–7.

(65) Abdehagh, N.; Gurnani, P.; Tezel, F. H.; Thibault, J. Adsorptive Separation and Recovery of Biobutanol from Abe Model Solutions. *Adsorption* **2015**, *21*, 185–194.

(66) Krishna, R.; van Baten, J. M. Hydrogen Bonding Effects in Adsorption of Water−Alcohol Mixtures in Zeolites and the Consequences for the Characteristics of the Maxwell−Stefan Diffusivities. *Langmuir* **2010**, *26*, 10854-10867.

(67) Milestone, N. B.; Bibby, D. M. Concentration of Alcohols by Adsorption on Silicalite. *J. Chem. Technol. Biotechnol.* **1981**, *31*, 732–736.

Chapter 4: Prospects and challenges for the recovery of 2-butanol produced by vacuum fermentation: a techno-economic analysis

Abstract The conceptual design of a bio-based process for 2-butanol production is presented for the first time. Considering a hypothetical efficient producing strain, a vacuum fermentation is proposed to alleviate product toxicity, but the main challenge is the energy-efficient product recovery from the vapor. Three downstream scenarios were examined for this purpose: 1) multi-stage vapor recompression; 2) temperature swing adsorption; and 3) vapor absorption. The processes were simulated using Aspen Plus, considering a production capacity of 101 kton/yr. Process optimization was performed targeting the minimum selling price of 2-butanol. The feasibility of the different configurations was analyzed based on the global energy requirements and capital expenditure.

The use of integrated adsorption and absorption minimized the energy duty required for azeotrope purification, which represents 11% of the total operational expenditure in Scenario 1. The minimum selling price of 2-butanol as commodity chemical was estimated as 1.05 $/kg, 1.21 $/kg, and 1.03 $/kg regarding the fermentation integrated with downstream scenarios 1), 2), and 3), respectively. Significant savings in 2-butanol production could be achieved in the suggested integrated configurations if more efficient microbial strains were engineered, and more selective adsorption and absorption materials were found for product recovery.

Keywords: Biomaterials; bioprocess engineering; integrated product recovery; modeling; process economics

Abbreviations: CAPEX, total capital expenditure; **CEPCI**, chemical engineering plant cost index; **CW**, cooling water; **FCI**, fixed capital investment; **LPS**, low pressure steam; **MBSP**, minimum 2-butanol selling price; **MPS**, medium pressure steam; **OPEX**, total operating expenditure; **TDC**, total direct costs; **TIC**, total indirect costs; **TSA**, temperature swing adsorption; **VOC**, variable operating costs.

Published as: Pereira, J.P.C., Lopez-Gomez, G., Reyes, N.G., van der Wielen, L.A.M., and Straathof, A.J.J., Prospects and challenges for the recovery of 2-butanol produced by vacuum fermentation - a techno-economic analysis. *Biotechnol. J.* 2017, *12*, 1600657.

Contents

4.1 Introduction

The production of biofuels and commodity chemicals from biomass-derived feedstock has received increased attention in the last decade, mainly due to the sustainability and volatile cost of fossil feedstocks. Although various bio-based chemicals have reached high market shares, with alcohols (ethanol, 1-butanol, isobutanol) and carboxylic acids (acetic, citric and lactic acid) as noticeable examples [1], the commercialization of bioprocesses is still hindered by low titers and yields, typically related to microbial robustness and product toxicity [2]. The fermentation products must be kept below inhibiting concentrations to avoid microbial inhibition, but then purification of diluted product, for instance by conventional distillation, becomes highly energy-consuming [3]. For this reason, it has been estimated that productivities below 2.0 g/(L h) are unfeasible for industrial production of commodity chemicals, as they lead to high capital costs [4].

To overcome these issues, in addition to strain engineering for enhanced product tolerance and yield [5,6], several *in situ* product recovery techniques have been developed to alleviate product toxicity. Alternative vapor-based techniques, such as gas stripping [7-10] and vacuum stripping [11,12], have proved effective to circumvent inhibition, increase productivities, and reduce energy requirements in the recovery of volatile fermentation products, namely in ABE and ethanol fermentation. Gas stripping, however, relies on high gas flow rates and has low selectivity, while vacuum stripping enhances the relative volatility of products such as 1-butanol, resulting in higher selectivity and faster removal rates [12]. Most recently, hybrid strategies based on membrane-assisted vapor-stripping also revealed efficient for product recovery, providing higher selectivity and mass flux than other membrane-based technologies [13,14].

Albeit many studies have proved the technical feasibility of stripping, it is not yet clear how to efficiently recover the product from the vapor-phase, also containing significant amounts of CO_2 and water. Customarily, energy-intensive methods as condensation and distillation are used [14]. Therefore, finding more energy-efficient technologies to recover fermentation products from the stripped vapor is crucial for process development.

The aim of this study is to evaluate and compare the techno-economic feasibility of promising separation technologies for efficient product recovery from stripped fermentation vapor. Compared to 1-butanol and isobutanol, the fermentative production of 2-butanol has been largely overlooked so far. We focused on 2-butanol, given its potential as biofuel and biocommodity chemical, which has attracted the attention of researchers over the last few years [15-17]. Among the different butanol isomers, 2-butanol is particularly interesting as biofuel

candidate, given its superior octane rating and lower boiling temperature. 2-Butanol is also the key intermediate for the potential bio-based production of methyl propionate, where the overall process involves the fermentation of lignocellulosic sugars into 2-butanol, pursuing a metabolic route via butanone (a.o.) [18]. Bio-based 2-butanol was first observed in the wine-making industry, produced by *Lactobacillus* strains able to dehydrate 2,3-butanediol into butanone, and hydrogenate the latter to 2-butanol [19]. Based on this observation, Ghiaci *et al.* [16] attempted to introduce 2-butanol production in *S. cerevisiae*. The production of 2-butanol was vestigial, mainly due to low precursor supply and low activity of the diol dehydratase, but the study suggested that the enzyme-expressing constructs were functional to be used in other hosts. Most recently, Chen *et al.* [17] extended the natural meso-2,3-butanediol pathway in *K. pneumoniae*, and achieved a titer of 1030 mg/L 2-butanol directly from glucose. Although the titers are still far from commercial targets, competitive strains can be reached in the near future if sufficient investment exists for strain development, similarly to what happened to 1,4-butanediol [20], a related fermentation product. Therefore, evaluating the prospects of the integrated production and recovery of 2-butanol is crucial to identify process bottlenecks and understand the process economics at an early stage. Engineering a strain to achieve competitive production levels, however, is outside the scope of the present study.

Herein, we use engineering software Aspen Plus (Aspen Technologies, Inc., USA) for simulation purposes, considering a production capacity of 101 kton/yr 2-butanol, and operating time of 8000 h/yr. A vacuum fermentation is proposed to prevent the severe inhibition of microbes by 2-butanol, when product concentration reaches about 1 wt.% [21]. Three distinct downstream scenarios for product recovery from the vapor-phase were investigated: 1) multi-stage vapor recompression train; 2) temperature swing adsorption; and 3) vapor absorption combined with multicomponent distillation. The performance of each configuration was evaluated based on global energy requirements and capital expenditure. Process optimization was investigated aiming at the minimization of the product selling price. The economics were estimated from the outcome of each configuration under a consistent framework, and served as basis for a fair comparison among the different scenarios.

It is known that 2-butanol/water systems form a homogeneous azeotrope similar to that found in ethanol/water systems, and such mixtures cannot be separated using conventional distillation methods. By contrast, 1-butanol/water systems form a heterogeneous azeotrope that facilitates the purification of 1-butanol up to 99.9 wt.% by conventional distillation combined with decantation [3]. Even though, purifying a feed containing 1 wt.% 1-butanol requires 36 MJ/kg 1-

butanol, a value as high as its energy content [22], which makes conventional distillation unfeasible for dilute solutions. Thus, we discarded such conventional configuration for 2-butanol recovery, since it was proven poor a *priori*. Based on the thermodynamic properties of 1-butanol/water mixtures, adsorption and liquid-liquid extraction have been often suggested as attractive recovery options, presenting high selectivity for 1-butanol and low energy requirements [22,23]. Although several adsorbent materials have been identified for the selective recovery of 1-butanol from fermentation broths, namely activated carbon F-400 [24], silicalite pellets [25], high-silica zeolite CBV28014 [26] and poly(styrene-co-divinylbenzene) resins [27], only few studies focused on alcohol adsorption from vapor phase [28,29]. Extraction has also been thoroughly investigated [30-33], and it has been suggested to offer significant energy savings over distillation [23]. Ionic liquids and alcohols, namely Guerbet alcohols, depicted the highest capacities with fair selectivity for 1-butanol [32]. The adsorption or absorption of 2-butanol from fermentation vapor is expected to avoid well-known process bottlenecks occurring with fermentation medium, namely fouling of the adsorbent, emulsion formation, and extractant accumulation and toxicity in the fermentation [32].

4.2 Materials and methods

The process models were developed using engineering software Aspen Plus® V8.8 (Aspen Technologies, Inc., USA). MATLAB® R2014b (The MathWorks, Inc., USA) was used to determine the parameters in the adsorption isotherms and fermentation kinetics, and to optimize the bioreactor productivity. The thermodynamic model used to describe vapor-liquid equilibrium (VLE) was the modified UNIFAC group contribution model, accounting for the non-idealities in dilute 2-butanol/water mixtures. The model predictions were compared against experimental data with good correlation. The NRTL (non-random two-liquid) model was used to predict the liquid-liquid equilibrium (LLE) in phase separation, using the pure component parameters taken from the LLE-Aspen database. The McCabe-Thiele method was used to analyze binary distillations. The overall design procedure followed the guidelines provided by Seider *et al*. [34] and Humbird *et al*. [35]. Flowsheet analysis provided the mass and energy balances from which the feedstock and energy requirements were calculated. The utilities considered in the process design are LPS (2 bar/125°C), MPS (17 bar/210°C), CW, and electricity. Heat integration was performed by pinch analysis to optimize the energy duty in each scenario [36]. The scenarios were designed under the same underlying assumptions, and can be fairly compared based on the

MBSP determined for each case. Issues related to biomass pretreatment, substrate utilization, and waste management are not taken into account in the present study.

4.2.1 Vacuum fermentation with in situ stripping

A continuous vacuum fermentor was simulated using a stoichiometric reactor model combined with a flash vessel, both set at 33°C and 0.066 bar. An aqueous mixture containing 120 g/L glucose is fed into the bioreactor, as an attempt to mimic the typical sugar concentration of corn stover hydrolysate. Given the fact that no experimental data are available to support the current process design, the microbial growth rate (0.03 h^{-1}), maximum growth rate (0.26 h^{-1}) and half-velocity constant (0.2 g/L) were assumed based on reasonable values [37]. Also, strain engineering is currently focused on the metabolic pathway optimization, aiming at the minimization of by-product formation. If the required metabolic rates are achieved, other metabolic products can be neglected. The overall process reaction is depicted in equation (1). Based on previous considerations [4], a volumetric productivity of 2.0 g/(L h) was assumed. Equilibrium is reached between the liquid and the vapor phases in the bioreactor, and the flash vessel is used to perform phase separation while upholding the vacuum pressure. Two distinct 2-butanol-containing phases are obtained from this configuration: the dilute aqueous broth is first centrifuged for biomass separation/recycle and sent to a distillation task for product recovery, while the enriched vapor is sent to one of the downstream processing scenarios enumerated below. Due to the vacuum pressure, the amount of CO_2 dissolved in the liquid was neglected.

$$C_6H_{12}O_6 + 0.084NH_4^+ \rightarrow 0.420CH_{1.8}O_{0.5}N_{0.2} + 0.926C_4H_{10}O + 1.874CO_2 + 1.115H_2O + 0.084H^+ \quad (1)$$

4.2.2 Integrated vapor-phase product recovery

4.2.2.1 Scenario 1: multi-stage vapor recompression train, combined with decantation and distillation

Scenario 1 combines the aforementioned vacuum fermentation with a multi-stage recompression train, where the CO_2 is removed from the 2-butanol-enriched vapor mixture. The design has been optimized aiming at the lowest energy consumption, and the process flow diagram is shown in Fig. 1. The recompression train is comprised of 4 stages in which the pressure is increased step-wise up to atmospheric pressure. The isentropic efficiency was

assumed as 0.8. The condensate stream is sent to a decanter at 33°C (D-401), where the solubility properties of the 2-butanol/water mixture facilitate phase separation into an aqueous and an organic phase. The aqueous phase is subsequently sent to a distillation task (C-401), along with the centrifuged broth from the fermentor. In the distillation, a near-azeotropic 2-butanol/water mixture is obtained, containing 72.5 wt.% 2-butanol. This is combined with the organic phase from the decanter to obtain the final product (70.6 wt.% 2-butanol).

In the recompression train, losses up to 5% of 2-butanol occurred along with the discharged CO_2. To minimize these losses, a countercurrent absorption unit was designed (C-501), using recycled water as absorbent.

4.2.2.2 Scenario 2: temperature swing adsorption, coupled to distillation

Scenario 2 combines the vacuum fermentation with a temperature swing adsorption task. A preliminary screening was performed to find a suitable adsorbent for the selective recovery of 2-butanol. Based on reported adsorption capacities, hydrophobicity, and efficiency of regeneration [24-27], four different adsorbents were tested: powdered high-silica zeolite CBV28014, provided by Zeolyst International (USA); silicalite pellets HiSiv3000 (1/16), provided by UOP Molsiv Adsorbents (USA); activated carbon FILTRASORB 400 (F-400), supplied by Chemviron Carbon (Belgium); and polymeric resin SEPABEADS® SP207, supplied by Resindion S.R.L. (Italy). The pure compound isotherms were determined at 30°C for CO_2, water vapor, and 2-butanol vapor. Gas adsorption was performed by volumetric method, using a high-pressure gas adsorption system BELSORP-HP (BEL Japan, INC). Vapor adsorption was performed using a Quantachrome Autosorb 1C volumetric adsorption analyzer, equipped with a vapor-dosing system. Saturated vapor equilibrium experiments were performed in sealed, depressurized desiccators under controlled temperature.

In the process design, a fixed bed adsorption column with plug flow was considered. Overall mass and heat transfer coefficients were derived from well-known correlations and approximations according to the guidelines provided in the literature [38,39]. The linear driving force approximation was used to determine transfer resistances [40], and the low operating pressure allowed for the use of the ideal gas theory to describe the thermodynamic process.

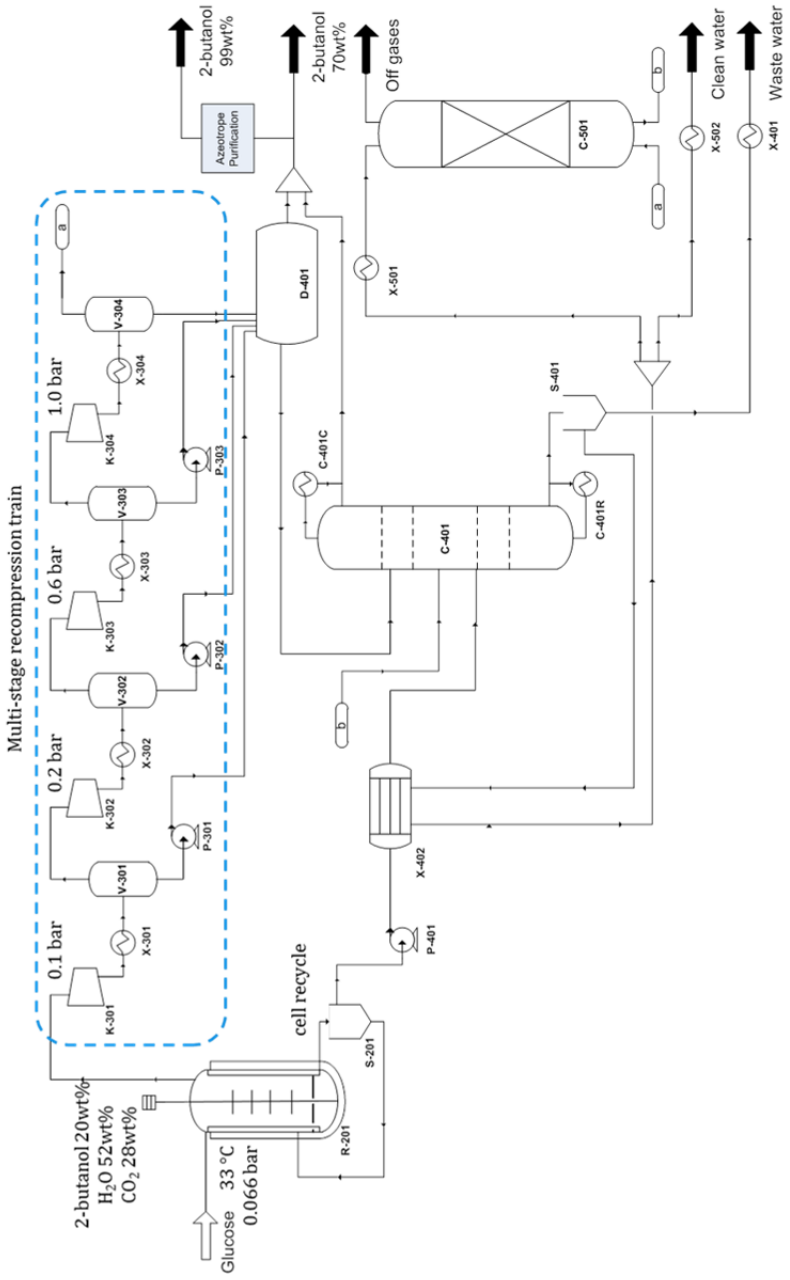

Figure 1. Process flow diagram for 2-butanol production using vacuum fermentation with *in situ* stripping, integrated with Scenario 1

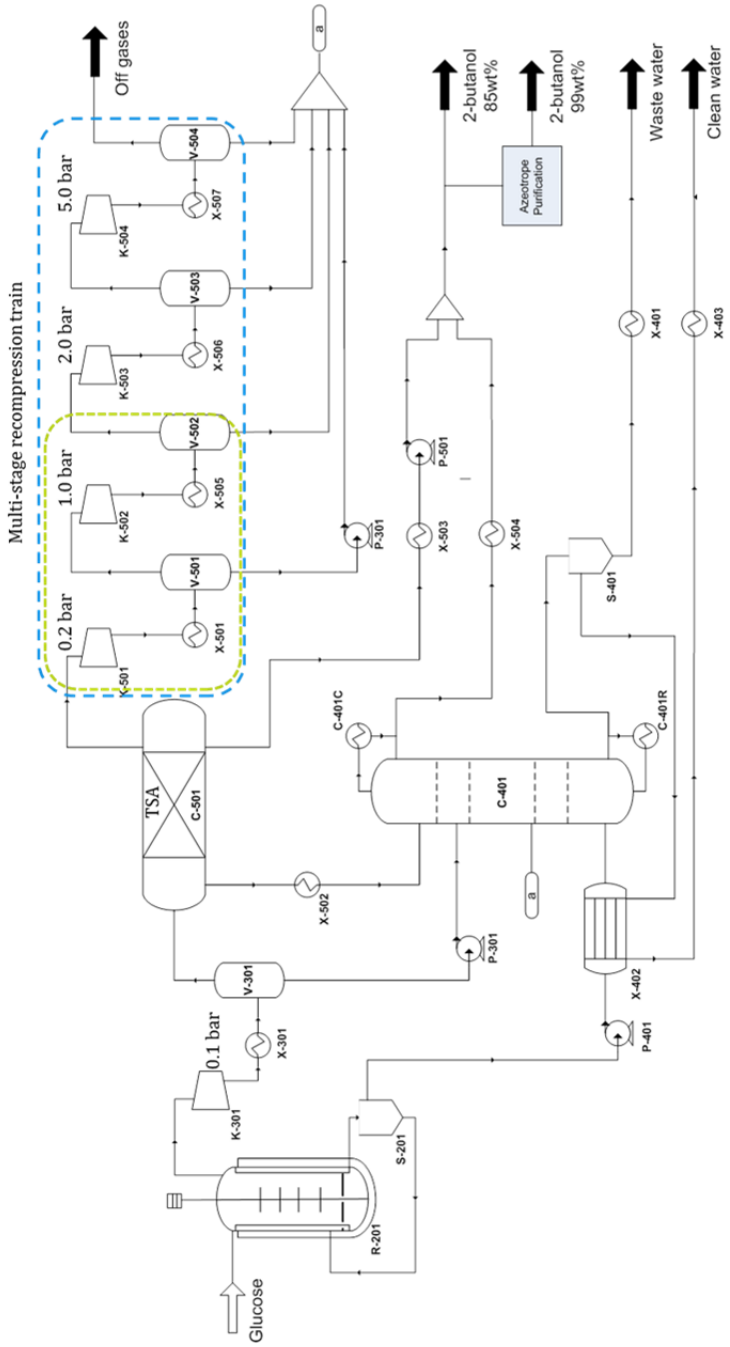

Figure 2. Process flow diagram for 2-butanol production using vacuum fermentation with *in situ* stripping, integrated with Scenario 2

Temperature swing adsorption (TSA) was used for adsorbent regeneration, assuming a cyclic steady state [38,39]. Temperature-programmed desorption was investigated to first recover the water at lower temperature, followed by 2-butanol recovery at higher temperature. The TSA cycles accounted for the following steps: i) adsorption; ii) water desorption; iii) 2-butanol desorption; and iv) cooling. Temperature control during adsorption and desorption was performed using cooling water and steam, respectively. 2-Butanol recovery has been primarily set as main target for the process design, however, to be used as commodity chemical, product purity must also be considered. Two approaches were thus investigated: *Ads1* and *Ads2*, aiming at the maximum product recovery (>99%) and product purity (99 wt.%), respectively.

In *Ads1*, the breakthrough limit was defined accounting for the loss of 0.5% 2-butanol, and the desorption step was tuned to avoid additional alcohol losses. In *Ads2*, the adsorption step time was set to maximize the adsorbed 2-butanol, taking advantage of competitive adsorption. The outcome of these approaches was compared based on adsorption performance indicators, namely product recovery, purity, productivity, and energy requirement, determined according to equations 2–5, respectively.

$$R = \frac{n_{BuOH,out}}{n_{BuOH,in}} \quad (2)$$

$$\alpha = \frac{n_{BuOH} M_{BuOH}}{\sum_i N_i M_i} \quad (3)$$

$$\eta = \frac{n_{BuOH} M_{BuOH}}{t m_{ads}} \quad (4)$$

$$E = \frac{Q}{n_{BuOH} M_{BuOH}} \quad (5)$$

The main parameters used in the simulation, namely properties of Silicalite HiSiv3000, 2-butanol, and water, can be found in the supporting data. The adsorption unit was first designed using ADSIM™, by simultaneously solving dynamic mass, heat and momentum balances, and further incorporated in Aspen Plus by means of a Sep block. A block flow diagram illustrating the modeling approach for Scenario 2 is shown in Fig. 2. As the streams resulting from the adsorption task in *Ads1* and *Ads2* differed on product composition, the downstream processing was adjusted for each option: in *Ads1*, the adsorption gas is compressed up to atmospheric

pressure in 2-stages before discharge, while in *Ads2* further compression up to 5.0 bar is required to fully recover the remaining product.

4.2.2.3 Scenario 3: vapor absorption, coupled to multicomponent distillation and decantation

Scenario 3 combines the vacuum fermentation with an absorption task, using a liquid with a high affinity for 2-butanol and low affinity for water and CO_2. Although suitable solvents exist for 1-butanol extraction [30-32,41], absorption studies are scarce [42,43], and 2-butanol extraction/absorption has been overlooked so far. Fortunately, when no experimental data are available, suitable solvents can be evaluated based on predictive group contribution methods [44]. First, we ranked the best solvents found in the literature for 1-butanol extraction based on their capacity, selectivity, and availability. Then, according to the methodology proposed by Gmehling and Schedemann [44], we used the modified UNIFAC model, along with the Raoult's law accounting for non-ideal solutions, to predict the distribution coefficient and selectivity of these solvents for a 2-butanol/water vapor mixture. The solvents with higher affinity for 2-butanol at 33ºC and 0.066 bar are shown in Table 1. Based on the results, 1-hexanol was chosen for the preliminary analysis, mainly because it is readily available, it has fairly high distribution coefficient and selectivity for 2-butanol, and it has the lowest boiling point, which might decrease operating costs in product purification via distillation.

Table 1. Estimated distribution coefficients D and selectivity S for 2-butanol (T=33°C, P=0.066 bar)

Solvent	D_{2-BuOH}	S_{2-BuOH}	T_b (°C)
3-Methyl-2,4-heptanediol	1.63	4.5	233.1
2-Ethyl-1,3-hexanediol	1.61	4.6	244.0
1-Hexanol	1.49	7.8	157.6
1-Heptanol	1.47	8.7	176.4
1-Octanol	1.46	9.5	195.2
1-Decanol	1.42	10.7	231.1
1-Dodecanol	1.39	11.6	259.0
2-Butyl-1-octanol	1.36	11.4	246.5

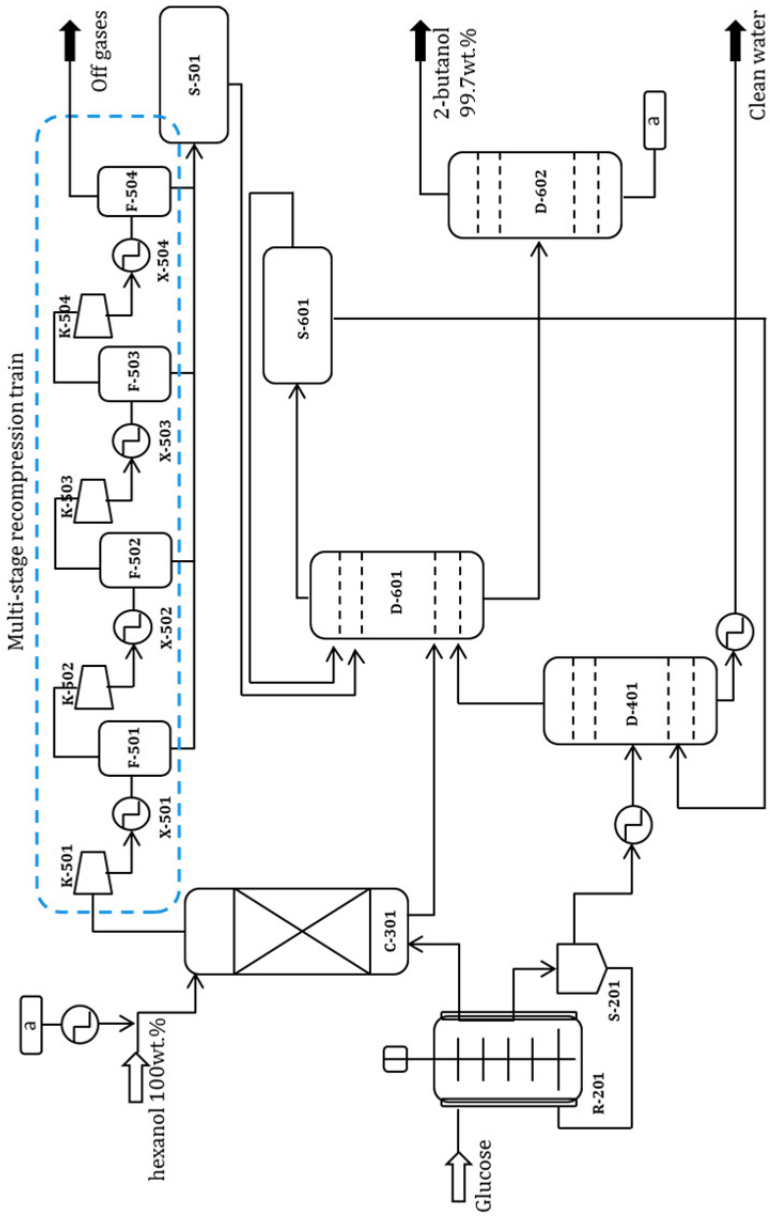

Figure 3. Process flow diagram for 2-butanol production using vacuum fermentation with *in situ* stripping, integrated with Scenario 3

The process flow diagram illustrating Scenario 3 is shown in Fig. 3. The absorption task was modeled using the RadFrac module in Aspen Plus. The vapor stream, at 33°C and 0.066 bar, is sent to the absorption task (C-301) where it is contacted with 1-hexanol (hereafter referred to as hexanol) in countercurrent flow, aiming at 99% 2-butanol recovery efficiency. At the absorption outlet, the vapor phase contains mostly CO_2, but also 2-butanol, hexanol, and water. It is thus sent to an optimized 4-stage recompression train, with an identical design to that described in Scenario 1. Three streams result from this unit operation: a gaseous stream containing 97.7 wt.% CO_2, an aqueous stream containing 99.4 wt.% water, and an organic stream containing 92.5 wt.% hexanol. The former two streams are discharged, and the latter is sent to the purification task. This unit operation, comprising two distillation columns (D-601/2) and a decanter (S-601), has been thoroughly investigated so that solvent and product were fully recovered and purified with minimum losses. Thus, the solvent is never contacted with the microbial hosts.

The first distillation column is used for water separation, and the bottom stream contains only hexanol and 2-butanol (2.5 wt.%), which are fully separated in the second distillation column. The distillate, on the other hand, contains 2-butanol (16.6 wt.%), hexanol (42.4 wt.%) and water (41.0 wt.%), and splits into two phases in the decanter. Both organic and aqueous phases are recycled back to distillation.

4.2.3 Azeotrope purification train

2-Butanol aqueous solutions are characterized by an azeotrope with an alcohol composition of ca. 68 wt.%, which restricts the use of conventional distillation for further product purification. In ethanol/water systems, extractive distillation is commonly applied to purify ethanol, using ethylene glycol as entrainer [45]. As the LLE behavior of aqueous 2-butanol solutions resembles that of ethanol, this approach was also investigated. A preliminary thermodynamic study was performed, and according to the LLE of the ternary mixture, complete regeneration of ethylene glycol was not possible, leading to an economically unfavorable process. Hexanol, on the other hand, showed great efficacy for 2-butanol separation (recall Scenario 3). The azeotrope purification train was thus designed using a configuration similar to that in the product purification task in Scenario 3, with hexanol as entrainer. The azeotrope is fed to a first distillation column, along with hexanol. The mixture of 2-butanol and hexanol obtained in the bottom is sent to a second distillation column, where pure 2-butanol (99 wt.%) and hexanol are

obtained. The distillate is a ternary mixture, which is sent to a decanter for phase separation. Both phases are recycled back to distinct columns in the distillation task for performance boost.

4.2.4 Economic analysis

The equipment sizing was defined based on the simulations results (see supporting data for more detail), and the economics were estimated for each scenario following well-known methodologies [34,35,46]. The purchase cost of most equipment was estimated from equipment cost databases, namely Matches (available from www.matche.com) and DACE [47], and adjusted using widely known correlations [34,46]. The cost of decanters and distillation columns was estimated using built-in cost models in Aspen. The purchase cost was corrected to current year using the CEPCI, and the installation cost was estimated using suitable factors from the literature [34,46]. Additionally, piping, warehouse, and site development were considered respectively as 4.5, 4.0, and 9.0% of the equipment purchase cost. These are the total direct costs (TDC). The total indirect costs (TIC) were determined as 60% of the TDC. Together, the TDC and TIC represent the fixed capital investment (FCI). The total capital expenditure (CAPEX) was finally determined based on the FCI and the working capital costs (5% of FCI).

The variable operating costs (VOC) were calculated based on the mass and energy balances resulting from the simulations. The feedstock price was estimated based on the sugar content in corn stover hydrolysate [35]. The adsorbent and absorbent costs were provided by suppliers. The cost of utilities was estimated based on consumption and corresponding CEPCI according to well-known methodologies [48]. The total operating expenditure (OPEX) was calculated based on the VOC and other additional fixed costs such as salaries, labor burden, maintenance, and insurance.

A discounted cash flow analysis was ultimately performed to determine the minimum 2-butanol selling price for each of the scenarios investigated, according to the NREL procedure [35]. The price of petrochemical 2-butanol was estimated as 1.59 $/kg, based on its precursors price in a 50-months interval (Straathof and Bampouli, unpublished data).

4.3 Results and Discussion

4.3.1 Vacuum fermentation with *in situ* stripping

The microbial productivity and maintenance rate in this process were determined as 0.065 $mol_P/(mol_X\ h)$ and 0.034 $mol_P/(mol_S\ h)$ respectively. It is important to recall that using cell

recycle in continuous bioreactors can lead to significantly improved productivity [49,50]. Thus, the fermentation performance was investigated and optimized based on a trade-off between cell density within the reactor (49.4 g/L), cell recycle (85%), and reactor volume (1963 m^3, from which 70% is working volume). These parameters were used in the detailed Aspen simulation. The volumetric productivity was enhanced to roughly 9.5 g/(L h), and while 83% of the produced 2-butanol leaves the fermentor as vapor, 17% of the total remains in the aqueous phase. As a result of the vacuum stripping, the concentration of 2-butanol in the aqueous phase was kept below inhibiting levels, around 7 g/L. After fermentation, other metabolic and lignocellulosic products may also be present. Vacuum stripping, however, is particularly suitable to recover products that are more volatile than water. Since the impurities expected to be found in the broth are usually nonvolatile, these will eventually be purged along with process wastewater (e.g. residual sugars). Volatile impurities that might be stripped (e.g. furans) are easily recoverable by distillation, but were not considered in this study for the sake of simplification.

4.3.1.1 Vacuum fermentation with *in situ* stripping integrated with Scenario 1

The solubility of 2-butanol in water (16.1 wt.% at 33°C), much higher than that of 1-butanol, added an unexpected complexity to product recovery and purification. Under the current operational conditions in the decanter, the concentrations obtained in the organic phase after phase-separation (67.8 wt.% 2-butanol) are lower than that of the azeotrope. This leads to a lower final product concentration, requiring higher energy requirement for product purification by distillation. The overall energy consumption without heat integration was 326.9 GJ/h, mainly due to the distillation task (43%) and the recompression train (29%). Taking advantage of heat integration, the energy duty was reduced to 192.3 GJ/h, determined based on the CW (134.4 GJ/h), LPS (49.8 GJ/h) and electricity (8.1 GJ/h) requirements. The recompression train used most of the electricity, and 62% of the total CW requirements. The first compression/condensation stage was the major CW consumer (38%), mostly due to the processing of large amounts of vapor at vacuum pressure.

For 2-butanol to be used as commodity chemical, the product requires further purification up to 99 wt.%. The capital costs related to the azeotrope purification train are defined from the material and energy balances. Interestingly, when determining the MBSP, the capital costs were not significant, since the yearly operational costs became dominant. Having this in mind, the costs related to the azeotrope purification train were considered as an additional utility. In Scenario 1, the final product contains 70.6 wt.% 2-butanol, slightly lower than the azeotrope

composition, and purification up to 99 wt.% results in additional energy consumption of 130.1 GJ/h. The utility requirements for this process add up to 0.106 $/kg-2-butanol. Overall, the energy duty estimated for this scenario is increased by 68% when 2-butanol is to be produced as commodity chemical, rendering 25.3 MJ/kg-2-butanol.

4.3.1.2 Vacuum fermentation with *in situ* stripping integrated with Scenario 2

Selective adsorption was observed for 2-butanol using silicalite HiSiv3000, for which the isotherm parameters, estimated using the Langmuir adsorption model, are depicted in Table 2. The maximum adsorption capacity appears to be similar for CO_2, water and 2-butanol vapor, but the affinities are widely different, as can be seen by the values of b_i: at 30°C and 0.066 bar, a very low affinity was observed for CO_2, while the highest affinity was found for 2-butanol. Due to this fact, CO_2 adsorption was neglected in the overall process design. The vapor adsorptive equilibrium behavior was described using the extended Langmuir equation [51] based on the pure compound isotherm data.

Table 2. Pure compound isotherm parameters estimated using the Langmuir model for the adsorption of CO_2, water vapor and 2-butanol vapor onto silicalite HiSiv3000 at 30°C

Parameter	CO_2	Water	2-butanol
$q_{max,i}$ (mg/g)	85.30	68.48	108.50
b_i (1/kPa)	0.0107	0.8297	40.944
R^2	0.998	0.943	0.973

Preliminary studies showed that pressure drop, coupled to particle size and mass transfer resistance, significantly limited the gas velocity within an adsorption column. Using the vapor stream directly from the fermentor, the maximum attainable gas velocity (0.08 m/s) led to an outsized cross section area (~2700 m^2). Trying to overcome this issue, the effect of partial condensation of the feed on the design was assessed. The molar and volumetric flows, as well as 2-butanol/water mole fractions, and energy and equipment requirements were analyzed for each option. To reduce the equipment requirements while keeping the adsorptive recovery of 2-butanol feasible, feed compression up to 0.1 bar is recommended. Further compression increases the energy duty, without significantly improving the process. The effect of the vapor feed velocity on the adsorption performance was also simulated, and the best compromise

between cross section area reduction and adsorption capacity was obtained using a vapor velocity of 0.15 m/s, which resulted in a column with a so-called pancake geometry. In such cases, when large cross section areas are required, the use of horizontal vessels is recommended [52]. Accordingly, the feed was distributed through 30 adsorption units, running in parallel. Using the selected design parameters, isothermal adsorption was simulated, and the results are shown in Fig. 4. Despite the low concentration of 2-butanol in the feed, both water and 2-butanol are adsorbed at nearly the same rate at the beginning of the process (Fig. 4A). Given the higher silicalite selectivity for 2-butanol, this is strongly adsorbed when reaching the available adsorption sites, while water flows to the subsequent layers. However, as the 2-butanol adsorption front reaches the water-saturated layers, competitive adsorption takes place, and water is displaced by 2-butanol. This is particularly clear at t > 1 h, when the amount of adsorbed water in the column decreases almost linearly, whereas adsorbed 2-butanol increases until saturation is reached. The water displacement induced by competitive adsorption is also observed in the breakthrough curve (Fig. 4B): the amount of water in the effluent increases steeply, becoming higher than that in the feeding mixture, which indicates additional water desorption. This phenomenon, known as "roll-up", has also been reported in previous adsorption studies using butanol/water mixtures [53].

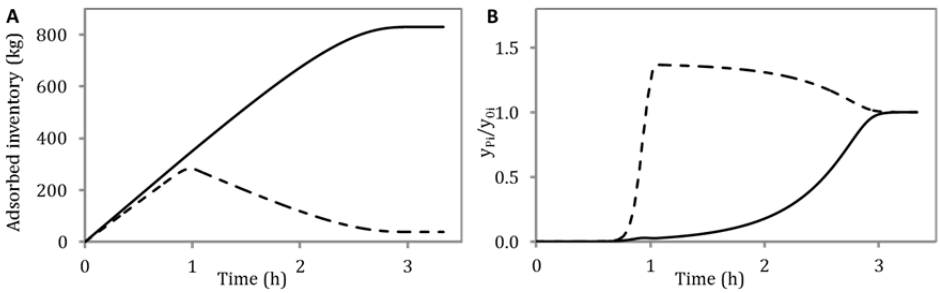

Figure 4. Isothermal adsorption of a 2-butanol (solid line)/water (dashed line) vapor mixture at 33°C, as simulated in ADSIM: (**A**) adsorbed component inventory; (**B**) breakthrough curves

2-Butanol recovery efficiency was found to be very sensitive to the temperature at which water desorption was performed, particularly above 60°C, and thus this temperature was not exceeded. Alcohol dehydration by zeolite catalysis was considered when selecting the temperature for 2-butanol desorption. Despite the fact that dehydration of 1-butanol to 1-butene was observed in zeolite material (ZSM-5) at temperatures higher than 118°C [54], 2-

butanol hardly reacted without a catalyst over several mesoporous materials in the range of 150–350°C [55]. As a precaution, 2-butanol desorption was performed at 180°C. Upon complete desorption, the bed was cooled to 33°C before the next cycle. It was observed that, using this TSA configuration, the adsorbates were almost fully desorbed in both cases, and only a small amount of water and 2-butanol (<1%) remained loaded onto the adsorbent. According to simulations, this had a minor effect on the efficiency of the subsequent cycles. The performance of configurations *Ads1* and *Ads2* was compared based on the indicators depicted in Table 3.

Table 3. Performance indicator values determined for the adsorption task, considering two adsorption options: maximum product recovery (99%), and maximum product purity (99 wt.%)

Parameter		*Ads1*	*Ads2*
R	(%)	99.6	89.2
α	(wt.%)	69.8	98.7
η	(kg_{BuOH}/(h ton_{ads}))	0.54	0.74
Heating duty	(MJ/cycle)	2305	2610
E	(MJ/kg_{BuOH})	7.6	3.8
TSA duration	(h)	2.8	4.2

By defining the adsorption step time as 2.2 h in *Ads2*, as opposed to *Ads1* (0.9 h), the water was desorbed by displacement, and the 2-butanol concentration in the column was maximized. It is clear that, despite the larger TSA cycle time required for *Ads2*, this appears as the most effective option: the recovery efficiency is roughly 10% lower, but the productivity increased by 37% when compared to *Ads1*, reducing by half the energy requirements per kilogram of 2-butanol produced. Both *Ads1* and *Ads2* were incorporated in the overall process simulations in Aspen. In *Ads1* 2-butanol is fully adsorbed in the column, and thus the effluent resulting from water desorption, as well as the gaseous stream, are sent out of unit's battery limits, with negligible loss of product. In *Ads2*, due to the water displacement phenomenon, these effluents contain a significant amount of 2-butanol (4.0% and 4.3% respectively). The gaseous stream is hence compressed in an optimized 4-stage train up to 5 bar to recover all the product. The effluent resulting from 2-butanol desorption, containing 69.8 wt.% 2-butanol in *Ads1*, and 98.7 wt.% 2-butanol in *Ads2*, is ultimately combined with the azeotropic mixture from distillation. The overall energy requirement was estimated as 277.8 GJ/h in *Ads1* and 215.3 GJ/h in *Ads2.* The lower value in *Ads2* results from the cooling/heating requirements related to the adsorption task, 2.2

times lower than in *Ads1*. Similarly to what was observed in Scenario 1, the compression/condensation tasks are the major expenditures for electricity and CW, adding up to 32% and 46% of the total energy duty in *Ads1* and *Ads2*, respectively. Overall, the final products from *Ads1* and *Ads2* contain 70.4 wt.% and 85.1 wt.% 2-butanol, respectively. Further purification up to 99 wt.% was investigated, using the same approach as in Scenario 1 (recall the azeotrope purification train). Remarkably, the final 2-butanol concentration in *Ads2* exceeds that of the azeotrope, and the energy requirements for product purification drop by half: 63.7 GJ/h against 131.0 GJ/h in *Ads1*. As a result, the overall energy duty per unit mass of product is 32% lower in *Ads2,* rendering 21.9 MJ/kg-2-butanol.

4.3.1.3 Vacuum fermentation with *in situ* stripping integrated with Scenario 3

The distribution coefficients and 2-butanol selectivity in a ternary mixture containing water/2-butanol/solvent were estimated by means of the UNIFAC model, which has provided reliable estimates for the LLE of ternary mixtures comprising water/1-butanol and the solvents tested herein [31], and thus a similar level of accuracy can be assumed in this case.

The process design was first assessed using the alcohol with lower boiling point, hexanol, aiming at the maximum product recovery. The outcome of Scenario 3 is a stream containing 99.3 wt.% 2-butanol, in which more than 99% of the product is recovered. To achieve this performance, a solvent flow of 510825 kg/h is required in the absorption column. Although most of the solvent is recovered and recycled within the process, the make-up flow required is 185 kg-hexanol/h. The breakdown of the energy consumption per unit operation is depicted in Fig. 5.

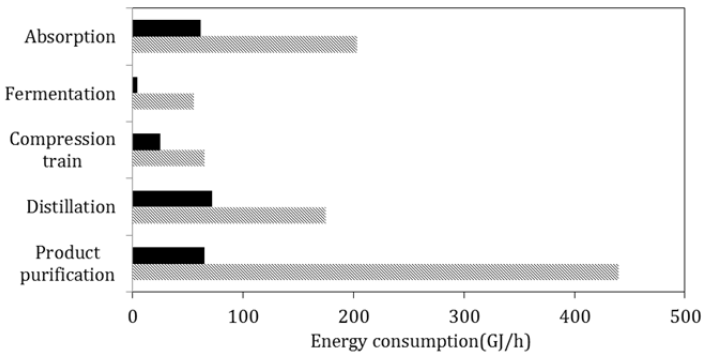

Figure 5. Breakdown of the energy consumption with (solid fill) and without (pattern fill) heat integration per unit operation in Scenario 3

Without heat integration, the overall energy requirements for the process were as high as 936.2 GJ/h, mainly due to the duty of the purification task (47%). To minimize the energy duty, heat integration was implemented considering the flows of the three distillation columns involved in the overall process, the streams from the absorption column, and the feed to the fermentor. The greatest energy savings were observed for the absorption task (90%), as the main duty was related to solvent cooling. The overall energy duty after heat integration decreased to 458.7 GJ/h, 64% of which is due to the product purification. As an attempt to further improve the overall economics, the operating conditions affecting the process were inspected and optimized, aiming at the MBSP (more details can be found in the supporting data). First, the pressures and temperatures used in each distillation column (distillation and purification tasks) were adjusted to enhance heat integration. By performing the first distillation in the purification task under vacuum (0.066 bar), instead of atmospheric pressure, larger equipment is required, leading to an increase of 22% in the capital expenditure. However, the savings are reflected in the utility requirements, reducing the fermentation, distillation, and purification energy duties by 84%, 24%, and 46%, respectively. This decreased the overall energy duty to 316.8 GJ/h. Other opportunities for optimization were sequentially investigated, namely the minimum temperature gradient used to perform heat integration, and the operating temperature and pressure in the absorption task. Finally, the process design was assessed using a less volatile alcohol with higher selectivity, 1-decanol. Lowering the temperature gradient used for heat integration increases the heat exchanger size and thus the equipment costs; on the other hand, the steam and cooling requirements are reduced, for which the overall energy duty decreases by 8% when the gradient is decreased from the original 10°C to 5°C. Additional energy savings were observed when the absorption operating conditions were explored: decreasing the absorption feed temperature from 33°C to 15°C saved 20% on the energy duty, and reduced the MBSP by 7%. This is mainly justified by the higher distribution coefficient for 2-butanol at lower temperatures, which reduced the solvent flowrate in the absorption task by 34%. Further optimization was achieved by partially compressing the feed of the absorption task. Curiously, the minimum product selling price was observed when the feed was compressed up to 0.085 bar. Above this pressure, the energy duty related to the compression step became dominant. At the optimized conditions, the overall energy requirements of Scenario 3 were 227.4 GJ/h (Fig. 5), equivalent to 17.6 MJ/kg-2-butanol.

Surprisingly, the use of 1-decanol as absorbent resulted in higher overall energy and equipment requirements, leading to an increased product selling price. Commonly, the use of high-boiling-point solvents such as oleyl alcohol [33], Guerbet alcohols [32], or ionic liquids [30,41] is suggested in the literature for 1-butanol recovery. Yet, it was herein observed that although solvent losses were minimized due to the lower volatility, the higher temperatures required in the distillation and solvent purification tasks led to increased energy consumption, such that the process became economically unfavorable.

4.3.2 Economic analysis

The estimated OPEX and CAPEX for the overall process considering the different downstream processing scenarios, are presented in Table 4, accounting for the variable and fixed costs. All the cases considered annual plant capacity of 101 kton 2-butanol with 99 wt.% purity, and overall product recovery of 99%. Given the better performance observed for *Ads2* as opposed to *Ads1*, the latter was precluded from further economic studies. In Scenario 2 and Scenario 3, the auxiliary phases used for product separation are also included as raw materials. Susarla *et al*. [56] assumed a lifetime of 1.5 years for zeolite material used in continuous vacuum swing adsorption. Since thermal regeneration is known to promote adsorbent degradation, 1 year was assumed for the silicalite under the current operational conditions. In Scenario 3, the energy duty is much lower than in the other scenarios considering the same product purity. This results largely from the scrupulous optimization involving important operating parameters and process integration, which decreased significantly the process variable costs.

The yearly operational cost was estimated as \$0.99, \$1.08 and \$0.97 per kg 2-butanol, considering the vacuum fermentation integrated with Scenario 1, Scenario 2, and Scenario 3, respectively. The hydrolysate was clearly the major cost regarding all the cases studied, within a range of 63–69% of the total OPEX. This is in agreement with other techno-economic analysis reporting that feedstock costs generally comprise the majority of the operational costs in biorefineries [57,58]. The azeotrope purification required in Scenario 1 and Scenario 2 is also a significant variable in the process, accounting respectively for roughly 11% and 5% of the yearly OPEX. Additionally, the adsorbent represents 9% of the operational expenditure in Scenario 2. In Scenario 3, on the other hand, the absorbent is a negligible part of the cost (3%).

Regarding the CAPEX, the installed equipment costs represent a share within 56–61% of the FCI. Among all the scenarios, the highest FCI was observed for Scenario 2 (79.3 M \$), driven by the

numerous adsorption units required for the TSA task. As expected, the lowest CAPEX was found for Scenario 1, given the absence of an auxiliary phase task for product recovery. In this scenario, the fermentation cost exceeds half of the installed equipment costs (56%). In Scenario 3, the absorption task is only a small fraction of the total CAPEX (8%), but the purification task represents 18% of the total capital, given the distillation units involved.

Table 4. Overall operational costs (M $/yr) and capital costs (M $) estimated for the production of 101 kton 2-butanol/yr using vacuum fermentation with *in situ* stripping integrated with each scenario

	Scenario 1	Scenario 2 *Ads2*	Scenario 3
Total variable costs	98.8	106.3	96.2
Total fixed operational costs	1.7	2.7	1.9
Total OPEX (M $/yr)	100.5	109.0	98.1
Total direct costs	14.2	49.5	18.6
Total indirect costs	8.6	29.7	11.2
Fixed capital investment	22.8	79.3	29.8
Total CAPEX (M $)	24.0	83.2	31.2
Minimum Selling Price ($/kg)	1.05	1.21	1.03

Based on the results, a discounted cash flow analysis has been performed so that the MBSP could be determined for the three scenarios. The MBSP estimated under the conditions described in this paper was determined as $1.05, $1.21, and $1.03 per kg 2-butanol for Scenarios 1, 2 and 3, respectively. The impact of the OPEX on the MBSP is significantly higher than that of the CAPEX: even though the CAPEX required for Scenario 3 is 30% higher than that required for Scenario 1, the annual costs are 2% lower, leading to a slightly lower MBSP in this case.

Having in mind that the hydrolysate cost represents most of the total OPEX in all the case-studies, the price volatility generally associated to this type of feedstock must also be taken into account throughout the project's lifetime. A simplified sensitivity analysis was conducted to investigate the effect of the hydrolysate price on the MBSP, by fluctuating its market price within the range of 6–55 $/ton. As expected, a strong linear correlation is observed between the

hydrolysate price and the MBSP (data not shown). Under these conditions, the 2-butanol selling prices ranged between 0.5–1.6 $/kg-2-butanol.

4.4 Concluding remarks

The technical and economic feasibility of 2-butanol recovery from fermentation vapor has been assessed in the present work, considering an anaerobic fermentation with *in situ* vacuum stripping, and three distinct integrated downstream processing scenarios. Since severe microbial inhibition occurs when 2-butanol concentrations reach 1 wt.%, only integrated product removal can improve titer, yield, and productivity. We believe that a rational design targeting fermentation integrated with product recovery can help achieve the goal of cost-effective bio-2-butanol production, which cannot be achieved using conventional methods in the present case. The energy requirements per kg of highly-pure 2-butanol (99 wt.%) were determined as 25.3 MJ/kg, 21.9 MJ/kg, and 17.6 MJ/kg considering Scenario 1, Scenario 2 and Scenario 3, respectively. The energy requirements for 1-butanol recovery have been previously estimated as 24 MJ/kg for steam stripping , 22 MJ/kg for gas stripping, 8 MJ/kg for adsorption, and 13 MJ/kg and 5 MJ/kg for extraction with oleyl alcohol and mesitylene, respectively [23,33]. Most recently, membrane-assisted vapor-stripping systems were found to be 65% more energy efficient than conventional distillation, but the stripping rate in these processes can be limited by the membrane flux, causing solvents to circulate back to the fermentor [13]. Other issues, such as membrane selectivity, thermal stability, and cleaning downtime, also affect process performance, and can lead to significantly increased production costs [59]. Even though the results herein presented for 2-butanol recovery systems are still far from the desired requirements, defined as 10% of its combustion energy (3.6 MJ/kg [23]), they are within the ranges reported for its isomer 1-butanol. Interestingly, Scenarios 2 and 3 partially avoided the azeotrope formation and revealed lower energy requirements than those reported for 1-butanol using steam stripping or gas stripping [23]. Additional savings could be achieved in these configurations if adsorbent stability and selectivity was improved in Scenario 2, or a more selective solvent with low boiling point would be used in Scenario 3. Still, the hydrolysate represents the most significant expenditure for all the scenarios.

Overall, the production of commodity chemicals via fermentation is still greatly hindered by the feedstock market price and the low product titers, and this study reflects the metabolic targets that must be achieved for the bio-based production of 2-butanol to be economically feasible.

Significant savings in 2-butanol production can only be reached if more efficient microbial strains are used in a suitably integrated configuration, such as the ones suggested herein.

4.5 Acknowledgements

The authors would like to acknowledge Filipe Vidal Lopes, Eduardo Andrés García, Yi Song, Max Zomerdijk and Stef van Hateren, for their wise advice and analytical support. This project is financially supported by The Netherlands Organization for Scientific Research (NWO) under the framework of Technology Area TA-Biomass.

4.6 Nomenclature

Δ	kJ/kmol	Enthalpy of adsorption
b	1/Pa	Langmuir affinity constant
b_0	1/Pa	Extended Langmuir affinity constant
C	kJ/(kmol °C)	Heat capacity
d	m^2/s	Diffusion coefficient
D	–	Distribution coefficient
E	MJ/kg_{BuOH}	Energy requirement
M	kg/kmol	Molecular weight
m	kg	Mass
n	kmol	Number of moles
P	bar	Pressure
Q	MJ	Heat
q	kg/kg_{ads}	Adsorbent capacity
R	–	Product recovery
r	µm	Particle size
T	°C	Temperature
t	h	Time
U	$W/(m^2 K)$	Heat transfer coefficient
x	–	Molar fraction in the liquid phase
Greek Symbols		
α	%	Product purity

η	$kg_{BuOH}/(h\ kg_{ads})$	Adsorption productivity
ρ	kg/m^3	Density
ε	–	Porosity
τ	–	Tortuosity
Subscripts		
ads		Adsorbent
b		Boiling
$BuOH$		2-butanol
$cool$		Cooling
$heat$		Heating
i		Component i
in		Inlet
max		Maximum
out		Outlet
p		Particle

4.7 References

(1) Straathof, A. J. J. Transformation of Biomass into Commodity Chemicals Using Enzymes or Cells. *Chem. Rev.* **2014**, *114*, 1871–1908.

(2) Qureshi, N.; Ezeji, T. C. Butanol, 'a Superior Biofuel' Production from Agricultural Residues (Renewable Biomass): Recent Progress in Technology. *Biofuels, Bioprod. Biorefin.* **2008**, *2*, 319-330.

(3) Vane, L. M. Separation Technologies for the Recovery and Dehydration of Alcohols from Fermentation Broths. *Biofuels, Bioprod. Biorefin.* **2008**, *2*, 553–588.

(4) Van Dien, S. From the First Drop to the First Truckload: Commercialization of Microbial Processes for Renewable Chemicals. *Curr. Opin. Biotechnol.* **2013**, *24*, 1061–1068.

(5) Atsumi, S.; Liao, J. C. Metabolic Engineering for Advanced Biofuels Production from *Escherichia Coli. Curr. Opin. Biotechnol.* **2008**, *19*, 414-9.

(6) Buijs, N. A.; Siewers, V.; Nielsen, J. Advanced Biofuel Production by the Yeast *Saccharomyces Cerevisiae. Curr. Opin. Chem. Biol.* **2013**, *17*, 480-488.

(7) Xue, C.; Zhao, J.; Lu, C.; Yang, S. T.; Bai, F.; Tang, I. C. High-Titer N-Butanol Production by *Clostridium Acetobutylicum* Jb200 in Fed-Batch Fermentation with Intermittent Gas Stripping. *Biotechnol. Bioeng.* **2012**, *109*, 2746-56.

(8) Xue, C.; Zhao, J.; Liu, F.; Lu, C.; Yang, S.-T.; Bai, F.-W. Two-Stage in Situ Gas Stripping for Enhanced Butanol Fermentation and Energy-Saving Product Recovery. *Bioresour. Technol.* **2013**, *135*, 396–402.

(9) de Vrije, T.; Budde, M.; van der Wal, H.; Claassen, P. A. M.; López-Contreras, A. M. "*In Situ*" Removal of Isopropanol, Butanol and Ethanol from Fermentation Broth by Gas Stripping. *Bioresour. Technol.* **2013**, *137*, 153–159.

(10) Lu, C.; Dong, J.; Yang, S. T. Butanol Production from Wood Pulping Hydrolysate in an Integrated Fermentation-Gas Stripping Process. *Bioresour. Technol.* **2013**, *143*, 467–475.

(11) Nguyen, V. D.; Auresenia, J.; Kosuge, H.; Tan, R. R.; Brondial, Y. Vacuum Fermentation Integrated with Separation Process for Ethanol Production. *Biochem. Eng. J.* **2011**, *55*, 208–214.

(12) Mariano, A. P.; Qureshi, N.; Filho, R. M.; Ezeji, T. C. Assessment of in Situ Butanol Recovery by Vacuum During Acetone Butanol Ethanol (Abe) Fermentation. *J. Chem. Technol. Biotechnol.* **2012**, *87*, 334–340.

(13) Xue, C.; Wang, Z.; Wang, S.; Zhang, X.; Chen, L.; Mu, Y.; Bai, F. The Vital Role of Citrate Buffer in Acetone–Butanol–Ethanol (Abe) Fermentation Using Corn Stover and High-Efficient Product Recovery by Vapor Stripping–Vapor Permeation (Vsvp) Process. *Biotechnol. Biofuels* **2016**, *9*, 146.

(14) Cai, D.; Chen, H.; Chen, C.; Hu, S.; Wang, Y.; Chang, Z.; Miao, Q.; Qin, P.; Wang, Z. et al. Gas Stripping–Pervaporation Hybrid Process for Energy-Saving Product Recovery from Acetone–Butanol–Ethanol (Abe) Fermentation Broth. *Chem. Eng. J.* **2016**, *287*, 1–10.

(15) Bramucci, M. G.; Flint, D.; Miller, E. S.; Nagarajan, V.; Sedkova, N.; Singh, M.; Van Dyk, T. K. Method for the Production of 2-Butanol. U.S. Patent 8426174, 2013.

(16) Ghiaci, P.; Norbeck, J.; Larsson, C. 2-Butanol and Butanone Production in *Saccharomyces Cerevisiae* through Combination of a B12 Dependent Dehydratase and a Secondary Alcohol Dehydrogenase Using a Tev-Based Expression System. *PLoS One* **2014**, *9*, e102774.

(17) Chen, Z.; Wu, Y.; Huang, J.; Liu, D. Metabolic Engineering of Klebsiella Pneumoniae for the De Novo Production of 2-Butanol as a Potential Biofuel. *Bioresour. Technol.* **2015**, *197*, 260–265.

(18) van Beek, H. L.; Romero, E.; Fraaije, M. W. Engineering Cyclohexanone Monooxygenase for the Production of Methyl Propanoate. *ACS Chem. Biol.* **2016**,

(19) Speranza, G.; Corti, S.; Fontana, G.; Manitto, P.; Galli, A.; Scarpellini, M.; Chialva, F. Conversion of Meso-2,3-Butanediol into 2-Butanol by Lactobacilli. Stereochemical and Enzymatic Aspects. *J. Agric. Food. Chem.* **1997**, *45*, 3476–3480.

(20) Park, S. J.; Lee, S. H.; Lee, S. Y.; Lee, E. J. Mutants Having Capability to Produce 1,4-Butanediol and Method for Preparing 1,4-Butanediol. U.S. Patent 9096860, 2009.

(21) Pereira, J. P. C.; Verheijen, P. J. T.; Straathof, A. J. J. Growth Inhibition of S. Cerevisiae, B. Subtilis, and E. Coli by Lignocellulosic and Fermentation Products. *Appl. Microbiol. Biotechnol.* **2016**, *100*, 9069–9080.

(22) Xue, C.; Zhao, J.-B.; Chen, L.-J.; Bai, F.-W.; Yang, S.-T.; Sun, J.-X. Integrated Butanol Recovery for an Advanced Biofuel: Current State and Prospects. *Appl. Microbiol. Biotechnol.* **2014**, 3463–3474.

(23) Oudshoorn, A.; van der Wielen, L. A. M.; Straathof, A. J. J. Assessment of Options for Selective 1-Butanol Recovery from Aqueous Solution. *Ind. Eng. Chem. Res.* **2009**, *48*, 7325–7336.

(24) Abdehagh, N.; Tezel, F. H.; Thibault, J. Adsorbent Screening for Biobutanol Separation by Adsorption: Kinetics, Isotherms and Competitive Effect of Other Compounds. *Adsorption* **2013**, *19*, 1263–1272.

(25) Águeda, V. I.; Delgado, J. A.; Uguina, M. A.; Sotelo, J. L.; García, Á. Column Dynamics of an Adsorption–Drying–Desorption Process for Butanol Recovery from Aqueous Solutions with Silicalite Pellets. *Sep. Purif. Technol.* **2013**, *104*, 307–321.

(26) Oudshoorn, A.; van der Wielen, L. A. M.; Straathof, A. J. J. Adsorption Equilibria of Bio-Based Butanol Solutions Using Zeolite. *Biochem. Eng. J.* **2009**, *48*, 99–103.

(27) Nielsen, D. R.; Prather, K. J. In Situ Product Recovery of N-Butanol Using Polymeric Resins. *Biotechnol. Bioeng.* **2009**, *102*, 811–821.

(28) Hashi, M.; Thibault, J.; Tezel, F. H. Recovery of Ethanol from Carbon Dioxide Stripped Vapor Mixture: Adsorption Prediction and Modeling. *Ind. Eng. Chem. Res.* **2010**, *49*, 8733-8740.

(29) Cao, Y.; Wang, K.; Wang, X.; Gu, Z.; Gibbons, W.; Vu, H. Butanol Vapor Adsorption Behavior on Active Carbons and Zeolite Crystal. *Appl. Surf. Sci.* **2015**, *349*, 1–7.

(30) Ha, S. H.; Mai, N. L.; Koo, Y.-M. Butanol Recovery from Aqueous Solution into Ionic Liquids by Liquid–Liquid Extraction. *Process Biochem.* **2010**, *45*, 1899–1903.

(31) Kurkijärvi, A.; Lehtonen, J.; Linnekoski, J. Novel Dual Extraction Process for Acetone–Butanol–Ethanol Fermentation. *Sep. Purif. Technol.* **2014**, *124*, 18–25.

(32) Gonzalez-Penas, H.; Lu-Chau, T. A.; Moreira, M. T.; Lema, J. M. Solvent Screening Methodology for in Situ Abe Extractive Fermentation. *Appl. Microbiol. Biotechnol.* **2014**, *98*, 5915–5924.

(33) Kraemer, K.; Harwardt, A.; Bronneberg, R.; Marquardt, W. Separation of Butanol from Acetone–Butanol–Ethanol Fermentation by a Hybrid Extraction–Distillation Process. *Comput. Chem. Eng.* **2011**, *35*, 949–963.

(34) Seider, W. D.; Seader, J. D.; Lewin, D. R. *Product and Process Design Principles: Synthesis, Analysis and Design*, Wiley Global Education, 2008.

(35) Humbird, D.; Davis, R.; Tao, L.; Kinchin, C.; Hsu, D.; Aden, A.; Schoen, P.; Lukas, J.; Olthof, B. et al. *Process Design and Economics for Biochemical Conversion of Lignocellulosic Biomass to Ethanol - Dilute-Acid Pretreatment and Enzymatic Hydrolysis of Corn Stover*, NREL - National Renewable Energy Laboratory, 2011.

(36) Kemp, I. C. *Pinch Analysis and Process Integration: A User Guide on Process Integration for the Efficient Use of Energy*, Elsevier Science, 2011.

(37) Jarzębski, A. B.; Goma, G.; Soucaille, P. Modelling of Continuous Acetonobutylic Fermentation. *Bioprocess Eng.* **1992**, *7*, 357-361.

(38) Bonjour, J.; Chalfen, J.-B.; Meunier, F. Temperature Swing Adsorption Process with Indirect Cooling and Heating. *Ind. Eng. Chem. Res.* **2002**, *41*, 5802–5811.

(39) Joss, L.; Gazzani, M.; Hefti, M.; Marx, D.; Mazzotti, M. Temperature Swing Adsorption for the Recovery of the Heavy Component: An Equilibrium-Based Shortcut Model. *Ind. Eng. Chem. Res.* **2015**, *54*, 3027–3038.

(40) Sircar, S.; Hufton, J. R. Why Does the Linear Driving Force Model for Adsorption Kinetics Work? *Adsorption* **2000**, *6*, 137–147.

(41) Simoni, L. D.; Chapeaux, A.; Brennecke, J. F.; Stadtherr, M. A. Extraction of Biofuels and Biofeedstocks from Aqueous Solutions Using Ionic Liquids. *Comput. Chem. Eng.* **2010**, *34*, 1406–1412.

(42) Chen, J.; Razdan, N.; Field, T.; Liu, D. E.; Wolski, P.; Cao, X.; Prausnitz, J. M.; Radke, C. J. Recovery of Dilute Aqueous Butanol by Membrane Vapor Extraction with Dodecane or Mesitylene. *J. Membr. Sci.* **2017**, *528*, 103-111.

(43) Liu, D. E.; Cerretani, C.; Tellez, R.; Scheer, A. P.; Sciamanna, S.; Bryan, P. F.; Radke, C. J.; Prausnitz, J. M. Analysis of Countercurrent Membrane Vapor Extraction of a Dilute Aqueous Biosolute. *AIChE J.* **2015**, *61*, 2795-2809.

(44) Gmehling, J.; Schedemann, A. Selection of Solvents or Solvent Mixtures for Liquid–Liquid Extraction Using Predictive Thermodynamic Models or Access to the Dortmund Data Bank. *Ind. Eng. Chem. Res.* **2014**, *53*, 17794–17805.

(45) Meirelles, A.; Weiss, S.; Herfurth, H. Ethanol Dehydration by Extractive Distillation. *J. Chem. Technol. Biotechnol.* **1992**, *53*, 181–188.

(46) Couper, J. R.; Penney, W. R.; Fair, J. R.; Walas, S. M. *Chemical Process Equipment: Selection and Design*, Elsevier Science, 2005.

(47) DACE *Price Booklet - Cost Information for Estimation Aand Comparison*, Michael Sprong, The Hague, 2014.

(48) Ulrich, G. D.; Vasudevan, P. T. How to Estimate Utility Costs. *Chem. Eng.* **2006**, 66–69.

(49) Malaviya, A.; Jang, Y.-S.; Lee, S. Y. Continuous Butanol Production with Reduced Byproducts Formation from Glycerol by a Hyper Producing Mutant of Clostridium Pasteurianum. *Appl. Microbiol. Biotechnol.* **2012**, *93*, 1485-1494.

(50) Zheng, J.; Tashiro, Y.; Yoshida, T.; Gao, M.; Wang, Q.; Sonomoto, K. Continuous Butanol Fermentation from Xylose with High Cell Density by Cell Recycling System. *Bioresour. Technol.* **2013**, *129*, 360-5.

(51) Markham, E. C.; Benton, A. F. The Adsorption of Gas Mixtures by Silica. *J. Am. Chem. Soc.* **1931**, *53*, 497–507.

(52) Woods, D. R. *Rules of Thumb in Engineering Practice*, Wiley, 2007.

(53) Sowerby, B.; Crittenden, B. D. Vapour Phase Separation of Alcohol-Water Mixtures by Adsorption onto Silicalite. *Gas Sep. Purif.* **1988**, *2*, 177–183.

(54) Saravanan, V.; Waijers, D. A.; Ziari, M.; Noordermeer, M. A. Recovery of 1-Butanol from Aqueous Solutions Using Zeolite Zsm-5 with a High Si/Al Ratio; Suitability of a Column Process

for Industrial Applications. *Biochem. Eng. J.* **2010**, *49*, 33–39.

(55) Jeong, S.; Kim, H.; Bae, J.-h.; Kim, D. H.; Peden, C. H. F.; Park, Y.-K.; Jeon, J.-K. Synthesis of Butenes through 2-Butanol Dehydration over Mesoporous Materials Produced from Ferrierite. *Catal. Today* **2012**, *185*, 191–197.

(56) Susarla, N.; Haghpanah, R.; Karimi, I. A.; Farooq, S.; Rajendran, A.; Tan, L. S. C.; Lim, J. S. T. Energy and Cost Estimates for Capturing Co2 from a Dry Flue Gas Using Pressure/Vacuum Swing Adsorption. *Chem. Eng. Res. Des.* **2015**, *102*, 354–367.

(57) Mariano, A. P.; Dias, M. O. S.; Junqueira, T. L.; Cunha, M. P.; Bonomi, A.; Filho, R. M. Butanol Production in a First-Generation Brazilian Sugarcane Biorefinery: Technical Aspects and Economics of Greenfield Projects. *Bioresour. Technol.* **2013**, *135*, 316–323.

(58) Moncada, J.; El-Halwagi, M. M.; Cardona, C. A. Techno-Economic Analysis for a Sugarcane Biorefinery: Colombian Case. *Bioresour. Technol.* **2013**, *135*, 533–543.

(59) Vane, L. M.; Alvarez, F. R. Effect of Membrane and Process Characteristics on Cost and Energy Usage for Separating Alcohol–Water Mixtures Using a Hybrid Vapor Stripping–Vapor Permeation Process. *J. Chem. Technol. Biotechnol.* **2015**, *90*, 1380-1390.

Chapter 5: Perspectives for the microbial production of methyl propionate integrated with product recovery

Abstract A new approach was studied for bio-based production of methyl propionate, a precursor of methyl methacrylate. Recombinant E. coli cells were used to perform a cascade reaction in which 2-butanol is reduced to butanone using alcohol dehydrogenase, and butanone is oxidized to methyl propionate and ethyl acetate using a Baeyer-Villiger monooxygenase (BVMO). Product was removed by in-situ stripping. The conversion was in line with a model comprising product formation and stripping kinetics. The maximum conversion rates were 1.14 g-butanone/(L h), 0.11 g-ethyl acetate/(L h), and 0.09 g-methyl propionate/(L h). The enzyme regioselectivity towards methyl propionate was 43% of total ester. Starting from biomass-based production of 2-butanol, full-scale ester production with conventional product purification was calculated to be competitive with petrochemical production if the monooxygenase activity and regioselectivity are enhanced, and the costs of bio-based 2-butanol are minimized.

Keywords: Biomaterials; bioprocess engineering; integrated product recovery; modeling

---

Published as: Pereira, J.P.C., van der Wielen, L.A.M., and Straathof, A.J.J., Perspectives for the microbial production of methyl propionate integrated with product recovery. *Bioresour. Technol.* 2018, *256*, 187–194.

Contents

5.1 Introduction

Polymethyl methacrylate (PMMA) is a valuable thermoplastic known for its excellent performance characteristics, and its vast application in several fields [1]. Its market size is expected to exceed USD 11 billion by 2022 [2]. Nonetheless, industrial production methods rely on fossil carbon sources and precious metal catalysts, and generate greenhouse gases [3,4]. To mitigate these issues, the producers seek opportunities for biomass-based approaches for methyl methacrylate production.

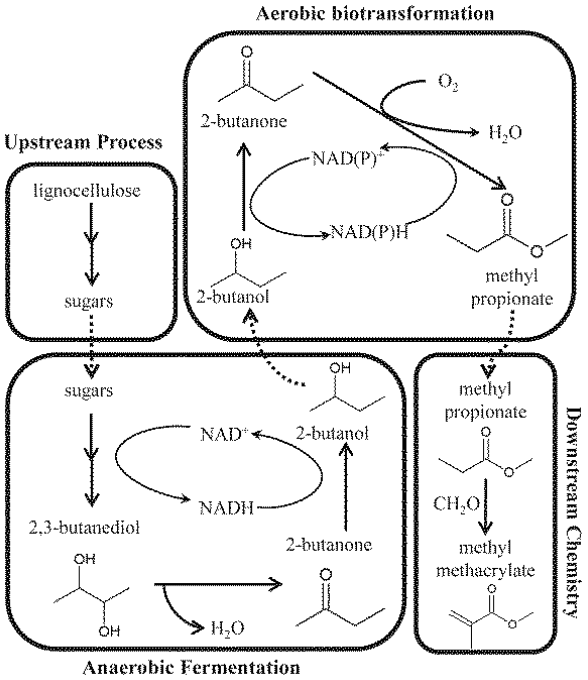

Figure 1. Pathway for the production of methyl methacrylate from lignocellulose via 2-butanol and methyl propionate

In the present work, we propose a pathway for biomass-based methyl methacrylate that comprises a series of reactions under distinct oxygen regimes, which is summarized in Fig. 1.

First, fermentable sugars such as lignocellulosic hydrolysate are converted into butanone by anaerobic fermentation [5,6]. This fermentation includes butanone conversion into 2-butanol by a suitable NADH-dependent alcohol dehydrogenase (ADH), to generate the essential NAD^+

required for closing the redox balance. The conditions for profitable bio-based 2-butanol production have been determined [7]. Next, in an aerobic biotransformation, 2-butanol is oxidized back to butanone by a $NADP^+$-dependent ADH, and butanone is further oxidized by O_2 using cyclohexanone monooxygenase (CHMO). CHMO inserts one oxygen atom in butanone, while the other atom is reduced with NADPH to water. Although oxygen insertion next to the most substituted carbon yields the so-called normal product, ethyl acetate, the regioselectivity of this reaction has been shifted to the abnormal product, methyl propionate [8]. Methyl propionate is finally condensed with formaldehyde to form methyl methacrylate, in a downstream chemistry step which is outside the scope of this study, as it resembles the last part of the existing Alpha process for methyl methacrylate production [9].

The current research evaluates an integrated biotransformation for methyl propionate production, aiming to identify the major process bottlenecks at an early stage of strain engineering and process design. Recombinant *Escherichia coli* cells expressing two distinct fused redox-complementary enzymes [10] have been used to determine the conversion rate of 2-butanol and identify the rate-limiting step in the cascade reaction.

As this is a strictly aerobic conversion, the continuous aeration promotes the stripping of the volatile biotransformation products along with the exhaust gas. Although stripping is useful to alleviate product toxicity and enhance product recovery costs [11,12], uncontrolled product loss makes the ester quantification a challenging task, demanding full understanding of the stripping process. Using stripping and product formation kinetics, the performance of a conceptual 120 kton/a process for bio-based methyl propionate production will be assessed.

The inevitable by-product, ethyl acetate, is an environmentally friendly solvent with broad application range, and its commercial value is close to that of methyl propionate itself [13]. Despite its current petrochemical-based production, numerous yeast species are natural ethyl acetate producers, particularly *Kluyveromyces marxianus* with an outstanding formation rate of 0.67 g/g/h, and 56% of the maximum theoretical yield [14]. Recently, Kruis et al. [15] reported ethyl acetate production using recombinant *E. coli*, reaching 33% of the maximum theoretical yield. In the two-step process proposed herein, the maximum achievable theoretical yield is 0.453 $g_{ester}/g_{glucose}$, similar to that of direct glucose conversion [16]. This suggests the high potential of the proposed process for bio-based ester production.

5.2 Material and methods

5.2.1 Bacterial strains and culture media

Fusion constructs containing the cyclohexanone monooxygenase (TmCHMO) gene from *Thermocrispum municipale*, and either the alcohol dehydrogenase TbADH obtained from *Thermoanaerobacter brockii*, or the MiADH obtained from *Mesotoga infera*, have been developed by Aalbers and Fraaije [10]. *E. coli* NEB® 10-beta cells (New England Biolabs), harboring the plasmids which contained the gene fusions, were kindly provided by the Molecular Enzymology Group, Groningen Biomolecular Sciences and Biotechnology Institute.

Recombinant cells from -80°C glycerol stocks were used in the experiments. Pre-cultures were first grown overnight at 37°C and 200 rpm, in 15 mL Luria Broth (LB) medium containing 10.4 g/L tryptone peptone, 10.4 g/L sodium chloride, 4.8 g/L yeast extract, and 50 mg/L ampicillin.

Terrific Broth (TB) contained 12.0 g/L tryptone peptone, 24.0 g/L yeast extract, 5.0 g/L glycerol, 2.4 g/L KH_2PO_4, 12.5 g/L K_2HPO_4, and 50 mg/L ampicillin. Minimal Medium (MM) contained 3.0 g/L KH_2PO_4, 7.3 g/L K_2HPO_4, 2.0 g/L NH_4Cl, 5.0 g/L $(NH_4)_2SO_4$, 8.4 g/L MOPS, 0.5 g/L NaCl, 0.5 g/L $MgSO_4 \cdot 7H_2O$, 4.0 g/L glucose$\cdot H_2O$, and 1 mL/L trace element solution. The trace element solution contained 3.6 g/L $FeCl_2 \cdot 4H_2O$, 5.0 g/L $CaCl_2 \cdot 2H_2O$, 1.3 g/L $MnCl_2 \cdot 2H_2O$, 0.4 g/L $CuCl_2 \cdot 2H_2O$, 0.5 g/L $CoCl_2 \cdot 6H_2O$, 0.9 g/L $ZnCl_2$, 0.03 g/L H_3BO_4, 20.0 g/L $Na_2EDTA \cdot 2H_2O$, 0.1 g/L $Na_2MoO_4 \cdot 2H_2O$, and 1.0 g/L thiamine HCl. The media were supplemented with 50 mg/L ampicillin and 40 mg/L L-leucine, and the final pH was adjusted to 7 using 1 mol/L K_2HPO_4.

5.2.2 Methyl propionate formation in shake flasks

The pre-cultures were used to inoculate 50 mL of MM or TB medium (1% v/v) in 2 L polycarbonate baffled flasks with vent cap (Thermo Fisher), and these were incubated at 24°C and 200 rpm. When the optical density at 600 nm (OD600) reached 0.5, L-arabinose and 2-butanol (Sigma-Aldrich, the Netherlands), were added to final concentrations of 0.2 g/L and 0.75 g/L, respectively. Samples for metabolite analysis were taken immediately, 24 h, and 40 h after induction. The samples were centrifuged at 4000 g for 10 min, and both supernatant and cell pellet were stored at -20°C until further analysis. The experiments were performed in duplicate.

5.2.3 Ester formation integrated with product recovery

5.2.3.1 Preliminary gas stripping studies

To characterize the *in-situ* removal of biotransformation products by gas stripping, model solutions were prepared using accurately weighed amounts of demi-water, 2-butanol, butanone, methyl propionate, and ethyl acetate (Sigma-Aldrich, the Netherlands).

Before each experiment, the glassware was cleaned with water and soap, dried overnight at 70°C, and accurately weighed at room temperature. A 3.0 L Biostat fermentor (Applikon, the Netherlands), fitted with typical sensors for dissolved oxygen, temperature, pressure, and pH, was used with a working volume of 1.0 L. The reactor was operated at 24.0±0.5°C, 500 rpm, and the air flow was varied between 1–2.5 vessel volumes per minute (vvm). The off-gas port of the reactor was attached to the condensation system (Fig. 2), which comprised an Erlenmeyer containing 128 g of butyl acetate in an ice bath, and a series of two 50 cm Graham-type condensers connected to 250 mL Erlenmeyer flasks, submerged in the cryostat at -7 °C (ECO RE 620, Lauda). Before being released to the atmosphere, the stripped vapor was additionally bubbled in 150 mL of chilled water in an ice bath.

The system was monitored using MFCS/win 3.0 software (Sartorius), and aqueous samples were collected hourly for GC analysis. Upon termination of the experiment, the volume, mass and composition of the media and condensates were determined. The experiments were performed in duplicate.

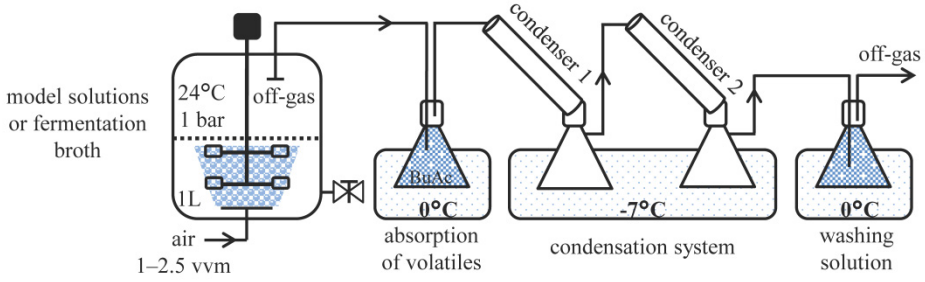

Figure 2. Schematic diagram of the experimental set-up for biotransformation integrated with *in-situ* product recovery by gas stripping and absorption

5.2.3.2 Biotransformation integrated with in-situ stripping and absorption

Ester biotransformation integrated with in-situ stripping and absorption was performed using the experimental set-up described in Fig. 2, under aseptic conditions. The reactor was operated at 24.0±0.5°C and 500 rpm, the air flow was 1 vvm, and the pH was controlled at 7.0±0.2 using either KOH (4 mol/L) or H_2SO_4 (0.5 mol/L). Pre-cultures were used to inoculate 1.0 L working volume of sterile TB or MM (10% v/v), supplemented with glycerol or glucose, respectively, to obtain 40 g/L of these carbon sources. Once the OD_{600} reached ~0.5, L-arabinose and 2-butanol were added. Samples from the bulk were collected hourly for metabolite analysis.

5.2.4 Analytical Methods

Cell growth was monitored by measuring the OD_{600} in a spectrophotometer (Biochrom Libra Instruments, Netherlands), and correlated to cell dry weight (CDW). CDW was determined by centrifuging 2 mL aliquots of several dilutions of broth in pre-weighed Eppendorf at 4000 g for 10 min, and drying the cell pellets at 70°C for 48 h before weighing.

To assess protein expression, cells grown in each medium were lysed using BugBuster Plus Lysonase™ solution (Novagen®). The cell pellet fraction was resuspended in 200 µL of KH_2PO_4 buffer (pH 7.5). Both supernatant and cell pellet fractions were loaded onto an SDS-PAGE gel (GenScript, Benelux), and analyzed according to the recommendations of the gel supplier.

Cell maintenance requirements were estimated from glucose consumption by non-growing cells during stationary phase. Glucose was quantified colorimetrically using the Megazyme Glucose Determination Reagent (Megazyme International Ireland). Glycerol was quantified by HPLC (Waters, USA), using an Aminex BioRad HPX-87Hf column (300 x 7.8 mm, particle size 9 µm) at 60°C, with phosphoric acid (147 mg/L) as eluent.

Aqueous concentrations of volatiles were determined via GC (InterScience, the Netherlands), using a Zebron™ ZB-WAX-PLUS column (30 m x 0.32 mm x 0.50 µm). 1-Pentanol (320 mg/L) was used as internal standard. The temperature was 30°C for 5 min, followed by a gradient of 20°C/min for 5 min. The temperatures of the injector and FI detector were 200°C and 250°C, respectively. Vapor concentrations of volatiles were determined via Compact GC 4.0 (InterScience, the Netherlands), using a Rtx®-1 column (30 m x 0.32 mm x 5.0 µm), with an isothermal program at 45°C for 14 min. For the low concentration range, an additional thermal desorption (TD) system, composed of a sorbent tube with Tenax® TA and a focusing trap U-T2GPH-2S, was used to concentrate the products.

5.2.5 Modeling studies

5.2.5.1 Integrated biotransformation and stripping of methyl propionate

The biotransformation model aims to describe the system where 2-butanol, butanone, ethyl acetate, methyl propionate, water, and O_2 are consumed/formed and stripped at specific rates. We consider batch mode with non-growing cells, but the equations can be modified to describe abiotic or continuous processes. Homogeneous vapor and liquid phases were assumed. The stripping of volatile biotransformation products has been modeled as a two-step process describing product transfer from the liquid to the vapor phase, followed by discharge via the off-gas (cf. Löser et al. [17] and Urit et al.[18]). The molar concentrations $C_{i,L}$ of each component i in the liquid phase, and respective molar fractions x_i, are:

$$C_{i,L} = \frac{n_{i,L}}{V_L} \quad (1)$$

$$x_i = \frac{n_{i,L}}{\sum n_{i,L}} \quad (2)$$

Analogously, the molar fractions in the vapor phase y_i are equal to:

$$y_i = \frac{n_{i,G}}{\sum n_{i,G}} \quad (3)$$

The following reactions are considered, assuming that cellular redox homeostasis is not limiting the reducing equivalent, NADPH, under non-growing conditions:

$$r_1: BuOH + NADP^+ \rightarrow But + NADPH + H^+ \quad (4)$$

$$r_2: But + O_2 + NADPH + H^+ \rightarrow MePr + H_2O + NADP^+ \quad (5)$$

$$r_3: But + O_2 + NADPH + H^+ \rightarrow EtAc + H_2O + NADP^+ \quad (6)$$

The catabolism of glucose required for cell maintenance was modeled as:

$$r_4: C_6H_{12}O_6 + 6\,O_2 \rightarrow 6\,CO_2 + 6\,H_2O \quad (7)$$

The material balance for each component in the liquid phase was:

$$\frac{dn_{BuOH,L}}{dt} = -\theta_{BuOH} - r_1 \times V_L \quad (8)$$

$$\frac{dn_{But,L}}{dt} = r_1 \times V_L - \theta_{But} - (r_2 + r_3) \times V_L \quad (9)$$

$$\frac{dn_{MePr,L}}{dt} = r_2 \times V_L - \theta_{MePr} \quad (10)$$

$$\frac{dn_{EtAc,L}}{dt} = r_3 \times V_L - \theta_{EtAc} \quad (11)$$

$$\frac{dn_{wat,L}}{dt} = (r_2 + r_3 + 6\, r_4) \times V_L - \theta_{wat} \quad (12)$$

$$\frac{dn_{O,L}}{dt} = -\theta_O - 6\, r_4 \times V_L - (r_2 + r_3) \times V_L \quad (13)$$

$$\frac{dn_{C,L}}{dt} = 6\, r_4 \times V_L - \theta_C \quad (14)$$

The formation rates of the enzymatic reactions, r, depend on the concentration of limiting substrate in the media, according to [19]:

$$r = r_{max} \times \frac{C_i}{K_{M_i} + C_i} \quad (15)$$

It is clear from eq. 15 that the rate of product formation resembles a zero-order reaction when the substrate concentration saturates the enzyme ($r = r_{max}$). When the substrate concentration becomes severely limiting ($K_{M_i} \gg C_i$), however, this resembles a first-order reaction where r is proportional to C_i. The binding affinities (K_{M_i}) for 2-butanol, butanone, oxygen, and NADPH have been previously determined using the non-fused enzymes, with experimental values of 8.63 mM, 381 µM, 18 µM, and 7 µM, respectively (Marco Fraaije et al., unpublished work), and the values have been used as starting point for eq. 15.

For the vapor phase, the material balances consider the molar air inflow (F_{in}) and gas outflow (F_{out}):

$$\frac{dn_{i,G}}{dt} = F_{in} \times y_{i,in} + \theta_i - F_{out} \times y_{i,out} \quad (16)$$

The air inflow was assumed to contain 20.95% O_2, 0.04% CO_2, and 79.01% N_2. Since N_2 is neither produced nor consumed during the fermentative process, the material balance considers that $dn_{N,L}/dt = 0$. The pressure in the headspace is constant and equal to 1 bar. The off-gas flow, F_{out}, can be written as a function of the total amount of moles in the headspace of the reactor:

$$F_{out} = F_{in} + \sum \theta_i \quad (17)$$

The transfer rate θ_i of volatile compounds through the vapor/liquid interface relates to the mass transfer coefficient $k_{L,i}a$ and the concentration at the liquid interface $C^*_{i,L}$:

$$\theta_i = k_{L,i}a \times (C_{i,L} - C^*_{i,L}) \times V_L \quad (18)$$

The mass transfer coefficient is strongly dependent on the equipment and medium composition, and once the $k_{L,O_2}a$ value is known within a given system, it can also be determined for the other components in that system based on diffusion coefficient values [20]:

$$k_{L,i}a = k_{L,O_2}a \times \frac{D_{i,L}}{D_{O_2,L}} \quad (19)$$

The value of $k_{L,O_2}a$ was determined experimentally using the dynamic method [21]. The Wilke–Chang estimation method was used to determine the diffusion coefficients of O_2 and CO_2 in water, while the Tyn–Calus method was applied to estimate the diffusion coefficients of 2-butanol, butanone, ethyl acetate and methyl propionate [22]. The stripping of water is mainly controlled by gas phase mass transfer resistance, and $k_{L,H_2O}a$ was thus determined using the diffusion coefficient of water vapor in air, according to Lennard-Jones correlation [22]. $C^*_{i,L}$ can be related to the partition coefficient K_i according to:

$$C^*_{i,L} = K_i \times y_i \times \frac{\rho_{wat}}{\sum x_i \times M_{w,i}} \quad (20)$$

K_i was predicted using the modified-UNIFAC model along with Raoult's law accounting for non-ideality [23]:

$$K_i = \frac{x_i}{y_i} = \frac{P}{\gamma_i P_i^{Sat}} \quad (21)$$

O_2 and CO_2 transfer through the interface depend on their saturation concentrations on the liquid phase, which were predicted using Henry coefficients:

$$C_{i,L}^{*} = y_i \times \frac{P}{H_i} \quad (22)$$

Using this structured model, the maximum rates of enzymatic reactions, r_{max}, were estimated by non-linear minimization of the sum of squared residuals between model estimates and experimental data, via Matlab R2014b (Mathworks). The experimental feed composition, expressed in terms of molar concentrations, was used as starting point for the simulations. Matlab ODE15s, appropriate for stiff differential equations, iteratively solved the equations 1–22, with t as the independent variable.

5.2.5.2 Process design for integrated product recovery

Aspen Plus® V8.8 (Aspen Technologies, Inc., USA) was used to simulate the biotransformation integrated with product recovery, aiming at a methyl propionate production capacity of 120 kton/a, operating time of 8000 h/a, and 98% recovery yield. The formation rate of methyl propionate, as determined from the batch biotransformation tests, was used to determine the cell mass requirements for the full-scale operation. The feedstocks considered were 2-butanol and corn stover hydrolysate, containing glucose at 120 g/kg [24]. The design procedures followed the guidelines provided by Seider et al. [25] and Humbird et al. [24]. The NRTL (non-random two-liquid model) model was selected as thermodynamic property method to predict liquid-liquid equilibrium and vapor-liquid equilibrium for non-ideal solutions.

It was assumed that the cells were first grown in a continuous seed-fermentor under inducing conditions, and then transferred to the production vessel to make up for cell washout. The metabolic equation for cell growth, based on the elemental and enthalpy balances as proposed by Heijnen and Roels [26], is:

$$0.258\ C_6H_{12}O_6 + 0.500\ O_2 + \ 0.200\ NH_4^+ \rightarrow CH_{1.8}O_{0.5}N_{0.2} + 0.550\ CO_2 + 0.950\ H_2O + 0.200\ H^+ \quad (23)$$

The production vessel was simulated as an ideally mixed continuous stoichiometric reactor at 24°C and 1 bar. The cells were kept under non-growing conditions using nitrogen limitation, and air was sparged at 1 vvm to avoid oxygen limitation and fulfil both cell maintenance and enzymatic conversion requirements. The broth concentrations of 2-butanol, butanone, and oxygen were defined based on their binding affinities (K_{M_i}). Product recovery and purification was performed by means of vapor compression, followed by distillation and decantation. Impurities resulting from cell metabolism and lignocellulose hydrolysis are mostly nonvolatile, and were thus considered to be purged along with the process wastewater. Volatile impurities recoverable by distillation (e.g. furans) were not considered in the present study for the sake of simplification.

The overall economic potential was evaluated using an economic black box model, where governing factors such as annual raw materials and utility costs were considered, while the capital costs were neglected. Recalling the CHMO selectivity for the isomers, 159 kton/a ethyl acetate is additionally produced. The price of petrochemical methyl propionate and ethyl acetate has been estimated as 0.91 €/kg and 0.93 €/kg, respectively [13].

5.3 Results and Discussion

5.3.1 Methyl propionate production in shake flasks

Recombinant cells containing the fusion constructs TmCHMO-MiADH and TbADH-TmCHMO revealed analogous growth behavior. Enzyme induction did not affect microbial growth. The highly enriched TB led to faster microbial growth, $\mu_{max} = 0.48\pm0.04\ h^{-1}$, as opposed to $0.27\pm0.02\ h^{-1}$ in MM. Although full glucose consumption has been observed in MM, the low cell density achieved (0.98±0.03 g/L) suggests that part of the energy source is used for maintenance and other non-growth related requirements. In TB, glycerol was fully depleted but the yeast extract could not be quantified. Cell density in this medium reached 2.41±0.11 g/L.

SDS-PAGE analysis confirmed that enzyme expression was poor in MM when compared to TB, and the target enzymes were mostly obtained in an insoluble form, probably aggregated within inclusion bodies [27]. Still, TmCHMO-MiADH enzymes exhibited higher activity in both media, particularly in TB, where full substrate conversion was achieved 24 h after induction. The

maximum concentrations of ethyl acetate and methyl propionate in the aqueous broth reached 349±1 mg/L and 206±1 mg/L, respectively, with a regioselectivity of 38±4% towards methyl propionate. Product loss due to the vented cap could not be entirely prevented, and it was estimated as 41.8±0.4 mol%. This value is in fair agreement with what was predicted using the UNIFAC model (38±5 mol%).

5.3.2 Process integration with in-situ gas stripping and absorption onto a liquid solvent

The gas stripping of 2-butanol, butanone, methyl propionate and ethyl acetate was examined abiotically using model solutions. The extent of product recovery was studied using air flows of 1.0 and 2.5 vvm, corresponding to $k_{L,O_2}a$ of 25 and 75 h^{-1}, respectively. The average of the results from duplicate tests is shown in Fig. 3 A. The high volatility of butanone, ethyl acetate and methyl propionate, with respective vapor pressures of 0.115 bar, 0.120 bar, and 0.109 bar at 24 °C, boosted mass transfer to the vapor phase, facilitating product evaporation: without an auxiliary absorbent, less than 5 wt.% was recovered by condensation.

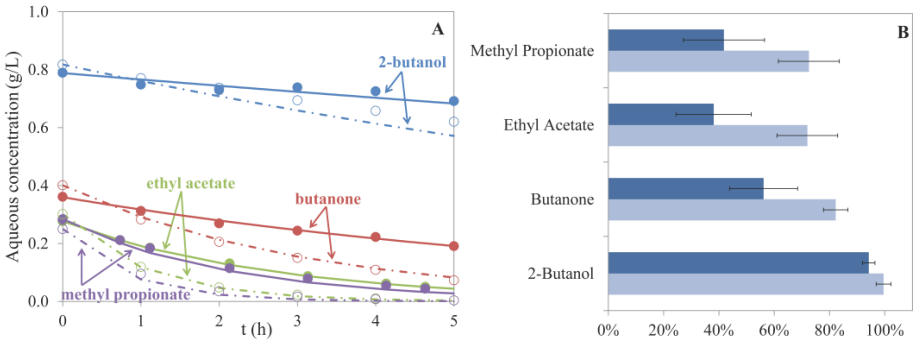

Figure 3. (A) Comparison between experimental (markers) and predicted (lines) concentrations of products in the aqueous phase during stripping of model solutions using flow rates of 1.0 vvm (solid lines, full markers) and 2.5 vvm (dash lines, open markers); **(B)** Yield of product recovery in the condensation system achieved in stripping tests with air flow rates of 1.0 vvm (light color) and 2.5 vvm (dark color)

To promote the laboratory-scale recovery of volatiles, absorbents were pre-screened among available esters, ketones, alcohols and ethers, using the methodology proposed by Gmehling and Schedemann [28]. The distribution coefficient (recall eq. 21) and selectivity ($\alpha_{MePr/wat} = K_{MePr}/K_{wat}$) of organic solvents for methyl propionate absorption from a representative vapor

mixture were predicted. Because of its ready availability, low volatility (T_b =126 °C), fairly high distribution coefficient (8.7) and selectivity (4.0) for methyl propionate, butyl acetate was used as absorbent in this study. Yet, full recovery could not be achieved (see Fig. 3B). Although 2-butanol could be fully condensed given its lower vapor pressure at the operational temperature (0.022 bar), great losses were observed for the other compounds. This shows the need for compressing the off-gas and cooling it below the dew point of the mixture. The mathematical model could describe the abiotic gas stripping process with a high coefficient of determination (Fig. 3A, R^2 = 0.998). Despite the slightly overestimated stripping rate of 2-butanol, the results suggest that the model is useful to quantify the stripping rates in the presence of product formation.

Biotransformations were performed using the cells containing TmCHMO-MiADH in both MM and TB media. As observed in shake flask experiments, the microbial growth was hindered in MM, and the dry cell concentration did not exceed 5.9±0.1 g/L, even when yeast extract was added to promote growth. Maintenance requirements for these *E. coli* cells (recall r_4) were estimated to be 0.0052 mol_S/(L h). When the biotransformation was terminated, the maximum butanone concentration in the media was 77.35±0.05 mg/L, and no esters were produced, suggesting that the CHMO activity was inhibited in the presence of glucose. This expression pattern is expected when the genes are under control of the arabinose promoter P_{BAD}. Therefore, P_{BAD} may not be suitable to express the genes of interest in this case, as the substrate for this process is lignocellulosic.

When the biotransformation was performed using TB media, during exponential cell growth only 2-butanone accumulated in the media without any ester formation. However, when the cells achieved stationary phase roughly 15 h later, 2-butanol was again added. Fig. 4 shows that the cascade conversion of 2-butanol into butanone, and butanone into the esters, was immediate, suggesting that the ADH is catalytically active during exponential growth, but the CHMO only becomes active during the stationary phase. This observation might be related to the unavailability of NADPH for the CHMO during microbial growth [29,30].

This exemplary biotransformation demonstrates the effectiveness of the model, represented by the lines in Fig. 4 (R^2 = 0.988), using as fitting parameters $r_{1,max}$ = 1.14±0.36 g_{But}/(L h), $r_{2,max}$ = 0.09±0.02 g_{MePr}/(L h), and $r_{3,max}$ = 0.11±0.01 g_{EtAc}/(L h). The formation rates of esters indicated an actual regioselectivity of 43±9% for the ester of interest, methyl propionate. The studies revealed that MiADH is converting 2-butanol into butanone 5.7-fold faster than TmCHMO is

converting butanone into esters and, as a result, full saturation of the CHMO occurred for the range of concentrations tested. These values were used to assess the performance of the full-scale biotransformation integrated with product recovery and purification.

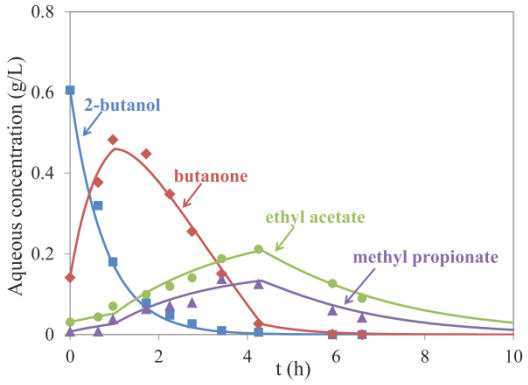

Figure 4. Aerobic biotransformation using *E.coli* TmCHMO-MiADH in TB medium, comparison between experimental (markers) and predicted (lines) concentrations in the aqueous phase; cell concentration = 7.1±0.8 g/L

5.3.3 Prospects for the biotransformation integrated with product recovery

A preliminary analysis was performed to assess the cell mass and feedstock needs for the proposed process, including seed fermentors and maintenance costs. Bioreactors of 500 m^3, with 70% working volume and maximum cell concentration of 50 g/L were considered. The results, shown in Table 1, uphold previous studies stating that volume-specific productivities below 2 g/(L h) are uncommercializable [31].

Given the discrepancy between the reaction rates of MiADH and TmCHMO, a significant fraction of the produced butanone either accumulates in the media or is stripped along with the vapor phase (>70 wt.%). To achieve the required ester productivity, more than 104.5 ton_{BuOH}/h are used, and the fermentation feedstock costs rise to ca. 944 million €/a. Also, due to the azeotropes that are formed between butanone, 2-butanol, water, and the esters, separation by conventional distillation becomes impracticable, anticipating severe operational costs. Ideally, the accumulation of butanone should be minimized while still allowing for full enzyme saturation. Hence, a different scenario was investigated where the observed MiADH productivity was used, and the TmCHMO productivity was tuned accordingly. As a result, the TmCHMO productivity used for design was ~7-fold the experimental, leading to accordingly decreased cell

mass, broth volume, and hydrolysate requirements (see Table 1). Under these conditions, the efficiency of product recovery becomes the major focus for the profitability of the overall process. Therefore, product recovery costs have been estimated. A flow diagram illustrating the integrated conceptual process is shown in Fig. 5, and the operational conditions used in the distillation units D1–D3 are depicted in Table 2.

Table 1. Requirements for the annual production of 120 kton methyl propionate, using the observed specific ADH/CHMO productivity, and tuned specific CHMO productivity

	Experimental		Tuned	
	CHMO	ADH	CHMO	ADH
Cell-mass specific productivity (kg/(kg$_X$ h))	0.012	0.158	0.082	0.158
Volume-specific productivity (kg/(m^3 h))	0.597	7.917	4.118	7.917
Volume broth required (m^3)	25629		3717	
Cell mass requirement (ton/a)	1281		186	
2-Butanol requirement (kton/a)	837		244	
Hydrolysate requirement (kton/a)	11094		1609	
Feedstock cost* (M €/a)	944		245	

*considering hydrolysate and 2-butanol

Table 2. Operational conditions in the distillation columns as defined by process design. See Fig. 5 for D1–D3

Distillation column	D1	D2	D3
Condenser P (bar)	1	1	1
Stages (minimum)	2	11	154
Stages (actual)	7	32	285
Feed stage	4	6	80
Reflux ratio	0.33	0.35	27.0
Distillate/feed ratio	0.03	0.99	0.67
T_{bottom} (ºC)	99.6	97.9	79.09
T_{top} (ºC)	94.8	72.2	68.05

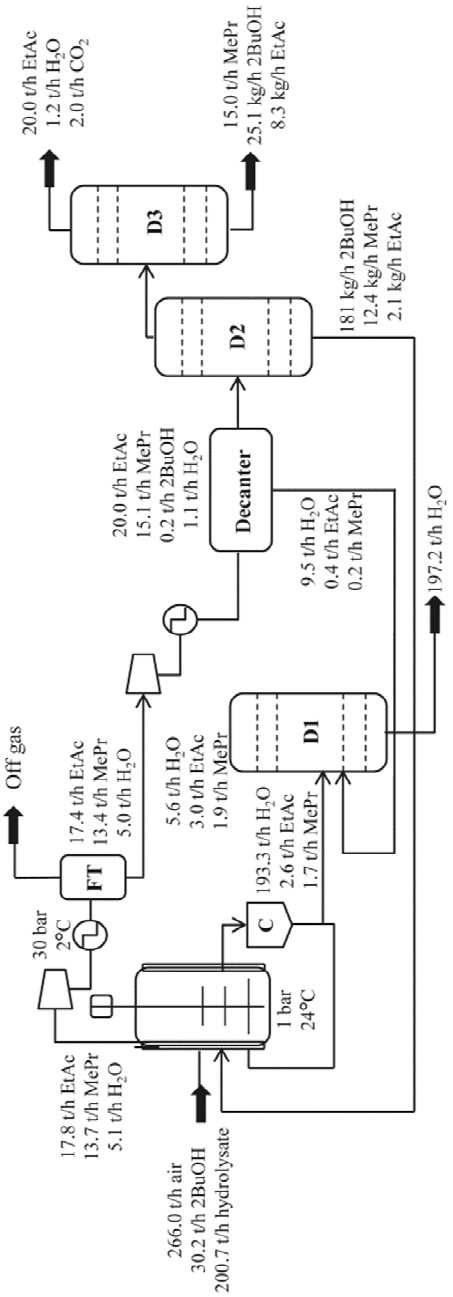

Figure 5. Process flow diagram for ester production using biotransformation integrated with product recovery and purification; C – centrifuge; FT – flash tank; D1/D2/D3 – distillation units

The aqueous broth containing ca. 8.5 g_{MePr}/L and 13.2 g_{EtAc}/L, concentrations below inhibiting threshold levels [32], was first centrifuged for cell mass separation and recycle (98.5 wt.%), and then distilled for water removal (D1). The enriched vapor, comprising 88 wt.% of the volatile biotransformation products, is compressed for inert gas removal. In this step, 99 wt.% of the vapor products are lost at room temperature and pressure, which was minimized to 2 wt.% using compression to 30 bar with cooling to 2°C.

The condensate was mixed with the distillate from D1 in a decanter, and the solubility properties of the resulting mixture enabled the concentration of esters in the organic phase beyond azeotropic compositions, facilitating further separation by distillation. 2-Butanol was first separated from the esters in D2, and the resulting stream, containing ca. 7.9 g_{EtAc}/L and 46.4 g_{MePr}/L, was recycled back to the production vessel. Due to a small relative volatility (1.077), methyl propionate and ethyl acetate can only be separated at the expense of extremely large distillation columns (D3). Under the current conditions, the distillate contained mainly ethyl acetate (85 wt.%), which was not purified further, while the bottom stream comprises the purified methyl propionate (99.78 wt.%), containing traces of 2-butanol (0.17 wt.%) and ethyl acetate (0.05 wt.%). Taking into account an assumed 20% penalty in the price of ethyl acetate, given its lower purity, the expected revenue for this process is 235 million €/a. The overall energy duty after heat integration was 1256 GJ/h (34.7 MJ/kg_{ester}). The cooling required for the biotransformation task represents a major energy sink in the process (41% of the total duty), along with the product purification task (41%), and vapor compression (15%). Under the present conditions, the total variable operating costs ascend to 335 million €/a (76% biotransformation; 14% vapor compression; 8% product purification). This translates into 1.16 €/kg_{ester}, which is beyond the petrochemical price of methyl propionate.

By shifting completely the TmCHMO selectivity to methyl propionate, the volume-specific productivity would double, and significant capital and operating savings would be achieved, as the biotransformation costs would decrease by ca. 57%. Additionally, the ester separation task could be avoided, as only 2-butanol would be recovered and recycled to the bioreactor. However, 2-butanol is the main substrate for the enzymatic conversion, with a requirement of 0.84 g/g_{ester}. Taking the bio-based 2-butanol selling price of ca. 0.9 €/kg [7], this represents 93% of the expected process revenues, and 69% of the total variable operating costs. In fact, even in case of full TmCHMO selectivity for methyl propionate, the 2-butanol demand would represent 83% of the product sales revenues. This suggests that the bio-based production of methyl propionate can only become profitable if the production cost of bio-based 2-butanol is

minimized. Using a dilute stream instead of pure 2-butanol would decrease its cost, but water distillation would become a significant expenditure in the present configuration. A biotransformation in which 2-butanol is produced in the same vessel as the esters at an appropriate rate, or a one-step conversion promoting methyl propionate formation directly from glucose, would avoid the need for 2-butanol recovery, and could enhance the maximum yield to 0.489 $g_{ester}/g_{glucose}$. Nevertheless, the microbial metabolic requirements and biotransformation are expected to be extremely demanding.

5.4 Conclusions

A novel bio-based approach for methyl propionate production has been assessed. Even though the pathway for bio-based methyl propionate has been implemented, significant strain optimization is still required. The enhancement of the activity/selectivity of the CHMO for methyl propionate can lead to significant feedstock and energy savings. Overall, the proposed two-step process appears to be suboptimal for microbial ester production due to substrate, product, and energy losses. This study suggests that avoiding 2-butanol recovery is crucial to achieve a profitable process, and a one-step microbial process for simultaneous 2-butanol and ester production should be aimed at.

5.5 Acknowledgments

The authors thank Prof. Dr. Marco Fraaije and Dr. Elvira Guzman, from the Molecular Enzymology Group, Groningen Biomolecular Sciences and Biotechnology Institute, for kindly providing the recombinant cells. Rosario Medici, Maria Cuellar, Bhargavi Ganesan, Yi Song, Max Zomerdijk, Stef van Hateren, and Linda Otten are to be acknowledged for their analytical support and fruitful advice.

5.6 Nomenclature

C	mol/L	Concentration
C^*	mol/L	Concentration at the liquid interface
D	cm^2/s	Diffusivity
F	mol/h	Mole flow rate
H	bar/(mol L)	Henry coefficient

$k_L a$	1/h	Volume-specific mass transfer coefficient
K_i	bar/bar	Distribution coefficient
K_M	mol/L	Michaelis constant
M_w	g/mol	Molecular mass
n	mol	Number of moles
P	bar	Pressure
r	mol/(L h)	Rate of formation
t	h	Time
T	K	Temperature
V	L	Volume
x	–	Mole fraction in the liquid phase
y	–	Mole fraction in the vapor phase
Greek Symbols		
γ	–	Activity coefficient
μ	1/h	Microbial growth rate
θ	mol/h	Transfer rate from liquid to gas phase
ρ	g/L	Density
Subscripts		
$BuOH$		2-Butanol
But		Butanone
C		Carbon dioxide
$EtAc$		Ethyl acetate
G		Gas phase
i		Component i
j		Component j
L		Liquid phase
$MePr$		Methyl propionate
N		Nitrogen
O		Oxygen
S		Substrate
sol		Organic solvent
X		Cell mass

5.7 References

(1) Ali, U.; Karim, K. J. B. A.; Buang, N. A. A Review of the Properties and Applications of Poly (Methyl Methacrylate) (Pmma). *Polym. Rev.* **2015**, *55*, 678–705.

(2) Global Market Insights, I., *Synthetic and Bio-Based Pmma (Polymethyl Methacrylate) Market Size by Product (Extruded Sheets, Pellets, Beads, Cell Cast Sheet & Blocks), by Application (Automotive, Electronics, Construction, Signs & Display), Industry Analysis Report, Regional Outlook, Downstream Application Development Potential, Price Trend, Competitive Market Share & Forecast, 2012-2022*. 2016. p. 190.

(3) Clegg, W.; R. J. Elsegood, M.; R. Eastham, G.; P. Tooze, R.; Lan Wang, X.; Whiston, K. Highly Active and Selective Catalysts for the Production of Methyl Propanoate Via the Methoxycarbonylation of Ethene. *Chem. Commun.* **1999**, 1877–1878.

(4) Liu, J.; Heaton, B. T.; Iggo, J. A.; Whyman, R.; Bickley, J. F.; Steiner, A. The Mechanism of the Hydroalkoxycarbonylation of Ethene and Alkene-Co Copolymerization Catalyzed by Pd(Ii)-Diphosphine Cations. *Chemistry* **2006**, *12*, 4417–4430.

(5) Yoneda, H.; Tantillo, D. J.; Atsumi, S. Biological Production of 2-Butanone in *Escherichia Coli*. *ChemSusChem* **2014**, *7*, 92–95.

(6) Chen, Z.; Sun, H.; Huang, J.; Wu, Y.; Liu, D. Metabolic Engineering of Klebsiella Pneumoniae for the Production of 2-Butanone from Glucose. *PLOS ONE* **2015**, *10*, e0140508.

(7) Pereira, J. P. C.; Lopez-Gomez, G.; Reyes, N. G.; van der Wielen, L. A. M.; Straathof, A. J. J. Prospects and Challenges for the Recovery of 2-Butanol Produced by Vacuum Fermentation - a Techno-Economic Analysis. *Biotechnol. J.* **2017**, *12*, 1600657.

(8) van Beek, H. L.; Romero, E.; Fraaije, M. W. Engineering Cyclohexanone Monooxygenase for the Production of Methyl Propanoate. *ACS Chem. Biol.* **2017**, *12*, 291–299.

(9) Eastham, G. R.; Johnson, D. W.; Straathof, A. J. J.; Fraaije, M. W.; Winter, R. T. Process for the Production of Methyl Methacrylate. EP2855689 A1, 2015.

(10) Aalbers, F. S.; Fraaije, M. W. Coupled Reactions by Coupled Enzymes: Alcohol to Lactone Cascade with Alcohol Dehydrogenase-Cyclohexanone Monooxygenase Fusions. *Appl. Microbiol. Biotechnol.* **2017**, *101*, 7557–7565.

(11) Xue, C.; Zhao, J.; Liu, F.; Lu, C.; Yang, S.-T.; Bai, F.-W. Two-Stage in Situ Gas Stripping for Enhanced Butanol Fermentation and Energy-Saving Product Recovery. *Bioresour. Technol.* **2013**, *135*, 396–402.

(12) de Vrije, T.; Budde, M.; van der Wal, H.; Claassen, P. A. M.; López-Contreras, A. M. "*In Situ*" Removal of Isopropanol, Butanol and Ethanol from Fermentation Broth by Gas Stripping. *Bioresour. Technol.* **2013**, *137*, 153–159.

(13) Straathof, A. J. J.; Bampouli, A. Potential of Commodity Chemicals to Become Bio-Based According to Maximum Yields and Petrochemical Prices. *Biofuels, Bioprod. Biorefin.* **2017**, *11*, 798–810

(14) Urit, T.; Li, M.; Bley, T.; Löser, C. Growth of Kluyveromyces Marxianus and Formation of Ethyl Acetate Depending on Temperature. *Appl. Microbiol. Biotechnol.* **2013**, *97*, 10359–10371.

(15) Kruis, A. J.; Levisson, M.; Mars, A. E.; van der Ploeg, M.; Garcés Daza, F.; Ellena, V.; Kengen, S. W. M.; van der Oost, J.; Weusthuis, R. A. Ethyl Acetate Production by the Elusive Alcohol Acetyltransferase from Yeast. *Metab. Eng.* **2017**, *41*, 92–101.

(16) Löser, C.; Urit, T.; Bley, T. Perspectives for the Biotechnological Production of Ethyl Acetate by Yeasts. *Appl. Microbiol. Biotechnol.* **2014**, *98*, 5397–5415.

(17) Löser, C.; Schröder, A.; Deponte, S.; Bley, T. Balancing the Ethanol Formation in Continuous Bioreactors with Ethanol Stripping. *Eng. Life Sci.* **2005**, *5*, 325–332.

(18) Urit, T.; Löser, C.; Wunderlich, M.; Bley, T. Formation of Ethyl Acetate by *Kluyveromyces Marxianus* on Whey: Studies of the Ester Stripping. *Bioprocess Biosyst. Eng.* **2011**, *34*, 547–559.

(19) Briggs, G. E.; Haldane, J. B. S. A Note on the Kinetics of Enzyme Action. *Biochem. J.* **1925**, *19*, 338–339.

(20) Truong, K. N.; Blackburn, J. W. The Stripping of Organic Chemicals in Biological Treatment Processes. *Environ. Prog.* **1984**, *3*, 143–152.

(21) Tribe, L. A.; Briens, C. L.; Margaritis, A. Determination of the Volumetric Mass Transfer Coefficient (K(L)a) Using the Dynamic "Gas out-Gas in" Method: Analysis of Errors Caused by Dissolved Oxygen Probes. *Biotechnol. Bioeng.* **1995**, *46*, 388–392.

(22) Poling, B.; Prausnitz, J.; Connell, J. O. *The Properties of Gases and Liquids*, McGraw-Hill Education, 2000.

(23) Lohmann, J.; Joh, R.; Gmehling, J. From Unifac to Modified Unifac (Dortmund). *Ind. Eng. Chem. Res.* **2001**, *40*, 957–964.

(24) Humbird, D.; Davis, R.; Tao, L.; Kinchin, C.; Hsu, D.; Aden, A.; Schoen, P.; Lukas, J.; Olthof, B. et al. *Process Design and Economics for Biochemical Conversion of Lignocellulosic Biomass to Ethanol - Dilute-Acid Pretreatment and Enzymatic Hydrolysis of Corn Stover*, NREL - National Renewable Energy Laboratory, 2011.

(25) Seider, W. D.; Seader, J. D.; Lewin, D. R. *Product and Process Design Principles: Synthesis, Analysis and Design*, Wiley Global Education, 2008.

(26) Heijnen, J. J.; Roels, J. A. A Macroscopic Model Describing Yield and Maintenance Relationships in Aerobic Fermentation Processes. *Biotechnol. Bioeng.* **1981**, *23*, 739–763.

(27) Rosano, G. L.; Ceccarelli, E. A. Recombinant Protein Expression in Escherichia Coli: Advances and Challenges. *Front. Microbiol.* **2014**, *5*, 172.

(28) Gmehling, J.; Schedemann, A. Selection of Solvents or Solvent Mixtures for Liquid–Liquid Extraction Using Predictive Thermodynamic Models or Access to the Dortmund Data Bank. *Ind. Eng. Chem. Res.* **2014**, *53*, 17794–17805.

(29) Walton, A. Z.; Stewart, J. D. An Efficient Enzymatic Baeyer-Villiger Oxidation by Engineered Escherichia Coli Cells under Non-Growing Conditions. *Biotechnol. Progr.* **2002**, *18*, 262–268.

(30) Julsing, M. K.; Kuhn, D.; Schmid, A.; Bühler, B. Resting Cells of Recombinant E. Coli Show High Epoxidation Yields on Energy Source and High Sensitivity to Product Inhibition. *Biotechnol. Bioeng.* **2012**, *109*, 1109–1119.

(31) Van Dien, S. From the First Drop to the First Truckload: Commercialization of Microbial Processes for Renewable Chemicals. *Curr. Opin. Biotechnol.* **2013**, *24*, 1061–1068.

(32) Pereira, J. P. C.; Verheijen, P. J. T.; Straathof, A. J. J. Growth Inhibition of S. Cerevisiae, B. Subtilis, and E. Coli by Lignocellulosic and Fermentation Products. *Appl. Microbiol. Biotechnol.* **2016**, *100*, 9069–9080.

Chapter 6: Concluding remarks on the integrated production and recovery of bio-based MMA

Contents

6.1 Opportunities and challenges in the biotransformation of methyl propionate from lignocellulosic sugars via 2-butanol

The findings discussed in the present thesis suggest that there are several opportunities for improvement in the different steps of the proposed approach. Overall, future developments regarding microbial engineering and separation process technology are crucial to achieve a techno-economically feasible bio-based process, which can compete with the current petrochemical processes for MMA production.

Widely used biotechnological platform producers, such as *E. coli* and *S. cerevisiae*, have good potential to be engineered and further established as hosts for the bio-based production of methyl esters, as suggested in Chapter 2. Directed evolution methods have already proved effective in improving microbial robustness and boosting the activity of biomolecules for diverse research and industrial applications [1], and can also be used to improve strain stability, alleviate inhibitor tolerance, and enhance production levels, ultimately promoting the bio-based methyl propionate production in the present case. Moreover, recently developed technologies for genome editing and targeted gene regulation, such as CRISPR/CRISPRi, are powerful tools expected to provide new insights and approaches for numerous metabolic engineering targets [2-4].

However, maximized tolerance does not necessarily result in maximized production, if the tolerance mechanism is not closely related to the metabolic pathway [1]. To reach the desired production levels at industrial scales, a large number of seed-train bioreactors and production-bioreactors must be operated intermittently to comply with the continuous product demand. Overall, the costs related to fermentation can account for a significant part of the total OPEX, as observed in Chapters 4 and 5. Attempting to increase productivity and minimize fermentation costs, fermentation strategies such as cell-recycling have been proposed (recall Chapters 4 and 5), and several examples of continuous fermentation processes with cell recycling and retention exist in the literature, typically reporting significant productivity improvements [5-7]. Most recently, self-cycling fermentation has also been demonstrated to improve volumetric and specific productivity in bioethanol production, potentially reducing capital and production costs [8].

Although it has been demonstrated that using an optimized microbial host could lead to a profitable bio-based process for the production of 2-butanol and methyl propionate, this is only possible if suitably integrated process configurations are used for product separation, mainly

due to the thermodynamic properties of the mixtures formed (Chapters 4 and 5). Overall, the proposed two-step approach facilitates process control and optimal aeration conditions in both biotransformations, eventually promoting higher productivities. Furthermore, a two-step process is expected to be more advantageous for product recovery and purification, as it minimizes the simultaneous removal of intermediate compounds, which would decrease the formation yields. It also mitigates the formation of complex alcohol-ketone-esters-water mixtures with relatively high product concentrations, that could compromise the efficiency of the downstream process. However, with a 2-butanol requirement of 0.84 g/g_{ester}, the precursor cost represents 83% of the final product sale revenues, even if an ideal strain is used (Chapter 5). Using a dilute stream of 2-butanol directly from the anaerobic fermentation would decrease its cost, but then water distillation would become the most significant expenditure in methyl propionate purification. Another option would be the direct sparging of the stripped fermentation vapor from the anaerobic 2-butanol fermentation through the aerobic ester production vessel, but this would require additional stream compression to atmospheric pressure, and the 2-butanol concentrations required in the vapor would be ca. 46-fold as high as those estimated in Chapter 4. Given the oxygen requirements in methyl propionate production, performing this biotransformation under vacuum pressure is unreasonable. Therefore, the outcome of this thesis indicates that further studies should focus on one-step approaches for ester production, bypassing the need for a 2-butanol stream.

6.1.1 One-step biotransformation of lignocellulosic sugars into methyl propionate

Pursuing a one-step conversion for methyl propionate formation directly from glucose would avoid the need for the recovery of chemical precursors, and could enhance the maximum yield to 0.489 $g_{ester}/g_{glucose}$. The pathway pursued in the one-step biotransformation of lignocellulosic sugars into methyl propionate is depicted in Fig. 1.

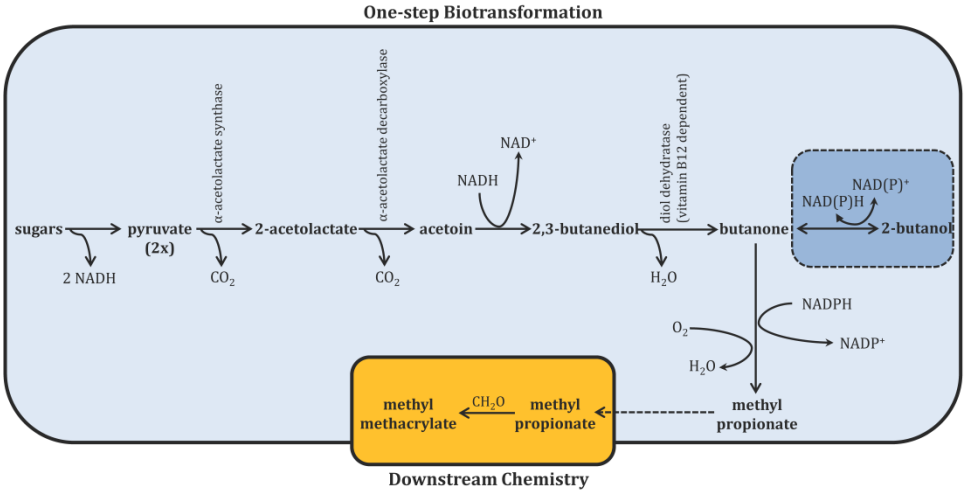

Figure 1. Suggested metabolic pathway for one-step production of methyl methacrylate from sugars (dotted box represents an alternative metabolic route via 2-butanol)

Ideally, the pathway would bypass 2-butanol formation, avoiding intermediate product accumulation and *in-situ* separation, but the microbial metabolic requirements are expected to be extremely demanding. As an example, the metabolic pathway requires full closure of the redox balance. As shown in Fig. 1, 2 NADH coenzyme molecules result from glycolysis, and while the synthesis of 2,3-butanediol (BDO) requires 1 NADH, the cyclohexanone monooxygenase (CHMO) oxidizing butanone into the esters is NADPH-specific [9]. For the present application, changing the NADPH-specificity of the CHMO towards NADH would be convenient to close the redox balance, also because NADH is considered to be a more stable coenzyme [10]. Although there are examples of successful reversal of coenzyme specificity in 4-hydroxyacetophenone monooxygenase (HAPMO), an enzyme catalyzing BV oxidations on several ketones, it has been suggested that the full reversal of coenzyme specificity in Type I BVMOs, such as CHMO, would require a great number of mutations [10]. If this is not achievable, the pathway calls for the simultaneous production of 2-butanol and ester to close the redox balance. In such a cascade reaction, butanone is first converted to 2-butanol by a suitable NADH-dependent alcohol dehydrogenase (ADH), and 2-butanol is oxidized back to butanone by a $NADP^+$-dependent ADH, as illustrated in the dotted box in Fig. 1. Matching enzyme kinetics would circumvent the accumulation and removal of the precursor from the broth.

Another major constraint in the one-step biotransformation relates to the oxygen requirements in each conversion step (recall section 1.2.1 of this thesis). The synthesis of 2,3-BDO from pyruvate is dependent on three key enzymes, namely α-acetolactate synthase, α-acetolactate decarboxylase, and 2,3-BD dehydrogenase [11]. Under aerobic conditions, α-acetolactate synthase is inactivated and acetyl-CoA is generated, which is further channeled to the tricarboxylic acid cycle. Under micro-aerobic conditions, α-acetolactate synthase, a.o., generates additional lactate and formate, at the expense of 2,3-BDO [11]. On the other hand, stoichiometric amounts of oxygen are required to catalyze methyl propionate production, without promoting cell growth (Chapter 5). To overcome this issue, an oxygen supply strategy must be implemented to optimize the final product formation. For instance, the conversion could be performed under limited oxygen supply, but this is expected to promote both respiration and mixed acid fermentation. A total knock-out of the mixed acid fermentation could be attempted in this case, similarly to what has been done to enhance the anaerobic production of itaconic acid by *E. coli* [12]. However, cell growth might be promoted at the expense of ester production, as has been observed regarding 2,3-BDO production in *E. coli* [13]. Another interesting, but demanding, option would be the (selective) blockage of the electron transport chain to reduce cell growth [14], and promote the BV oxidation.

Due to the aforementioned constraints, a promising approach to comply with the proposed one-step biotransformation relies on the use of two compartments in a single bioreactor, facilitating the control of different oxygen regimes in each compartment. The precursor 2-butanol would be formed in the anaerobic compartment, where the microorganisms would be retained, and taken up in the aerobic compartment for ester production. Such configuration could be achieved by means of membrane-separation, or microbial biofilms with aerobic/anaerobic layers. Examples of effective aerobic-anaerobic membrane bioreactors exist in wastewater treatment systems, but the major obstacle in their practical application is membrane fouling, which results in high energy demands [15-17]. Using a different approach, an upper aerobic biofilm reactor has been integrated with a lower anaerobic sludge digester in a single bioreactor with vertical configuration [18]. The two compartments were separated by a roof-like shape, preventing oxygen diffusion from the upper aerated compartment down to the anaerobic compartment. Despite the experimental verification, the industrial applicability of such design has not been proven [18].

6.1.2 Cobalamin requirements in anaerobic 2-butanol production

Possible additional bottlenecks in the anaerobic pathway for 2-butanol production relate to the production of butanone from 2,3-BDO, which is accomplished by a cobalamin-dependent diol dehydratase [19]. If required, the addition of this expensive coenzyme in the present process is expected to increase the overall cost. Endogenous 2-butanol producers such as *Lactobacilli brevis* are able to express this enzyme, but they do not possess the genes for cobalamin biosynthesis [20], nor do other model microorganisms with large industrial usage, such as *E. coli* and *S. cerevisiae*. Biosynthetic pathways for cobalamin production exist in *Pseudomonas denitrificans, Sinorhizobium meliloti*, and *Propionibacterium shermanii,* and although these strains are used at industrial scale for vitamin production, they require expensive media nutrients, and lack robustness for strain engineering [21]. Cobalamin biosynthetic genes have also been characterized in *Salmonella typhimurium* [22], which is closely related to *E. coli*. Based on this finding, it has been demonstrated that the de novo production of cobalamin can be achieved in *E. coli* under anaerobic conditions, by transferring 20 genes from the *S. typhimurium cob* operon [23]. Most recently, a recombinant *E. coli* strain harboring 22 cloned genes from *P. denitrificans* was able to produce 0.65 µg-cobalamin/g-cdw under both aerobic and anaerobic conditions [24]. Given the complexity of the metabolic regulation of cobalamin synthesis, this heterologous pathway still requires further development [24], but this approach has proved the potential of using *E. coli* for cobalamin production.

6.1.3 Using CHMOs in large-scale operations

The present research has shown that significant feedstock and energy savings can result from the enhancement of the CHMO activity/selectivity for methyl propionate. Although this might not be an easy task, it has been demonstrated that the enzyme regioselectivity for butanone can be further improved, in case of sufficient investment in enzyme engineering [25].

It is also important to note that the use of CHMOs in large scale operations is still restricted by severe limitations such as decreased microbial growth, low biocatalyst stability, low enzyme activity, and ineffective cofactor regeneration [26]. Additionally, both substrate and product inhibition occur [9]. These issues were also observed during the fermentative conversion of 2-butanol to methyl propionate (recall Chapter 5). Some valuable strategies to overcome these issues have been proposed for BV oxidations, namely separating the biomass growth (biocatalyst production) from the actual biotransformation (reactant conversion) [27]. This strategy has been

suggested in the conceptual process design presented in Chapter 5, but its application in a one-step biotransformation process would become even more challenging.

Following this strategy, and considering an industrial scale process, oxygen transfer is expected to become the rate-limiting step in the BV oxidation [28,29]. Previous studies using whole-cell biocatalysts have shown that the rates of reaction would decrease as a function of increasing cell concentrations, independently of the reactor scale used. The authors suggested that oxygen was preferentially used by the cells for maintenance reactions, leaving the remaining oxygen for the biotransformation [28]. Therefore, the optimum biocatalyst concentration allowed in the biotransformation is dependent on the maximum oxygen transfer rate. Although oxygen supply can be enhanced to certain extent by increasing air flow rates or stirrer speeds, feasible oxygen transfer rates at industrial scale range from 0.11–0.18 mol/(L h) [30]. As a result, if cell maintenance requirements were reduced to near-zero values, the maximum achievable ester productivity would range between 9.7–15.9 g/(L h). Considering the current enzyme regioselectivity of 43% for methyl propionate, the achievable productivities would range between 4.2–6.8 g/(L h), which appear to be feasible values for industrial production [31].

6.2 Other opportunities for the bio-based production of MMA

Although not many bio-based routes to MMA exist, some promising options start from glucose via methacrylic acid (MAA) or, alternatively, via methyl propionate (recall Chapter 1, Fig. 2).

6.2.1 Alternative bio-based routes via methacrylic acid

Methyl methacrylate can be obtained from the direct esterification of methacrylic acid with methanol, in the presence of highly active catalysts [32]. Currently, MAA is still produced from petrochemical resources, but several chemical processes have been proposed for its bio-based production via itaconic acid (IA), 2-hydroxyisobutyric acid (2-HIBA), and isobutene, which can be obtained from the fermentation of sugars [33].

The biotechnological production of IA is well established at industrial scale, with a yearly production of 80000 tons, using native and engineered *Aspergillus terreus* fungus. The glycolysis regulation system in *A. terreus* promotes the efficient biosynthesis of IA from glucose, and yields up to 0.58 g/g have been reported, corresponding to 80% of the theoretical maximum yield on glucose (0.72 g/g) [34,35]. An outstanding titer of ca. 160 g/L IA has been recently achieved, with a productivity of 1.0 g/(L h), using *A. terreus* in optimized 15-L scale reactors [35]. This value is in the

same range as the well-known citric acid production using *A. niger* [36]. High substrate concentrations, low pH-value, and phosphate-limited conditions are required for the successful production of IA [34,35]. Besides glucose, this strain is also able to utilize carbon sources such as starch, glycerol, pentose sugars (arabinose, xylose), and other hexose sugars (galactose, mannose), offering several opportunities for the use of lignocellulosic biomass [37]. Most recently, 43 g/L IA has been reached using engineered *E. coli* in a high-cell density fed-batch fermentation, with an average productivity of 1.4 g/(L h), and yield of ca. 0.6 g/g from glycerol [38]. However, it has been reported that productivities of ca. 2.5 g/(L h) are required for the bio-based process to fully replace the current petrochemical production [34].

One of the first proposed routes for the production of MAA from bio-based IA is based on the dehydration and decarboxylation of citric acid (CA) to IA, followed by a second decarboxylation yielding MAA [39]. The method uses sodium hydroxide (NaOH) as catalyst, but requires near-critical and supercritical water conditions (>276 bar) and high temperatures (400°C) [39]. Later developments on this method enhanced the selectivity of catalysis up to 99% under lower temperatures (255−265°C) and pressures (31−207 bar), while using Group I and Group II base catalysts [32]. The major drawback of this method is the formation of by-products such as propylene, which reduce the yield of MAA [32]. The selective decarboxylation of CA and IA using precious metal catalysts such as platinum, palladium, or ruthenium, has also been investigated, with reported yields of 0.51 mol/mol on IA and selectivities up to 84%,using Pt/Al_2O_3 catalyst at lower reaction temperatures (250°C) and pressures (38 bar) [40]. To avoid the basification and acidification steps through decarboxylation of the starting acid to MAA, Lansing et al. [41] recently described the decarboxylation of IA using catalytic ruthenium carbonyl propionate in an aqueous solvent system. The authors reported a selectivity higher than 90% at lower temperatures (190−250°C) and pressures (29 bar) [41].

On a different approach, Genomatica patented the bio-based production of MAA from 2-hydroxyisobutyric acid, based on the microbial conversion of 3-hydroxybutyryl-CoA, a product resulting from the acetate metabolism, into 2-hydroxybutyryl-CoA. The latter is hydrolyzed into 2-HIBA, which is excreted and then converted to MAA [42]. This approach requires the cobalamin-dependent 2-hydroxyisobutyryl-CoA mutase, which has been introduced into *Cupriavedus necator*, a PHB-producing bacterium. To date, 6.4 g/L 2-HIBA has been produced from fructose in a fed-batch fermentation, using recombinant *C. necator* H 16 [43]. Recently, the production of MAA from 2-HIBA has been demonstrated, using a single dehydration step with subcritical water at 275°C, depicting a yield of ca. 0.71 mol/mol [44].

The two-stage process involving the selective oxidation of isobutene to methacrolein, followed by oxidation of methacrolein towards MAA, has also been investigated by many researchers, widely using heteropolyacids as state-of-the-art catalysts [45-47]. These catalysts typically lack long-term stability, and attempts to improve catalysis have been focusing on the use of mixed oxide catalysts [47]. Chitin-$CsH_3PMo_{11}VO_{40}$ hybrid microspheres have been recently suggested as pivotal catalysts for the conversion of methacrolein to MAA, reaching conversions of 80% and selectivities around 94% [47]. Isobutene is currently produced via petrochemical routes, but promising bio-based routes include the direct fermentation from glucose [48], or the dehydration of isobutanol [49]. To date, the highest microbial production rate reported was 0.45 mg/(L h), using *Rhodotorula minuta* [48]. The enzymatic dehydration of isobutanol is still under research, and merely 0.006 g/(L h) isobutene have been obtained from isobutanol using oleate hydratases [50]. The existing bio-based routes to isobutanol are currently led by Gevo and Butamax [51]. While Gevo is the current leading producer of bio-isobutanol, with a plant capacity of ca. 4.5 kton/a, Butamax recently announced plans to produce bio-isobutanol with its acquisition of Nesika Energy, LLC and its ethanol facility in Scandia, Kansas [52].

6.2.2 Alternative bio-based routes via methyl propionate

In the Alpha Process, methyl propionate is formed as a result of the methoxycarbonylation of ethene in a catalytic cycle, using carbon monoxide and methanol [53,54]. The final step of this route is the condensation of methyl propionate with formaldehyde to yield MMA.

Besides the petrochemical route via steam cracking of petrochemicals, ethene can also be produced via acid-catalyzed dehydration of bio-based ethanol, using catalysts such as phosphoric acid, oxides, molecular sieves, or heteropolyacids [55,56]. Despite the low investment cost estimated per ton of product, ethanol dehydration is an endothermic process, and temperatures in the range of 300−500°C are required to increase the selectivity towards ethene. As a result, a recent techno-economic evaluation suggested that the bio-based process was not cost-competitive under the present feedstock and product prices [56].

Alternatively, methyl propionate can also be prepared by esterification of propionic acid (PA) with methanol. Currently produced from petrochemical feedstocks, possible bio-bases routes for PA include the succinate pathway, the acrylate pathway, and the propanediol pathway. Several studies have reported the production of PA from pentose and hexose sugars, as well as many renewable substrates, and an extensive review on the carbon sources used by

Propionibacterium can be found elsewhere [57]. The toxicity posed by PA to microbial producers has been successfully attenuated using metabolic engineering combined with adaptive evolution, and several *Propionibacterium* mutants exhibit high productivity and yields. To date, the highest PA titer has been observed for engineered *P. acidipropionici*, which produced 106 g-PA/L in a glycerol fed-batch fermentation (ca. 0.04 g/(L h)), with a yield of 0.56 g/g [58]. The highest volumetric productivity has been observed in high cell density batch fermentation, using another *P. acidipropionici* mutant: 2.98 g/(L h), with a yield of ca. 0.44 g/g glucose, and a PA titer of 40 g/L [59]. This is ca. 80% of the maximum theoretical yield on glucose, 0.55 g/g [33].

6.2.3 Methanol as reactant in the production of MMA

Methanol appears as reactant in the proposed bio-based routes for MMA production: it is required for the production of methyl propionate by direct esterification of PA, but also for the production of MMA by esterification of MAA. Moreover, the state-of-the-art downstream chemistry used by Lucite in the Alpha process involves formaldehyde, which is also produced via methanol oxidation. Therefore, the only bio-based route for formaldehyde is via bio-based methanol. The cost of methanol feedstock is estimated to account for 70% of the total manufacturing cost of formaldehyde [60].

Methanol, initially produced by wood distillation, can also be produced from several carbon-containing feedstocks, namely natural gases, biomass, or CO_2 [61]. Most methanol is produced via the conversion of natural gas at high temperature (200−300°C) and pressure (35−100 bar), in which the feedstock accounts for up to 90% of the production costs [61,62]. Bio-based methanol can be produced via the gasification of solid biomass (e.g. forest residues) or wastes at high temperatures (>1050°C), followed by catalytic conversion of the biogas generated [62,63]. A recent techno-economic assessment has shown that biomethanol produced via entrained flow gasification could compete with gasoline, if exempted from governmental tax [63]. Since conventional chemical catalysts require high temperatures and pressures, and are extremely sensitive to deactivation by pollutants, biological conversion appears as a promising alternative for biomethanol production [64]. It is known that native aerobic methanotrophs express methane monooxygenase (MMO), which oxidizes methane to methanol, while anaerobic methanotrophs express homologs of the methanogenesis enzymes [64]. A comprehensive review on the cultivation of methanotrophs and methanol production has been done by Ge et al. [65]. Although dependent on the cultivation conditions, the highest methanol titer ever reported was 1.12 g/L

[66], and the highest productivity was 0.171 g/(L h) [67], both observed using *Methylosinus trichosporium* cells. The expression of MMO in heterologous hosts is still under development, but it has been suggested that the anaerobic pathway might offer higher methanol yields, mostly due to the redox-balance, competition of oxidative phosphorylation, and critical gas transfer limitations occurring in the aerobic process [64]. The catalytic conversion of CO_2 to produce methanol by hydrogenation, using only renewable resources, has also become an attractive option, mainly due to the recent developments in CO_2 capture technologies [61]. In this case, the hydrogenation of CO_2 into formaldehyde would be more convenient, avoiding methanol. The synthesis of formaldehyde via catalytic hydrogenation of CO_2 in liquid media has been recently demonstrated [68].

6.3 Outlook

The research herein presented shows that, even though a novel pathway for bio-based methyl propionate has been implemented in *E. coli*, significant strain optimization is still required. Overall, a suitably integrated process could become techno-economically feasible, but future research should dedicate special attention to the numerous metabolic engineering targets discussed in this thesis. The outcome of this thesis indicates that the ideal microorganism for a one-step biotransformation of lignocellulosic sugars into methyl propionate would: 1) ferment lignocellulosic sugars; 2) harbor oxygen-insensitive enzymes; 3) form one methyl propionate per glucose equivalent, effectively closing the redox balance and circumventing the formation of ethyl acetate; 4) require no additional cobalamin; and 5) depict sufficient stability for cell retention and recycling.

6.4 References

(1) Mukhopadhyay, A. Tolerance Engineering in Bacteria for the Production of Advanced Biofuels and Chemicals. *Trends in Microbiology* **2015**, *23*, 498-508.

(2) Wu, M.-Y.; Sung, L.-Y.; Li, H.; Huang, C.-H.; Hu, Y.-C. Combining Crispr and Crispri Systems for Metabolic Engineering of E. coli and 1,4-Bdo Biosynthesis. *ACS Synthetic Biology* **2017**, *6*, 2350-2361.

(3) Jakočiūnas, T.; Bonde, I.; Herrgård, M.; Harrison, S. J.; Kristensen, M.; Pedersen, L. E.; Jensen, M. K.; Keasling, J. D. Multiplex Metabolic Pathway Engineering Using Crispr/Cas9 in Saccharomyces Cerevisiae. *Metabolic Engineering* **2015**, *28*, 213-222.

(4) Vanegas, K. G.; Lehka, B. J.; Mortensen, U. H. Switch: A Dynamic Crispr Tool for Genome Engineering and Metabolic Pathway Control for Cell Factory Construction in Saccharomyces Cerevisiae. *Microbial Cell Factories* **2017**, *16*, 25.

(5) Malaviya, A.; Jang, Y.-S.; Lee, S. Y. Continuous Butanol Production with Reduced Byproducts

Formation from Glycerol by a Hyper Producing Mutant of Clostridium Pasteurianum. *Appl. Microbiol. Biotechnol.* **2012**, *93*, 1485-1494.

(6) Ezeji, T. C.; Qureshi, N.; Blaschek, H. P. Bioproduction of Butanol from Biomass: From Genes to Bioreactors. *Curr. Opin. Biotechnol.* **2007**, *18*, 220-227.

(7) Westman, J. O.; Franzen, C. J. Current Progress in High Cell Density Yeast Bioprocesses for Bioethanol Production. *Biotechnol. J.* **2015**, *10*, 1185-95.

(8) Wang, J.; Chae, M.; Sauvageau, D.; Bressler, D. C. Improving Ethanol Productivity through Self-Cycling Fermentation of Yeast: A Proof of Concept. *Biotechnology for Biofuels* **2017**, *10*, 193.

(9) Aalbers, F. S.; Fraaije, M. W. Coupled Reactions by Coupled Enzymes: Alcohol to Lactone Cascade with Alcohol Dehydrogenase-Cyclohexanone Monooxygenase Fusions. *Appl. Microbiol. Biotechnol.* **2017**, *101*, 7557–7565.

(10) Kamerbeek, N. M.; Fraaije, M. W.; Janssen, D. B. Identifying Determinants of Nadph Specificity in Baeyer-Villiger Monooxygenases. *Eur J Biochem* **2004**, *271*, 2107-16.

(11) Ji, X. J.; Huang, H.; Ouyang, P. K. Microbial 2,3-Butanediol Production: A State-of-the-Art Review. *Biotechnol. Adv.* **2011**, *29*, 351-64.

(12) Vuoristo, K. S.; Mars, A. E.; Sangra, J. V.; Springer, J.; Eggink, G.; Sanders, J. P. M.; Weusthuis, R. A. Metabolic Engineering of the Mixed-Acid Fermentation Pathway of Escherichia Coli for Anaerobic Production of Glutamate and Itaconate. *AMB Express* **2015**, *5*, 61.

(13) Xu, Y.; Chu, H.; Gao, C.; Tao, F.; Zhou, Z.; Li, K.; Li, L.; Ma, C.; Xu, P. Systematic Metabolic Engineering of Escherichia Coli for High-Yield Production of Fuel Bio-Chemical 2,3-Butanediol. *Metab. Eng.* **2014**, *23*, 22-33.

(14) Shah, N. B.; Duncan, T. M. Aerobic Growth of Escherichia Coli Is Reduced, and Atp Synthesis Is Selectively Inhibited When Five C-Terminal Residues Are Deleted from the ϵ Subunit of Atp Synthase. *The Journal of Biological Chemistry* **2015**, *290*, 21032-21041.

(15) Chan, Y. J.; Chong, M. F.; Law, C. L.; Hassell, D. G. A Review on Anaerobic–Aerobic Treatment of Industrial and Municipal Wastewater. *Chemical Engineering Journal* **2009**, *155*, 1-18.

(16) Martin, I.; Pidou, M.; Soares, A.; Judd, S.; Jefferson, B. Modelling the Energy Demands of Aerobic and Anaerobic Membrane Bioreactors for Wastewater Treatment. *Environ Technol* **2011**, *32*, 921-32.

(17) Li, W.-W.; Yu, H.-Q. Advances in Energy-Producing Anaerobic Biotechnologies for Municipal Wastewater Treatment. *Engineering* **2016**, *2*, 438-446.

(18) Phattaranawik, J.; Leiknes, T. Study of Hybrid Vertical Anaerobic Sludge-Aerobic Biofilm Membrane Bioreactor for Wastewater Treatment. *Water Environ Res* **2010**, *82*, 273-80.

(19) Chen, Z.; Sun, H.; Huang, J.; Wu, Y.; Liu, D. Metabolic Engineering of Klebsiella Pneumoniae for the Production of 2-Butanone from Glucose. *PLOS ONE* **2015**, *10*, e0140508.

(20) Morita, H.; Toh, H.; Fukuda, S.; Horikawa, H.; Oshima, K.; Suzuki, T.; Murakami, M.; Hisamatsu, S.; Kato, Y. et al. Comparative Genome Analysis of Lactobacillus Reuteri and Lactobacillus Fermentum Reveal a Genomic Island for Reuterin and Cobalamin Production. *DNA Research: An International Journal for Rapid Publication of Reports on Genes and Genomes* **2008**, *15*, 151-161.

(21) Fang, H.; Kang, J.; Zhang, D. Microbial Production of Vitamin B(12): A Review and Future Perspectives. *Microbial Cell Factories* **2017**, *16*, 15.

(22) Lawrence, J. G.; Roth, J. R. Evolution of Coenzyme B12 Synthesis among Enteric Bacteria: Evidence for Loss and Reacquisition of a Multigene Complex. *Genetics* **1996**, *142*, 11-24.

(23) Raux, E.; Lanois, A.; Levillayer, F.; Warren, M. J.; Brody, E.; Rambach, A.; Thermes, C. Salmonella Typhimurium Cobalamin (Vitamin B12) Biosynthetic Genes: Functional Studies in S. Typhimurium and Escherichia Coli. *J Bacteriol* **1996**, *178*, 753-67.

(24) Ko, Y.; Ashok, S.; Ainala, S. K.; Sankaranarayanan, M.; Chun, A. Y.; Jung, G. Y.; Park, S. Coenzyme B12 Can Be Produced by Engineered Escherichia Coli under Both Anaerobic and Aerobic Conditions. *Biotechnol J* **2014**, *9*, 1526-35.

(25) van Beek, H. L.; Romero, E.; Fraaije, M. W. Engineering Cyclohexanone Monooxygenase for the Production of Methyl Propanoate. *ACS Chem. Biol.* **2017**, *12*, 291–299.

(26) Baldwin, C. V. F.; Wohlgemuth, R.; Woodley, J. M. The First 200-L Scale Asymmetric Baeyer−Villiger Oxidation Using a Whole-Cell Biocatalyst. *Organic Process Research & Development* **2008**, *12*, 660-665.

(27) Woodley, J. M. Microbial Biocatalytic Processes and Their Development. *Adv Appl Microbiol* **2006**, *60*, 1-15.

(28) Baldwin, C. V. F.; Woodley, J. M. On Oxygen Limitation in a Whole Cell Biocatalytic Baeyer–Villiger Oxidation Process. *Biotechnology and Bioengineering* **2006**, *95*, 362-369.

(29) Garcia-Ochoa, F.; Gomez, E. Bioreactor Scale-up and Oxygen Transfer Rate in Microbial Processes: An Overview. *Biotechnology Advances* **2009**, *27*, 153-176.

(30) Riet, K.; Tramper, J. *Basic Bioreactor Design*, Taylor & Francis, 1991.

(31) Van Dien, S. From the First Drop to the First Truckload: Commercialization of Microbial Processes for Renewable Chemicals. *Curr. Opin. Biotechnol.* **2013**, *24*, 1061–1068.

(32) Eastham, G. R.; Johnson, D. W.; Waugh, M. A Process for the Production of Methacrylic Acid and Its Derivatives and Polymers Produced Therefrom. WO 2013160702 A1, 2013.

(33) Straathof, A. J. J. Transformation of Biomass into Commodity Chemicals Using Enzymes or Cells. *Chem. Rev.* **2014**, *114*, 1871–1908.

(34) Klement, T.; Büchs, J. Itaconic Acid – a Biotechnological Process in Change. *Bioresour. Technol.* **2013**, *135*, 422-431.

(35) Krull, S.; Hevekerl, A.; Kuenz, A.; Prusse, U. Process Development of Itaconic Acid Production by a Natural Wild Type Strain of Aspergillus Terreus to Reach Industrially Relevant Final Titers. *Appl Microbiol Biotechnol* **2017**, *101*, 4063-4072.

(36) Max, B.; Salgado, J. M.; Rodríguez, N.; Cortés, S.; Converti, A.; Domínguez, J. M. Biotechnological Production of Citric Acid. *Brazilian Journal of Microbiology* **2010**, *41*, 862-875.

(37) Saha, B. C.; Kennedy, G. J.; Qureshi, N.; Bowman, M. J. Production of Itaconic Acid from Pentose Sugars by Aspergillus Terreus. *Biotechnology Progress* **2017**, *33*, 1059-1067.

(38) Chang, P.; Chen, G. S.; Chu, H. Y.; Lu, K. W.; Shen, C. R. Engineering Efficient Production of Itaconic Acid from Diverse Substrates in Escherichia Coli. *J Biotechnol* **2017**, *249*, 73-81.

(39) Carlsson, M.; Habenicht, C.; Kam, L. C.; Antal, M. J., Jr.; Bian, N.; Cunningham, R. J.; Jones, M., Jr. Study of the Sequential Conversion of Citric to Itaconic to Methacrylic Acid in near-Critical and Supercritical Water. *Industrial & Engineering Chemistry Research* **1994**, *33*, 1989-1996.

(40) Le Nôtre, J.; Witte-van Dijk, S. C. M.; van Haveren, J.; Scott, E. L.; Sanders, J. P. M. Synthesis of Bio-Based Methacrylic Acid by Decarboxylation of Itaconic Acid and Citric Acid Catalyzed by Solid Transition-Metal Catalysts. *ChemSusChem* **2014**, *7*, 2712-2720.

(41) Lansing, J. C.; Murray, R. E.; Moser, B. R. Biobased Methacrylic Acid Via Selective Catalytic Decarboxylation of Itaconic Acid. *ACS Sustainable Chemistry & Engineering* **2017**, *5*, 3132-3140.

(42) Burgard, A. P.; Burk, M. J.; Osterhout, R. E.; Pharkya, P. Microorganisms for the Production of 2-Hydroxyisobutyric Acid. US 8900837 B2, 2014.

(43) Hoefel, T.; Wittmann, E.; Reinecke, L.; Weuster-Botz, D. Reaction Engineering Studies for the Production of 2-Hydroxyisobutyric Acid with Recombinant Cupriavidus Necator H 16. *Appl Microbiol Biotechnol* **2010**, *88*, 477-84.

(44) Pirmoradi, M.; Kastner, J. R. Synthesis of Methacrylic Acid by Catalytic Decarboxylation and Dehydration of Carboxylic Acids Using a Solid Base and Subcritical Water. *ACS Sustainable Chemistry & Engineering* **2017**, *5*, 1517-1527.

(45) Weber, D.; Weidler, P.; Kraushaar-Czarnetzki, B. Partial Oxidation of Isobutane and Isobutene to Methacrolein over a Novel Mo–V–Nb(–Te) Mixed Oxide Catalyst. *Topics in Catalysis* **2017**, *60*, 1401-1407.

(46) Kanno, M.; Yasukawa, T.; Ninomiya, W.; Ooyachi, K.; Kamiya, Y. Catalytic Oxidation of Methacrolein to Methacrylic Acid over Silica-

Supported 11-Molybdo-1-Vanadophosphoric Acid with Different Heteropolyacid Loadings. *Journal of Catalysis* **2010**, *273*, 1-8.

(47) Cao, Y.-L.; Wang, L.; Xu, B.-H.; Zhang, S.-J. The Chitin/Keggin-Type Heteropolyacid Hybrid Microspheres as Catalyst for Oxidation of Methacrolein to Methacrylic Acid. *Chemical Engineering Journal* **2018**, *334*, 1657-1667.

(48) van Leeuwen, B. N.; van der Wulp, A. M.; Duijnstee, I.; van Maris, A. J.; Straathof, A. J. Fermentative Production of Isobutene. *Appl Microbiol Biotechnol* **2012**, *93*, 1377-87.

(49) Marlière, P. Method for Producing an Alkene Comprising Step of Converting an Alcohol by an Enzymatic Dehydration Step. WO 2011076691, 2011.

(50) Park, A. R.; J.J., Y. *Bio-Based Production of Isobutylene from Isobutanol by Biocatalysis*. in *Symposium on Biotechnology for Fuels and Chemicals*. 2016. Baltimore, MD.

(51) From the Sugar Platform to Biofuels and Biochemicals. Final Report for the European Commission, Contract No. Ener/C2/423–2012/Si2.673791. http://www.qibebt.cas.cn/xscbw/yjbg/201505/P020150520398538531959.pdf accessed 23 Dec 2017.

(52) Butamax Prepares for Bio-Isobutanol Commercialization. https://greenchemicalsblog.com/2017/04/12/butamax-prepares-for-bio-isobutanol-commercialization/ accessed 03 Jan 2017.

(53) Tooze, R. P.; Eastham, G. R.; Whiston, K.; Wang, X. L. Process for the Carbonylation of Ethylene and Catalyst System for Use Therein. WO 1996019434 A1, 1996.

(54) Dubois, J. L. Procede De Fabrication D'un Methacrylate De Methyle Derive De La Biomasse. WO 2010079293 A1, 2011.

(55) Morschbacker, A. Bio-Ethanol Based Ethylene. *Polymer Reviews* **2009**, *49*, 79-84.

(56) Mohsenzadeh, A.; Zamani, A.; Taherzadeh, M. J. Bioethylene Production from Ethanol: A Review and Techno-Economical Evaluation. *ChemBioEng Reviews* **2017**, *4*, 75-91.

(57) Ahmadi, N.; Khosravi-Darani, K.; Mortazavian, A. M. An Overview of Biotechnological Production of Propionic Acid: From Upstream to Downstream Processes. *Electronic Journal of Biotechnology* **2017**, *28*, 67-75.

(58) Zhang, A.; Yang, S.-T. Propionic Acid Production from Glycerol by Metabolically Engineered Propionibacterium Acidipropionici. *Process Biochemistry* **2009**, *44*, 1346-1351.

(59) Wang, Z.; Jin, Y.; Yang, S. T. High Cell Density Propionic Acid Fermentation with an Acid Tolerant Strain of Propionibacterium Acidipropionici. *Biotechnol Bioeng* **2015**, *112*, 502-11.

(60) Millar, G. J.; Collins, M. Industrial Production of Formaldehyde Using Polycrystalline Silver Catalyst. *Industrial & Engineering Chemistry Research* **2017**, *56*, 9247-9265.

(61) Dalena, F.; Senatore, A.; Marino, A.; Gordano, A.; Basile, M.; Basile, A. Methanol Production and Applications: An Overview, in: *Methanol;* (Eds.); 2018, pp 3-28.

(62) Iaquaniello, G.; Centi, G.; Salladini, A.; Palo, E. Waste as a Source of Carbon for Methanol Production, in: *Methanol;* Dalena, F., (Eds.); 2018, pp 95-111.

(63) Carvalho, L.; Furusjö, E.; Kirtania, K.; Wetterlund, E.; Lundgren, J.; Anheden, M.; Wolf, J. Techno-Economic Assessment of Catalytic Gasification of Biomass Powders for Methanol Production. *Bioresour. Technol.* **2017**, *237*, 167-177.

(64) Bennett, R. K.; Steinberg, L. M.; Chen, W.; Papoutsakis, E. T. Engineering the Bioconversion of Methane and Methanol to Fuels and Chemicals in Native and Synthetic Methylotrophs. *Current Opinion in Biotechnology* **2018**, *50*, 81-93.

(65) Ge, X.; Yang, L.; Sheets, J. P.; Yu, Z.; Li, Y. Biological Conversion of Methane to Liquid Fuels: Status and Opportunities. *Biotechnology Advances* **2014**, *32*, 1460-1475.

(66) Duan, C.; Luo, M.; Xing, X. High-Rate Conversion of Methane to Methanol by Methylosinus Trichosporium Ob3b. *Bioresour. Technol.* **2011**, *102*, 7349-7353.

(67) Mehta, P. K.; Ghose, T. K.; Mishra, S. Methanol Biosynthesis by Covalently Immobilized Cells of Methylosinus Trichosporium: Batch and Continuous Studies. *Biotechnol Bioeng* **1991**, *37*, 551-6.

(68) Chan, F. L.; Altinkaya, G.; Fung, N.; Tanksale, A. Low Temperature Hydrogenation of Carbon Dioxide into Formaldehyde in Liquid Media. *Catalysis Today* **2017**,

List of Publications

Part of the research conducted in this project led to the following publications:

Pereira, J.P.C., Verheijen, P.J.T., and Straathof, A.J.J. Growth inhibition of *S. cerevisiae*, *B. subtilis*, and *E. coli* by lignocellulosic and fermentation products. *Appl. Microbiol. Biotechnol*. **2016**, *100*, 9069.9080.

Pereira, J.P.C., Lopez-Gomez, G., Reyes, N.G., van der Wielen, L.A.M., and Straathof, A.J.J. Prospects and challenges for the recovery of 2-butanol produced by vacuum fermentation - a techno-economic analysis. *Biotechnol. J.* **2017**, *12*, 1600657.

Pereira, J.P.C., van der Wielen, L.A.M., and Straathof, A.J.J. Perspectives for the microbial production of methyl propionate integrated with product recovery. *Bioresour. Technol.* **2018**, *256*, 187.194.

Pereira, J.P.C., Overbeek, W., Gudiño-Reyes, N., Andrés-García, E., Kapteijn, F., van der Wielen, L.A.M., and Straathof, A.J.J. Integrated vacuum stripping and adsorption for the efficient recovery of 2-butanol produced by fermentation. Submitted for publication in *Ind. Eng. Chem. Res.*

Transcript of Records

Discipline-related skills

Courses:	Advanced Course Bioprocess Design	(Wageningen, the Netherlands)
	BIOPRO World Talent Campus 2016	(Copenhagen, Denmark)
	ISPT - Process Economics & Cost Engineering	(Eindhoven, the Netherlands)
	RENESENG - Renewable Systems Engineering	(Delft/Wageningen,the Netherlands)

Transferable skills

Courses:	Coaching project-oriented groups	Graduate School, TU Delft
	The art of presenting science	Graduate School, TU Delft
	Writing scientific articles	Graduate School, TU Delft
	Professional and career development	Graduate School, TU Delft

Research-related skills

Oral presentations:	In-situ recovery of volatile fermentation products, 11th European Symposium on Biochemical Engineering Science, 11-14 September 2016, Dublin, Ireland
	Integrated fermentative production of methyl esters, 10th World Congress of Chemical Engineering, 1-5 Oct 2017, Barcelona, Spain
	Integrated fermentative production of methyl esters and 2-butanol, The Netherlands Process Technology Symposium, 30-31 May 2018, Enschede, The Netherlands
Education assistance:	BSc. Course Sustainable Entrepreunership, TU Delft
	BSc. Biotechnology, Integrated Laboratory Course, TU Delft
	BSc. Course Thermodynamica van Levensprocessen, TU Delft
	MSc. Design Project, TU Delft
Supervision MSc. Projects:	Wouter Overbeek, “Characterization of vacuum stripping of intermediate 2-butanol in the bio-based production process of methyl propionate”, 2015
	Gustavo Lopez Gomez, “Techno-economic evaluation of a 2-butanol production process using vacuum fermentation and absorption for DSP”, 2016
	Noelia Gudiño-Reyes, “Conceptual design of an adsorptive bio-based process for 2-butanol production”, 2016
	Sebastiaan G.F. Keuter, “2-butanol recovery from vacuum stripping vapour through absorption - a preliminary selection and evaluation of solvents”, 2016
	Bhargavi Ganesan, “Fermentative production of methyl propionate integrated with in-situ recovery”, 2017

Curriculum vitæ

Joana Patrícia Carvalho Pereira was born on the 23rd May 1983, in the coastal city of Aveiro, Portugal. She finished her Higher Secondary Education in 2001, and started her Diploma Degree (Licenciatura) in Environmental Engineering at the University of Aveiro (UA). During her degree, she focused on Energy and Environmental Management. In 2005, she earned an Erasmus Scholarship that allowed her to study Environmental Sciences at Wageningen University and Researchcentrum, in the Netherlands. After returning to UA, she graduated in 2007 with her thesis entitled "Improving Environmental Management Systems in the Metallurgic Industry".

After she graduated, Joana moved to the Faculty of Engineering in the University of Porto (FEUP), to research fluid dynamics applied to biological wastewater treatment. Here, she grew passionate about academic research: up to 2014, she worked as research fellow on several research projects, namely "Study of the activated sludge process in oxidation ditches" (in LSRE, FEUP), "HIDROCORK – Utilization of cork wastes and by-products for elimination of oils and fats from waters" (in LSRE/LCM, FEUP), "MICROFCELLS – Miniaturization Direct Methanol Fuel Cells: design, modelling and optimization" (in CEFT, FEUP), and "Sustainable gold mining wastewater treatment by sorption using low-cost materials" (in IHE, Delft Institute for Water Education). In 2012, Joana pursued a Master of Science degree, graduating in 2013 with her thesis entitled "Passive Direct Ethanol Fuel Cells: experimental and modeling studies", under the supervision of Prof. dr. ir. António J.B. Samagaio (UA) and Prof. dr. ir. Alexandra M.P.S.F.R. Pinto (FEUP).

In January 2014, she joined the Bioprocess Engineering group (BPE), at Delft University of Technology, the Netherlands, and started her PhD research under the supervision of Dr. ir. Adrie J.J. Straathof, and Prof. dr. ir. Luuk A.M. van der Wielen. Up to January 2018, she assessed the techno-economic feasibility of a novel bio-based approach for the production of methyl propionate, as presented in this thesis.

As of April 2018, she holds a Postdoc position in the BPE.

LinkedIn: www.linkedin.com/in/joana-pereira-490b831a/

Acknowledgements

"As palavras proferidas pelo coração não tem língua que as articule, retém-nas um nó na garganta e só nos olhos é que se podem ler." – José Saramago

"Words that come from the heart are never spoken, they get caught in the throat and can only be read in one's eyes." – José Saramago

This is the last Chapter of this Thesis and, perhaps, the most important one. As I sit to write it, I truly understand the impact of this journey, and how much I have earned from it. And I feel so grateful for having had the privilege of knowing such remarkable people along the way.

Adrie Straathof, my promotor, supervisor, and, above all, my role model. I cannot find enough words to express my gratitude for your kindness, dedication, guidance, and support. Thank you for always finding the right words to keep me enthusiastic and motivated during this project. You are a brilliant researcher, an exceptional mentor, and I admire that you are truly committed to your students. I feel very proud and privileged to be part of your research group.

Luuk van der Wielen, it has been a pleasure to have you as my promotor. Thank you for always challenging me during our progress meetings, for showing me new perspectives on industrial engineering, and for teaching me so much, on so many (trivial and non-trivial) topics.

Peter Verheijen, I will never thank you enough for your availability and dedication, your patience and guidance, your friendship. It is because of such passionate, talented professionals that I love my work in academia. You are an inspiring professor, and it is a privilege to work with you.

I would like to extend my gratitude to the members of the MEBIO project, Graham Eastham, David Johnson, Henk Noorman, Marco Fraaije, Linda Otten, Ulf Hanefeld, Hugo van Beek, and Elvira Guzman, for their support and collaboration. Also, my dear friend Rosario Medici: we have struggled and thrived together, and I have learned so much from you, much more than science! Freek Kapteijn, Filipe Vidal Lopes, Eduardo Andrés Garcia, and Willy Rook, thank you for kindly sharing your knowledge (and your busy equipment!), it was a valuable contribution to this work.

My MSc students, Wouter, Sebastiaan, Gustavo, Noelia, Bhargavi, (and, for short time, Pari!), I have learned more from you than you will ever know. Each one of you taught me diverse and precious lessons, and helped me grow professionally, and personally. I am very proud of you, and of what you have accomplished in your projects, also after your MSc. Thank you, for also being my mentors. I would also like to acknowledge the (PDEngs) Maria, Diogo, Catarina, Rita, Rafaela, Sajan, Pilar, Harsha: your collaboration and enthusiasm in the initial phase of this project was crucial for its development.

I would like to thank the members of the BPE group, for making me feel part of the family: Maria, thank you for always supporting me. You are a true inspiration, not only for your

students, but for all the lucky ones that come upon you. Marcel, I have learned a lot from your work, thank you for sharing your expertise. Kawieta, I really appreciate that you are always willing to help everyone, always with a smile, you are wonderful. Max and Stef, it is a pleasure to work with you, thank you for your patience and perseverance, particularly for my analytical methods. Song, you are an extraordinary professional, and an extraordinary friend. Thank you for turning stressful experiments into amusing memories, and for giving your best every time.

All of you who accompanied me along this beautiful journey, making every day brighter: Rita, thank you for your contribution to the project, for being my office mate, for being a best friend. Silvia and Marcelo, we started this journey together, and I really loved my time with you. Thank you for this amazing experience (and our Colombian adventure)! Carlos, Susana, Deborah, thank you for all the laughs, innumerable discussions about "stuff", and quality time in the "new" office (Plantita Vive!). Victor, David, Alex, thank you for the muffin tradition, for teaching me so much, and for making it so much fun. Arjan, Mihir, Renato, thank you for the *gezelligheid* in the Julianalaan's office, and for the delicious food you have shared with me. Monica, Chema, Bianca, Shima, Marina, Joan, thank you for the great times we have spent together. Thank you for showing me the silver lining behind every cloud, and for making me a better person. Floor, Lisette, Ana, Francisca, Mariana, Mar, Monica, Jasmine, Giannis, Noa, Anja, Fabienne, Kirsten, Hugo, Camilo, Karel, Sushil, Cristina, Angel, Daniel, Simon, Florence, Yaya, Jelle, Vidhvath, Robin, Leonor, thank you for your kindness and camaraderie along these years. Geert-Jan, thank you for your contagious enthusiasm. Ton van Maris, Walter, Aljoscha, Rob, Kristina, John, Pilar, Patricia, Dirk, Cor, Angie, Johan, Apilena, Astrid, Jannie, Laura, Erik, thank you for your time, support, and dedication. You made it all better!

My dear Portuguese and International friends, Sara, Maria, Diogo, Filipe, Joana, Isabel, Tino, Joana, João, Pontus, Ana, Jan, Filipe, Carla, Luz, Inês, Edu, Cata, André, Paola, Lan, Angela, Gui, Midas, Bert, Sophie, Boris, famílias Pestana e Azevedo, thank you for all your love, during all these years, and for showing me that friends are - indeed - the family we choose. No matter where, or for how long, whenever I am with you, I feel at home.

Aos meus pais, Maria Fernanda e Manuel, por sempre me terem dado asas para voar, e a liberdade para as usar, o meu obrigada. Mamã, papá, obrigada por todos os valores que me passaram, por todo o vosso amor, por todo o vosso apoio. Obrigada por serem quem são, por serem a minha verdadeira fundação. Amo-vos muito. Avós Natalina e Esmeralda, tia Isabel e tio Luís, obrigada por todo o entusiasmo e carinho, trago-vos no coração.

Querido Douglas, obrigada por estares comigo nesta aventura, porque nada disto teria sido possivel sem ti! Obrigada por teres tomado conta de mim nestes 4 anos (na verdade, são quase 8!!), e por sempre me teres apoiado, em todos os momentos. Adoro partilhar a minha vida contigo, e não podia ser mais feliz! *"Te amo sin saber cómo, ni cuándo, ni de dónde, te amo directamente sin problemas ni orgullo: así te amo porque no sé amar de otra manera" (Pablo Neruda)*.